The Heat Transfer Problem in Optically Pumped Semiconductor Lasers

Diploma paper
by
Ulf Wiström

Lund Reports on Atomic Physics, LRAP-107
Lund, November 1989

Table of contents

Abstract
========

This thesis deals with the problem of heat transfer in optically pumped semiconductor lasers, which is the main complication when trying to obtain high output power from such lasers. Some proposals about how to reduce this problem are made, and some models of the laser heating in solids are discussed.
In order to investigate the effectiveness of the proposals and the validity of the proposals, some experiments have been carried out, including the construction of a semiconductor laser.
A major part of the work was done at TACAN Corporation in California, USA.

Introduction

Chapter 1 of this thesis is an introduction to lasers in general and optically pumped semiconductor lasers in particular. In the first section the general principles are mentioned. The second section is a review of different laser types. The third section is an introduction to some of the principles concerning optically pumped semiconductor lasers.

Chapter 2 deals with the heat transfer problem in optically pumped semiconductor lasers and some proposed solutions to that problem. The proposals are divided into different groups depending on which feature is to be improved. Each group has its own section in this chapter. Some parts of the calculations are presented in appendices.

Chapter 3 consists of some theory concerning the heat transfer problem in optically pumped semiconductor lasers. The first section is an introduction to the heat transfer theory in solids in general. Some simplifications for semiconductors are also mentioned. The second section presents four different models of laser heating of solids. For the last model a suggestion about for the convertion of the method into a computer program is made.

Chapter 4 describes the experiments carried out. In the first section the goals of the experiments are formulated, and the approach chosen to reach these goals is presented. The following sections describe how the experiments were carried out, from the choice of semiconductor to the construction of a semiconductor laser in order to investigate the red shift.

Chapter 5 contains a discussion and some conclusions.

Chapter 1. An introduction to lasers in general and to optically pumped semiconductor lasers in particular

What is a laser? General principles

The word LASER is an acronym from Light Amplification of Stimulated Emission Radiation. Lasers are used in many applications, and they are playing an important role in the development of man's knowledge. In order to understand how the laser works, we look at the atoms (or molecules) in a material. Depending on which energy they have, they are found in different energy levels.

Consider two energy levels in the material, E_1 and E_2. Let E_1 be the ground level, that is, the lowest possible energy level in the material.

If one irradiates the material with light of frequency ν, where ν is chosen so that $h\nu = E_2 - E_1$ (where h is Planck's constant), the energy of the radiation corresponds to the energy difference between the two levels.

There are three ways for an atom to make a transition between E_1 and E_2. (We assume that the transition is not forbidden.) See Fig. 1.

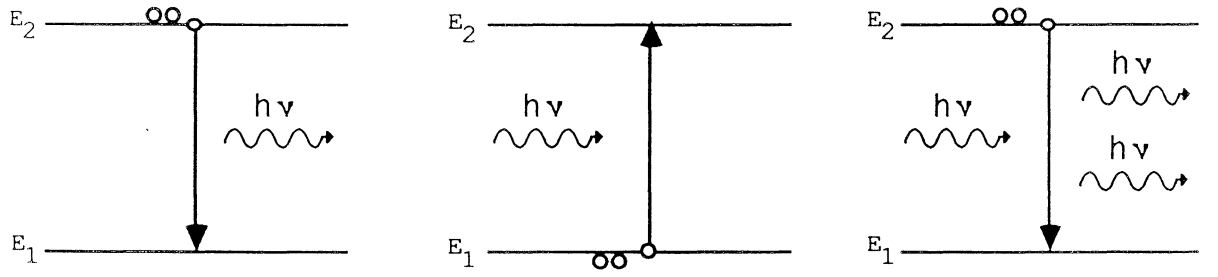

(a) Spontaneous emission (b) Absorption (c) Stimulated emission

Fig. 1. Different modes of transition.

Spontaneous emission

If the atom is in the level E_2, it can spontaneously make a transition to E_1, since $E_2 > E_1$ and the atom tries to achieve as low an energy as possible. The energy $E_2 - E_1$ is then released from the atom. If this energy is released by means of radiation, the process is called spontaneous emission. (See Fig. 1a.) The frequency of the radiation is determined by Planck's law

$$(1) \qquad \nu = \frac{E_1 - E_2}{h}$$

The transition can also occur when the atom collides with other atoms. Then the energy is released as kinetic energy, and no radiation occurs. This is called a non-radiative transition.

The transition rate for spontaneous emission is proportional to the

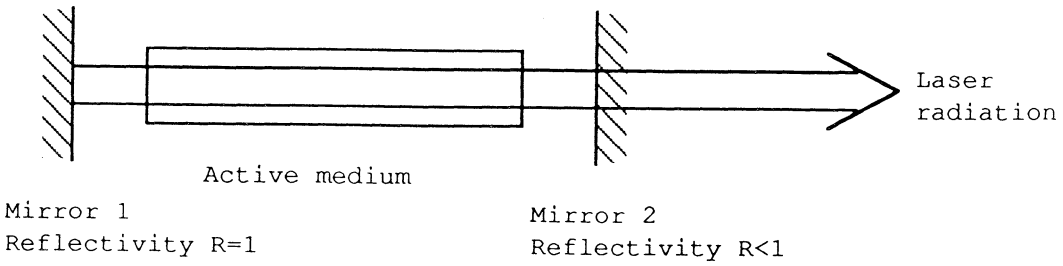

Fig. 3. Principles of a laser.

The process will start when some atoms spontanously decay from E_6 to E_5. Radiation is then emitted (spontaneous emission).

The radiation not perpendicular to the mirrors will soon disappear from the cavity, while the radiation emitted perpendicular to the mirrors will bounce back and forth between the mirrors and will start a chain reaction of stimulated emission.

Since the stimulated emmission has the same direction and the same phase as the incoming radiation, there will be more and more radiation bouncing back and forth between the mirrors, increasing the intensity all the time. This will continue until a steady state is reached. Then the losses in the cavity and the gain are equal. The main loss is the leaking light at mirror 2. This is the laser output.

Energy must be injected all the time in order to maintain the inversion. This process, the injection of energy to accomplish inversion, is called pumping.

But maintaining inversion is not enough to obtain lasing. The energy must be even higher, in order to take care of losses in the cavity due to e. g. nonperfect mirrors, light diversion and the laser output. When the energy injected is higher than this figure, called the pump threshold for lasing, the laser can work.

Optical pumping

If we try to construct a laser, using only two energy levels, we will not succeed. As already mentioned, inversion must be accomplished. But this is impossible using only two energy levels, since the population of the two levels in thermal equilibrium is given by the Boltzmann formula

$$\frac{N_6}{N_5} = \exp\left(-\left[\frac{E_6-E_5}{kT}\right]\right) \tag{10}$$

where k = Boltzmann's constant
T = the temperature in Kelvin

In order to obtain inversion, we have to use three or more energy levels. The principle for a three-level laser is illustrated in Fig. 4.

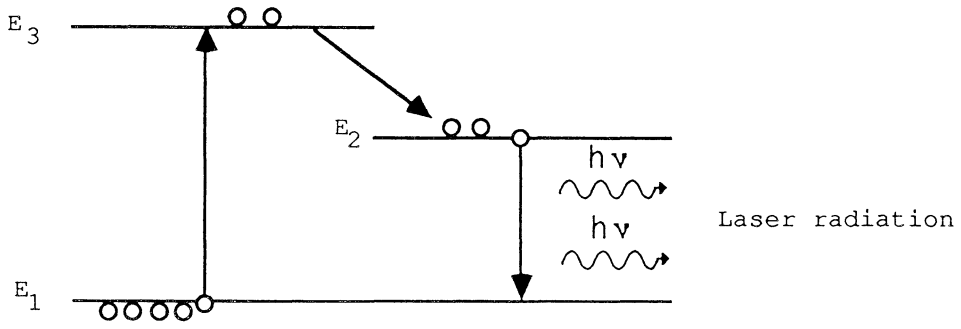

Fig. 4. The three-level laser.

Here E_1 is the ground level and E_2 is a metastable level (atoms here have a relatively long lifetime). The transition probability from E_3 to E_2 is high and must be much higher than the transition probability from E_3 to E_1.

By injecting energy atoms can be excited from E_1 to E_3. The conditions described above will lead to the collection of atoms in level E_2. In this way we can obtain the desired inversion between E_2 and E_1.

A brief laser review

The first laser was constructed by Maiman in 1960. It was a three-level laser, the active medium being a ruby rod.

Since then many lasers have been developed, and laser technology has become important. Lasers are used in a large number of applications; e. g. spectroscopy, optical communications, accurate measuring, fusion research and information processing.

We will look at some different types of lasers with spectroscopy in mind.

Fixed-frequency lasers

The ruby laser is a fixed-frequency laser. That is, radiation is obtainable only at certain, almost fixed, frequencies. Other lasers in this category are the Nd:YAG laser (with an active medium consisting of Nd3+ incorporated in an yttrium - aluminium garnet), the gas lasers (with an active medium consisting of gas e. g. He-Ne, Kr^+, Ar+) and the Eximer lasers (with an active medium consisting of e. g. KrF or XeCl).

Fixed-frequency lasers often have a good beam quality and can produce vast amounts of power. For instance, Q-switched lasers have produced pulses of more than 10^9 watt peak power during 10^{-9} seconds [1].

Q-switching is obtained by inserting an obstacle into the cavity. This leads to a dramatically increased lasing threshold. The inversion becomes stronger and stronger, trying to reach the threshold. If the obstacle is then suddenly removed, a giant pulse is emitted. Continuous repetition of this process (usually obtained by rapidly changing the transmission of the obstacle) produces a pulsed Q-switched laser.

Tunable lasers

The main disadvantage with fixed-frequency lasers is that they only have certain frequencies. Especially in spectroscopy, there is a need to be able to vary the frequency continuously. Let us take a look at the most common tunable lasers.

Dye lasers

The dye laser was the first tunable laser invented. It was in 1966 that Sorokin et al. and Schäfer et al. independently discovered lasing in organic dye solutions [2] [3].

Since then, many new dyes have been discovered, and dye lasers have become widespread in laboratories all over the world.

The active medium is often in the form of a fast moving sheet of dye solution. Dye lasers can be made to produce pulses as short as about 6 fs [4] and cw powers of several watts. They can operate in the range from 335 nm [5] to 1.12 µm [6] (using different dyes). However, when trying to extend further into the infrared region, they run into stability problems [7].

Colour-centre lasers

One can use colour-centre lasers between 1 μm and 4 μm [8]. Here the active medium is a cooled colour-centre crystal. The colour-centre is a certain defect in the crystal lattice.

These lasers have certain problems that reduce their usefulness. They must be cooled in order to lase, they are difficult to produce and they suffer from orientational bleaching after a while.

Solid state lasers

The recently developed solid state lasers can provide high output power and tunability in certain wavelength regions e. g. 700 - 800 nm (Alexandrite lasers) [9] and 1.6 - 2.1 μm ($CoMgF_2$ and $NiMgF_2$) [10]. However, there is a need for more research in order to find new crystals and dopants.

Semiconductor lasers

Another way of obtaining tunability is to use semiconductor lasers.

Semiconductor lasers can be of three kinds: electrically pumped junction lasers, optically pumped or electron beam pumped crystals.

Junction- or diode lasers are small p-n-doped crystals, with forward bias. Two surfaces of the crystal are polished to form a cavity. This means that we do not use an external cavity.

The lasing occurs in the transition area between the p-doped and the n-doped material, where electrons and holes recombine, driven against each other by the postive bias. When the electrons and holes recombine, laser radiation can be emitted, if the current is larger than a certain threshold value. The energy of the radiation approximately equals the band gap. Lasing effects in diodes were discovered in 1962 [11].

Commercial laser diodes cover a wide wavelength region from 670 nm to 40 μm [12]. The output can be high, and the light intensity can easily be modulated. The light has high spectral quality and these diodes have a high coupling factor to optical fibres [13]. This makes laser diodes very interesting for communication purposes, and of course also for spectroscopic purposes.

However, not all semiconductors can be turned into diodes. For instance, it is difficult to dope crystals with wide band gaps. But there are other ways to pump semiconductors. One way is to use an electron beam, which is focused onto a sample of semiconductor, causing it to lase. Although this method can give high output power, it is now seldom used, due to the difficulties in manipulating and focusing the electron beam. We can also use a laser to pump the semiconductor, which gives us an optically pumped semiconductor laser. Since this is the laser we are concerned with here, let us take a little closer look at it in the next section.

Optically pumped semiconductor lasers

The suggestion of using a laser beam to pump a semiconductor was first made as early as 1961 by Thomas and Hopfield [14]. They proposed lasing in CdS, and calculated the threshold for lasing. However, due to some erroneous considerations the calculated figure was far too low.

The first to obtain lasing in a semiconductor by optical pumping were Phelan and Rediker. 1965 they made an InSb crystal lase by pumping it with a GaAS junction laser. The lasing wavelength was 5.3 μm [15].

Let us look closer at the pumping process of a semiconductor laser.

One- and two-photon pumping

There are two methods of pumping the semiconductor sample optically.

The most common is one-photon pumping, where photons of an energy higher than the band gap are used to excite electrons in the semiconductor.

The other way is to use photons of an energy lower than the band gap, but of much higher intensities. Then the probability for two-photon absorption is not negligible. Two-photon absorption is the process in which an atom simultaneously absorbs two photons and becomes exited without the use of a real intermediate state. See Fig. 5.

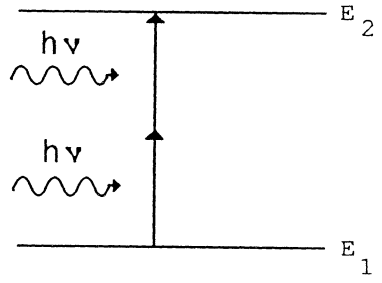

Fig. 5. Two-photon pumping.

Longitudinal - Transversel pumping

There is also to be made a choice between longitudinal and transversel pumping.

Longitudinal pumping is obtained when we focus the beam into a circular spot on the sample like in Fig. 6.

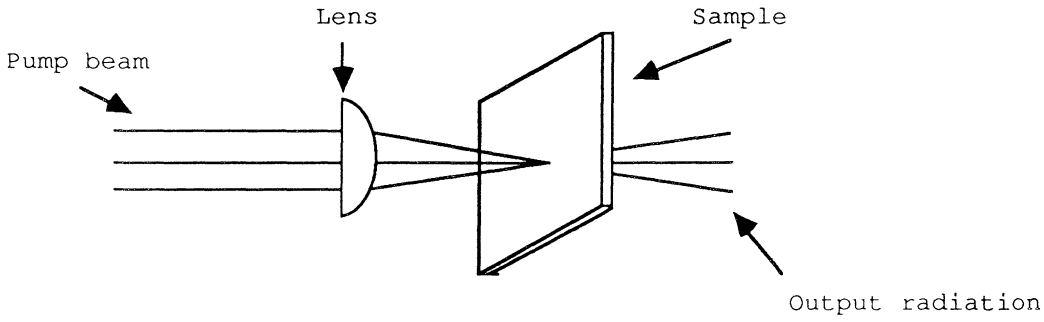

Fig. 6. Longitudinal pumping.

The active volume, that is the volume being pumped, is roughly (see Fig. 7)

(11) $V_a = a\pi d^2$

where a = the diffusion depth
d = the radius of the focused spot

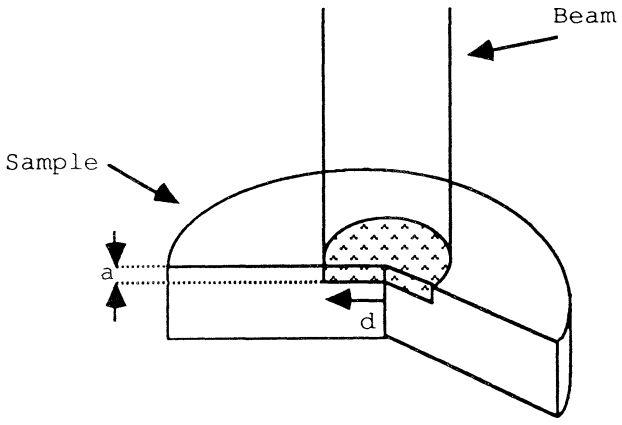

Fig. 7. Active region in longitudinal pumping.

To obtain transversel pumping we use a cylindrical lens which transforms the beam into a line. See Fig. 8.

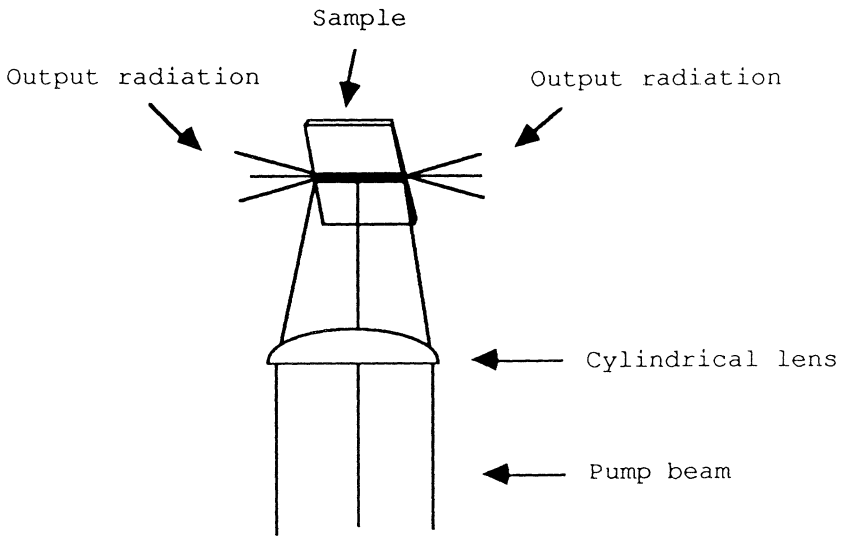

Fig. 8. Transversel pumping.

The active volume here is roughly (see Fig. 9.)

$$(12) \qquad V_a = \frac{\pi c^2}{2}$$

where L = the length of the pumped region of the sample

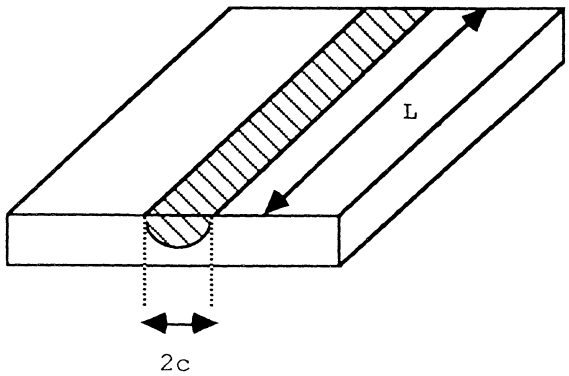

Fig. 9. The active volume in transversel pumping.

Example of configuration

Consider one of Roxlo's set-ups for longitudinal pumping. See Fig. 10. (Roxlo was the first, in 1981, to obtain a continuous wave (cw) optically pumped semiconductor laser in an external cavity [16]).

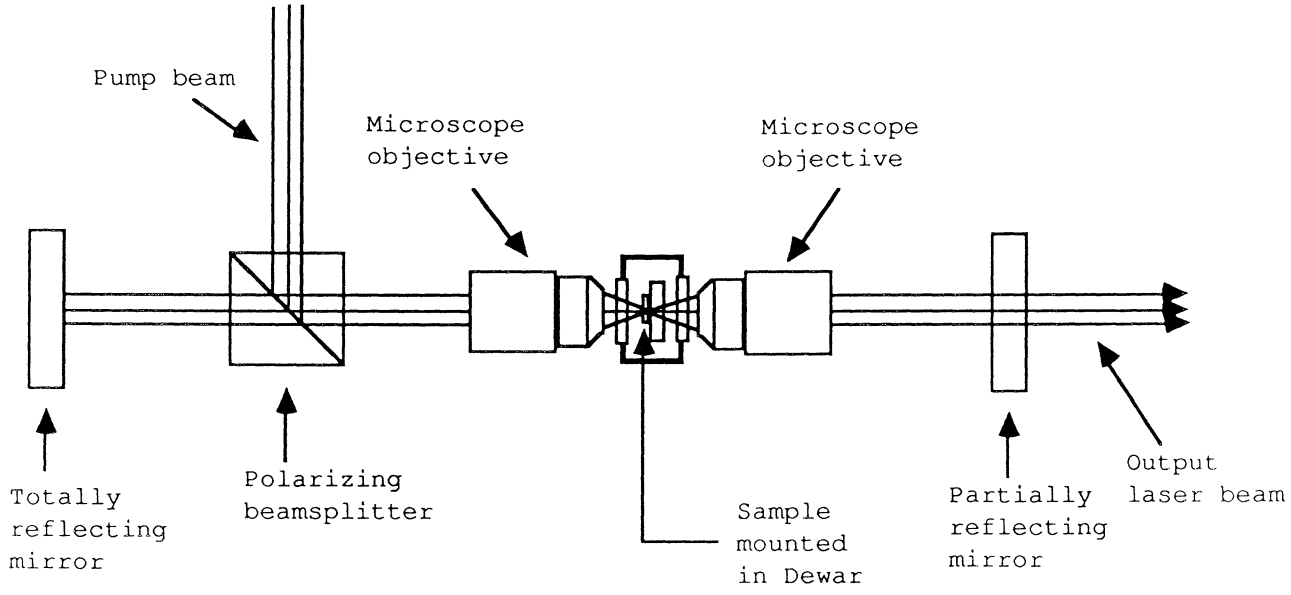

Fig. 10. An optically pumped semiconductor laser in an external cavity.

The sample is mounted on a sapphire window inside a cooled Dewar in order to reduce the heat problems. (See next section.)

One microscope objective focuses the pump beam into a small spot on the sample. The other is used to collimate the output beam from the sample.

The polarizing beamsplitter distinguishes between the vertically polarized pump beam and the horizontally polarized output.

Comparison between optically pumped semiconductor lasers and other lasers

It is interesting to compare optically pumped semiconductor lasers with dye lasers, solid-state lasers, colour-centre lasers and junction semiconductor lasers.

Compared with the dye laser, the optically pumped semiconductor laser has a larger spectral range, due to the large number of crystals with different energy gaps. It is also more convenient to handle, since we get rid of the often poisonous and messy dye solutions, and with them also the dye instability problem. Furthermore, since the optically pumped semiconductor laser can be pumped above the band gap, we have a wider variety of lasers to choose from when pumping the sample.

The Colour-centre lasers have, as we have seen, some serious problems. Also, they cover only small sections of the wavelength region above 1 μm.

Optically pumped semiconductor lasers may also have advantages over diode lasers. They ought to cover a broader wavelength region due to the variety of crystals available. Output power and frequency can be tuned independently of each other. This is not always possible in junction lasers, since an increase in output power requires a larger current. This heats the diode, which causes the band gap to decrease. The result is a lower frequency. Optically pumped semiconductor lasers usually have larger active volumes as well.

However, there might be some disadvantages with optically pumped semiconductor lasers. The most serious problem is probably the limited output power. This is due to heat problems.

Another, closely related, problem is that the pump threshold is very high, approximately 100 kW/cm^2 for one-photon pumping and 10 MW/cm^2 for two-photon pumping. Both values are approximate ones, since different materials have different cross sections for absorption.

If the heat problem can be reduced, the optically pumped semiconductor lasers can be even more useful, already being very valuable for spectroscopy. Let us look deeper into this problem in the next chapter.

Chapter 2. The heat transfer problem in optically pumped semiconductor lasers

In order to make a semiconductor lase, we must first obtain an inversion in the crystal. One way of doing this is (as mentioned earlier) by focusing a laser beam onto the semiconductor. The laser beam then deposits energy in the semiconductor. When the energy density is sufficiently high, the inversion is obtained and the semiconductor crystal starts to lase.

But the energy density required is very high, of the order of J/cm^3 [17]. Worst of all, most of the energy goes into heating the crystal. Increasing the pump power in order to get higher output from the crystal will soon melt it. Here we have the heating problem.

Now, how do we get rid of all this unwanted heat?

Several proposals have been made. We shall briefly describe them in the next section.

But first let us look at the present mounting technique of the crystal. This is required in order to understand some of the proposals. Fig. 11 shows the configuration.

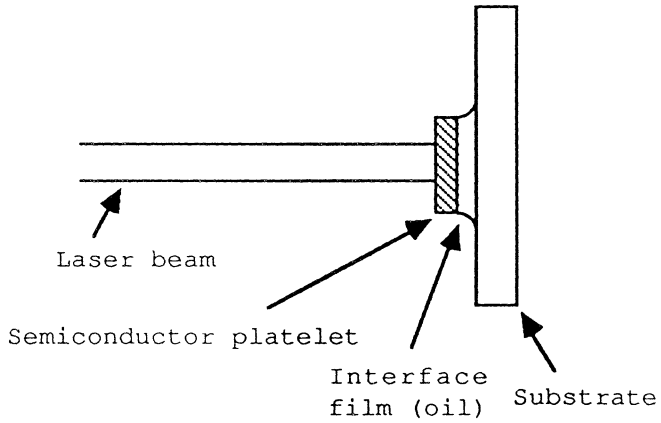

Fig. 11. Mounting configuration.

Here the sample is pumped longitudinally and with one-photon pumping.

Of course, many samples, if wished of different kinds, can be mounted on the same substrate. This enables us to cover a wide wavelength region.

Suggested solutions to the heat transfer problem

The proposals can be divided into four groups:

1. Proposals dealing with the pump beam and its interference with the crystal.

2. Proposals dealing with the crystal.

3. Proposals dealing with the interface between the crystal and the substrate.

4. Proposals dealing with the substrate.

Of course it is possible to combine different proposals. We will consider this later. Let us first take a look at the proposals in each group.

Group 1. Proposals dealing with the pump beam, and its interference with the crystal

A. A pulsed laser beam

This approach has been used in several cases. By pulsing the laser beam the sample has time to cool down between the pulses (mainly by conducting heat into the substrate). It is easy to obtain a pulsed laser beam. The disadvantage is that the output beam will also be pulsed.

B. A distributed pump source

The best way to obtain this is to rotate the sample. Then different spots of the sample will be heated, but the output will not be pulsed. See Fig. 12.

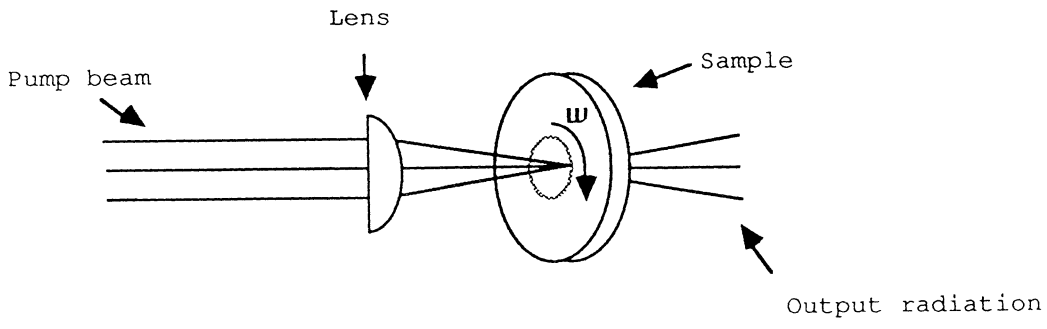

Fig. 12. Rotation of the sample.

The problem with this solution is of course the mechanical difficulties involved in rotating the sample with the required accuracy. (The beam must always be focused on the sample.)

C. Two-photon pumping

This is a technique mentioned earlier. The advantage compared with one-photon pumping is that the diffusion depth of the pump is greater. This allows thicker crystals. (Normally one wants to pump as much as possible of the thickness of the crystal, because the unpumped region reabsorbs the output light from the pumped region. This implies thin crystals. But, on the other hand, a thick crystal can conduct away more heat then a thin one. (Semiconductors have relatively good thermal conductivity.)

Conclusion: It is better (concerning the heat problem) to have as thick a crystal as possible. This is obtainable with two-photon-pumped crystals. (The diffusion depth in two-photon pumping is of the order of cm compared with μm [18] in one-photon pumping).

The disadvantage is that two-photon pumping is more complicated, and the pump power per unit area must be considerably higher (approx. 10 MW/cm^2 compared with approx. 100 kW/cm^2 for one-photon pumping) since the probability for two-photon excitation is much smaller than for one-photon excitation.

D. Transversel pumping

This technique has also been mentioned earlier. Like the method above, this technique increases the pumped volume of the semiconductor. This is desirable. The heating is five times greater than for longitudinal pumping with the same radius, but since the length of the pumped region can be very long, much higher outputs are obtained [19]. This means that we can use less pump power to obtain the same output as with longitudinal pumping. And lower pump power means lower heating. And since the pumped region is only at the surface, we can use thick crystals, which conduct heat more efficiently than thin crystals. However, since the active region is longer, we get problems with amplified spontaneous emission [19]. This is the main disadvantage with this method.

E. Beam radius

According to Roxlo [19] the temperature increases as the beam diameter squared. We ought to obtain better results if we can focus the beam better. It is difficult, however, to focus the beam to less than 5 μm diameter.

Group 2. Proposals dealing with the crystal

A. A protective coating

One way of solving the problem is perhaps to protect the sample with a coating. The ideal coating would have a very high thermal conductivity, in order to conduct heat away from the sample. Furthermore, it should not absorb any pump light or wanted emission. Perhaps the coating can also protect the crystal structure at high temperatures.

B. Thinner crystals

This has already been mentioned. See 2C.

Group 3. Proposals dealing with the interface between the crystal and the substrate

A. Growing the crystal on the substrate

This is a good suggestion, since we get rid of the interface oil film, which acts as a heat barrier, due to its low thermal conductivity [19]. Perhaps the substrate can be made as a mirror, which will further increase the value of this suggestion.

The disadvantages are the cost and the problems involved in the processing of this configuration. Some trials have been done, however [20]. Another problem that occurs when the crystal is heated is the stress which is caused by different thermal expansion of the substrate and the crystal. This problem seems not to be severe, however.

B. Obtaining optical contact by polishing the substrate and the sample

Perhaps it is possible to obtain optical contact and a surface force sufficient to fix the sample onto the substrate in this way. A positive indication is the observation by Roxlo [21] that thin crystals tend to stick to any surface. This solution also does away with the oil film. Furthermore, it is simple and cheap.

Perhaps also a protective coating can be fixed to the sample in this way.

If the force obtained is not sufficient, perhaps applied mechanical tension can achieve results.

A problem is the risk that the crystal will fall off the substrate.

C. Finding other interface materials

A very interesting configuration has been proposed by Holonyak and Scifres [22]. They use indium as interface material. See Fig. 13.

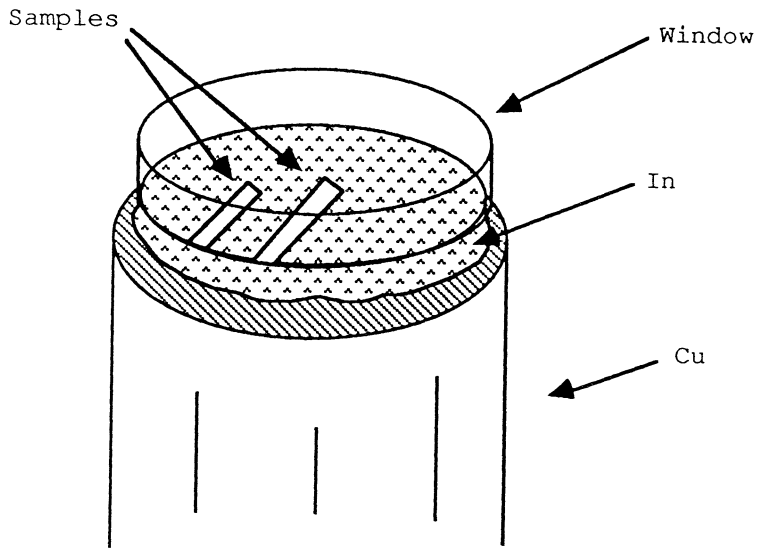

Fig. 13. Sandwich heat sink.

The samples are compressed into the indium with the window (indium is soft!) Since indium also is very good at forming strong contact forces with many smooth hard surfaces, it holds together the window, the sample and the copper substrate. Of course we can use sapphire as the substrate. Indium is probably also a good reflector, so we have the mirror too.

This solution is probably a very good one. We will get rid of the oil film, and probably obtain the mirror directly. The sample must be carefully polished, however. But this is not a problem, at least not with thicker crystals.

If the window causes problems, or we want a simpler approach, a solution is to use indium instead of the oil film in the configuration first considered. See Fig. 14.

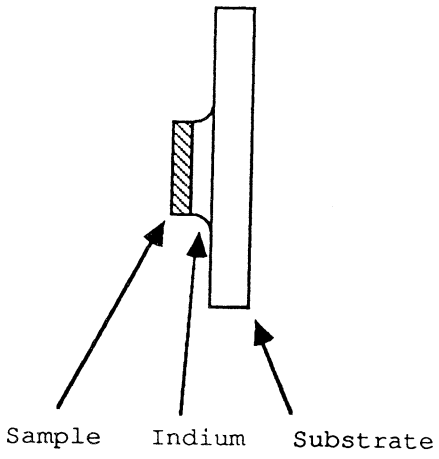

Fig. 14. Indium replaces oil.

If we have problems with the mirror formed by indium, we can grow a thin layer of silver on the sample before attaching it to the indium. This is, of course, possible in both configurations.

Perhaps it is also possible to find a better material than indium.

D. Improving the thermal properties of the oil film

One way to do this is to find another oil with higher thermal conductivity and lower viscosity. (The lower viscosity will make the film thinner.)

Another way to reduce the interface film thickness is by using the microcapillary interface suggested by Tuckerman [23]. See Fig. 15. This was originally a suggestion for an interface between integrated circuits and cold plates, but it can also be used here.

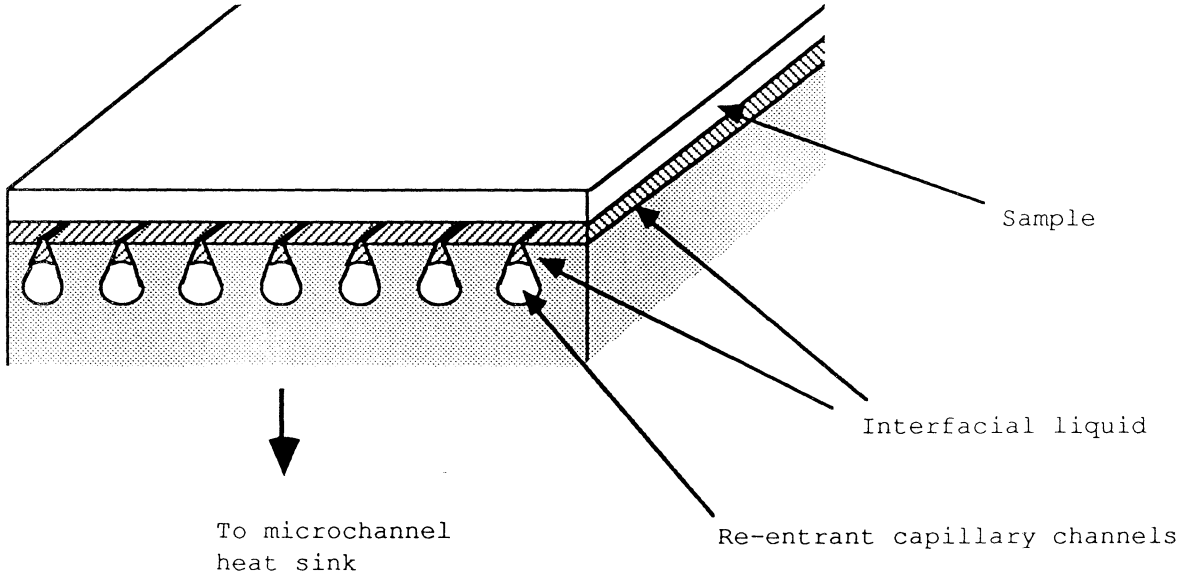

Fig. 15. Tuckerman's microcapillary thermal interface concept.

There are some disadvantages with this method. In order to pump the sample longitudinally, we must use the method with a silver layer grown on the back of the sample, otherwise the output beam will be scattered by the interface. The cost will also proably be high compared with the gain obtainable, unless the electronic industry makes interfaces that can be used.

Group 4. Proposals dealing with the substrate

A. Finding a substrate with higher thermal conductivity

Diamond, for example, is definitely better than sapphire, but the cost is probably higher.

B. Making cooling channels/ducts in the substrate and cooling it by pumping a liquid through these channels

See Fig. 16.

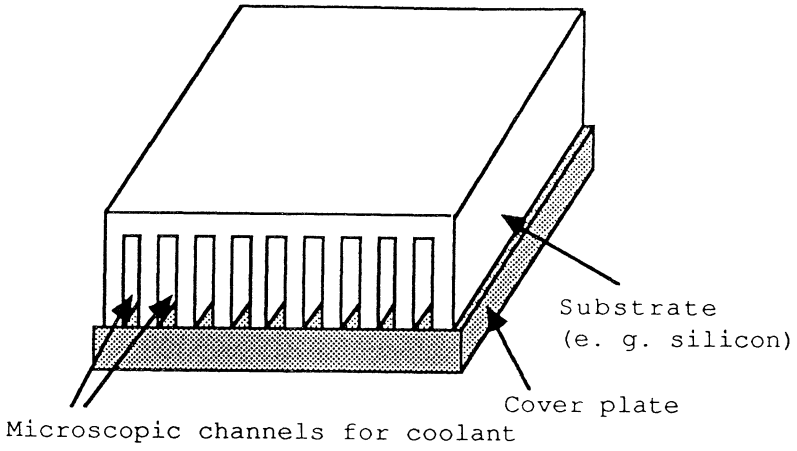

Fig. 16a. Microscopic heat sink.

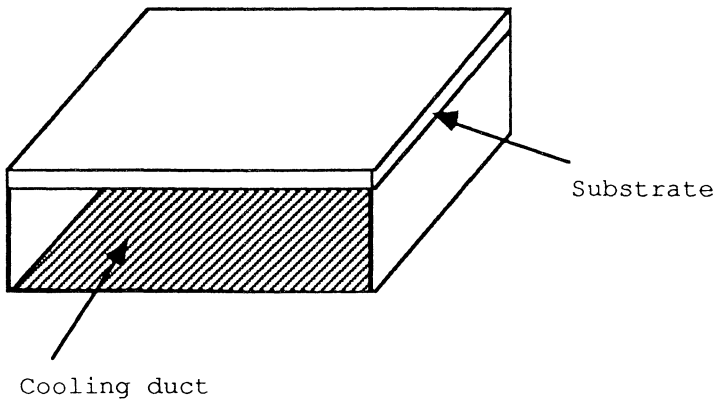

Fig. 16 b. A simple turbulent-flow cooling duct.

This was also proposed by Tuckerman [24]. The main disadvantage with these solutions is that it is impossible to use the original configuration. A new configuration must be obtained.

Combinations of various solutions

It can easily be seen that it is possible to combine solutions. One way to do this is to obtain solutions that deal with the sample, the interface and the substate at the same time.

Such a solution has been suggested by T. Call [25]. The proposal is to grow the crystals in holes in the substrate. See Fig. 17.

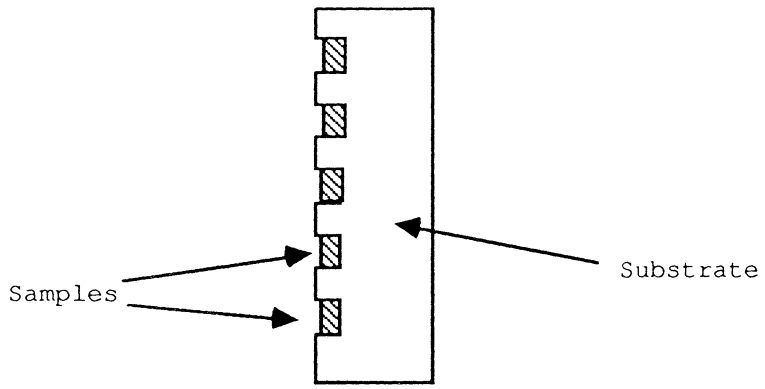

Fig. 17. T. Call's proposal.

He also considered the possibility of pumping the crystal through the substrate, thus obtaining better thermal properties.

There are several advantages with this proposal. It is a simple efficient configuration. Different samples can also be grown in different holes.

However, since it will be very difficult to produce this configuration, it is a proposal for the future. There might also be some problems with stress due to different thermal expansion coeffecients when the configuration is heated.

Chapter 3. Theory

Introduction to the theory of heat conduction in solids

Derivation of the partial differental equation of heat conduction

In order to make calculations for the various proposals, we must look at different models for laser heating of solids.

Since the starting point of all solutions is the partial differential equation of heat conduction, we will start by deriving that equation, using the method of Özisik [26].

When different parts of a body are at different temperatures, heat flows from the hotter part to the cooler part. This flow of heat can take place in three ways: radiation, convection or conduction. In a solid, conduction is by far the most important. This is our case. (We could also have assumed radiation from the heated semiconductor, but that heat transfer is negligible.)

Conduction is the process in which heat is transferred within the solid itself, by means of kinetic motion, or drift of electrons.

The basic law of heat conduction is Fourier's law. Let us look at it in the rectangular coordinate system. Here the law can be expressed as:

(13) $$q_x = -K\frac{\partial T}{\partial x}$$

or

(14) $$Q_x = -KA\frac{\partial T}{\partial x}$$

where q_x = the heat flux in the positive x direction (in W/m^2)

K = the thermal conductivity (in W/mK)

T = the temperature (in K)

$\frac{\partial T}{\partial x}$ = the temperature gradient in the pos. x direction

A = the area (in m^2)

The equations in the y and z directions are analogous.

Now, in order to derive the differential equation of heat conduction, consider an infinitesimal volume element $\Delta x \Delta y \Delta z$. See Fig. 18.

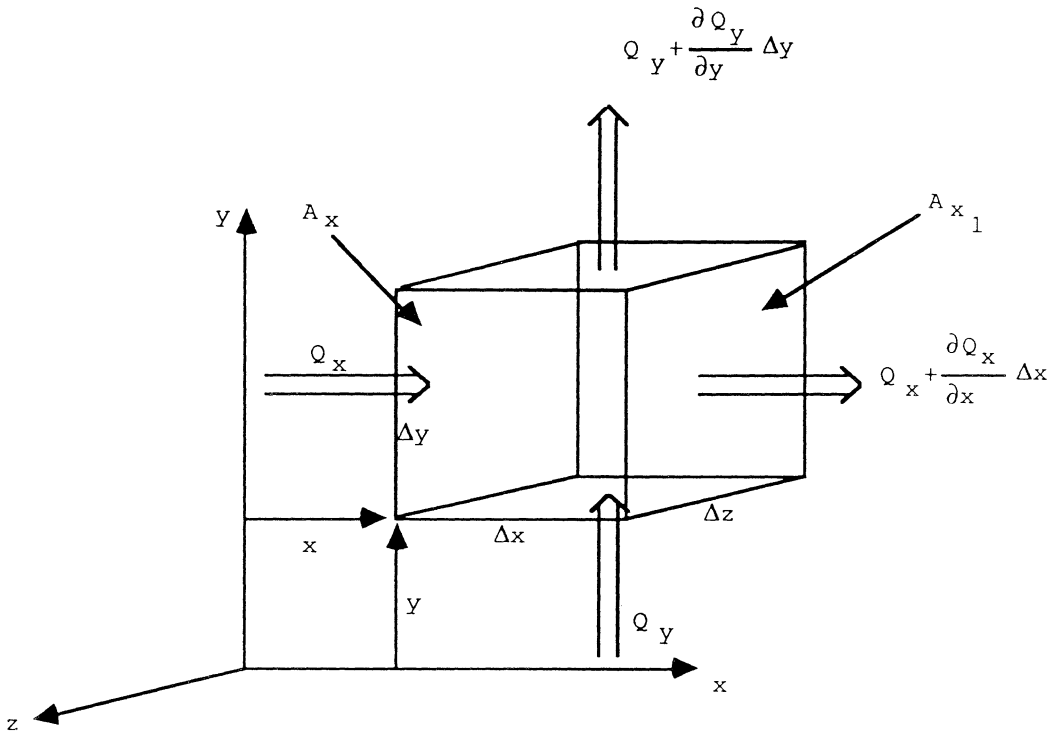

Fig. 18. An infinitesimal volume element with heat flow.

The energy balance for the element is:

A. Net rate of heat entering by conduction into the element $\Delta x \Delta y \Delta z$

+

B. Rate of energy generated in the element $\Delta x \Delta y \Delta z$

=

C. Rate of increase of internal energy of the element $\Delta x \Delta y \Delta z$.

Let us look at it term by term.

A: The first term is the heat gain in the element. Heat enters by conduction into the element in the x, y, and z directions, and leaves the element at the opposite surface. See Fig. 18.

The gain in, for instance, the x direction is

$$(15) \qquad Q_x - \left[Q_x + \frac{\partial Q_x}{\partial x}\Delta x \right] = - \frac{\partial Q_x}{\partial x} \Delta x = - \frac{\partial q_x}{\partial \chi} \Delta x \Delta y \Delta z$$

The heat gain in the y and z directions are obtained in the same way. The sum is

$$(16) \qquad A = - \left[\frac{\partial q_x}{\partial x} + \frac{\partial q_y}{\partial y} + \frac{\partial q_z}{\partial z} \right] \Delta x \Delta y \Delta z$$

B: the second term is called the source term. Assume that we have energy sources within the medium, generating the heat g(x,y,z,t) per unit time and volume (W/m^3). Then this term will be

$$(17) \qquad g\Delta x\Delta y\Delta z$$

C: The third term is the rate of energy storage within the medium. It is

$$(18) \qquad \rho c_p \frac{\partial T}{\partial x}\Delta x\Delta y\Delta z$$

where ρ = the density

c_p = the specific heat

Putting in the terms, we obtain

$$(19) \qquad - \left[\frac{\partial q_x}{\partial x} + \frac{\partial q_y}{\partial y} + \frac{\partial q_z}{\partial z} \right] + g = \rho c_p \frac{\partial T}{\partial t}$$

Using Fourier's law (13) gives

$$(20) \qquad \frac{\partial}{\partial x}\left[K\frac{\partial T}{\partial x} \right] + \frac{\partial}{\partial y}\left[K\frac{\partial T}{\partial y} \right] + \frac{\partial}{\partial z}\left[K\frac{\partial T}{\partial z} \right] + g = \rho c_p \frac{\partial T}{\partial t}$$

This is the partial differential equation of heat conduction.

Considered simplifications for semiconductors

Here we will consider different ways to simplify the partial differential equation of heat conduction.

In order to obtain a linear equation, we often assume uniform thermal conductivity. That is, the thermal conductivity is independent of position and temperature. In this case, we can use the Laplacian operator.

$$(21) \qquad \nabla^2 T = \frac{\partial^2 T}{\partial x^2} + \frac{\partial^2 T}{\partial y^2} + \frac{\partial^2 T}{\partial z^2} \qquad \text{(rectangular coord. sys.)}$$

or

$$(22) \qquad \nabla^2 T = \frac{1}{r}\frac{\partial}{\partial r}\left[r\frac{\partial T}{\partial r} \right] + \frac{1}{r^2}\frac{\partial^2 T}{\partial \Phi^2} + \frac{\partial^2 T}{\partial z^2} \qquad \text{(cylindrical coord. sys.)}$$

to simplify (20). We get

$$(23) \qquad \nabla^2 T + \frac{g}{K} = \frac{1}{\kappa}\frac{\partial T}{\partial t}$$

where $\kappa = \frac{K}{\rho c_p}$ = the thermal diffusivity (in m^2/s).

This simplification is dangerous, however, as will be seen, and we will therefore later try to improve some of the simpler models.

Another simplification used in the simpler models is the assumption that we have a surface source. That is, the source term equals zero. This assumption gives a rough estimation, but since the diffusion depth is 1 - 2 μm [27] and the crystals are relatively thick, this simplification is not included in the more complicated models.

Furthermore, we assume ρ to be a constant, as well as c_p, at least in the simpler models.

If we assume that the temperature does not vary with time, we have a situation that is called steady state. Here $\frac{\partial T}{\partial t}$ vanishes. This is a very interesting case, since the goal is to be able to continuously pump a semiconductor without melting it. Rykalin et al. have estimated the time required to obtain steady state to be 10ms [28].

Boundary conditions

To be able to solve the partial differential equation of heat conduction, we must specify certain boundary conditions for the medium involved. We must also, in the time-dependent cases, have an initial condition, the temperature distribution at time t=0.

The boundary conditions for a medium can be of three kinds.

The first type is when the temperature distribution at a boundary surface is given. For example, see Fig. 19.

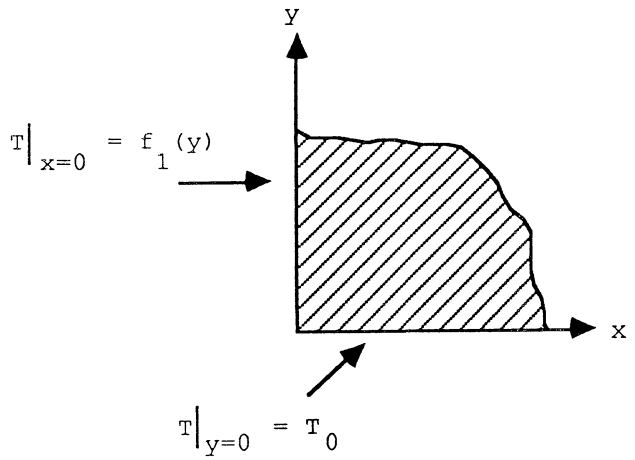

Fig. 19. Example of boundary condition of the first type.

The second type is when the heat flux at a boundary is given. Since the heat flux is defined as

$$q_x = \frac{\partial T}{\partial x} \qquad \text{(in the positive x direction)}$$

we can also say that the derivative of temperature normal to the surface is defined. For example see Fig. 20.

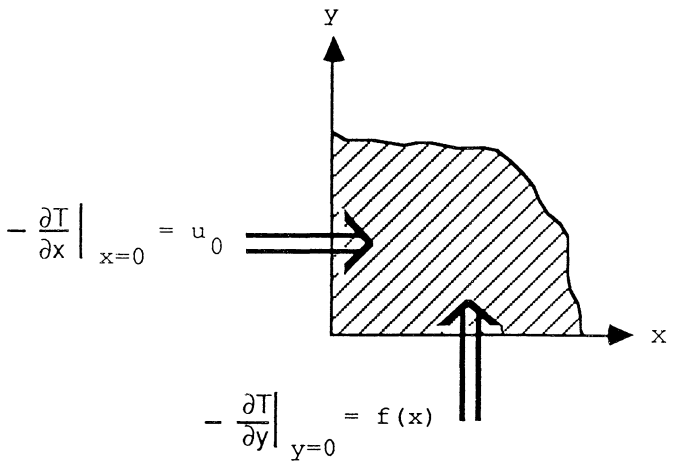

Fig. 20. Example of boundary condition of the second type.

The third type occurs when heat flows from the medium itself into another medium at a given temperature, by means of convection. The equation for this process is

$$(24) \qquad q = h(T_f - T_w)$$

where q = the heat flux (in W/m^2K)
T_f = the temperature of the fluid
T_w = the temperature of the surface of the solid)

For example, consider a thick slab. Consider one surface, x=0. (See Fig. 21.) Let us say that the slab is in an environment with a given temperature.

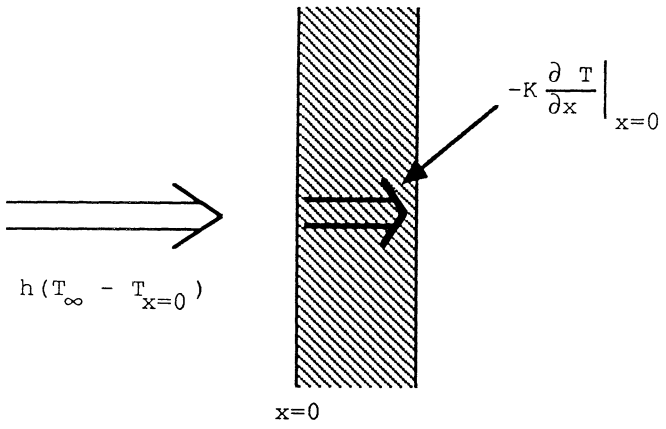

Fig. 21. Example of boundary conditions of the third type.

The energy balance must be obtained. This means that the heat entering by convection has to equal the heat leaving by conduction. See Fig. 21. We get

$$(25) \qquad \left[-K\frac{\partial T}{\partial x} + hT \right]_{x=0} = h_1 T_- = f_1$$

Four linear models of laser heating

1. The semi-infinite solid irradiated by a Gaussian beam

Configuration see Fig. 22.

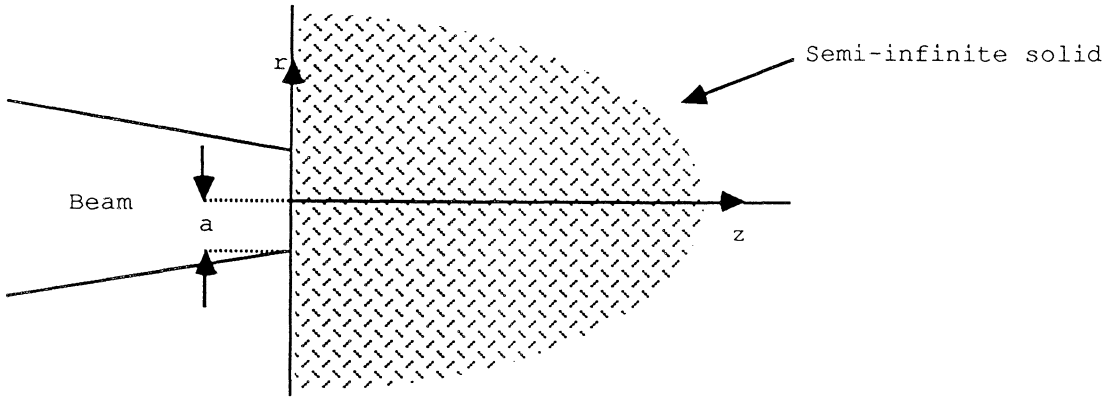

Fig. 22. Irradiated semi-infinite solid.

We assume uniform thermal conductivity and a surface source (no sources within the material. This also means that the absorption coeffecient α is infinite.)

The beam has a Gaussian shape

$$(26) \qquad F = F_0 \exp\left[-\frac{r^2}{a^2} \right]$$

where F = the intensity on the surface (in W/m^2)
F_0 = the intensity at the centre of the spot
a = the Gaussian beam radius (in m)

In solving this problem we adopt a method used by Ready, and Duley [29].

Carslaw - Jaeger [30] give the partial differential equation of heat conduction for an instantaneous point source in an infinite medium as

$$(27) \qquad \frac{\partial^2 T}{\partial x^2} + \frac{\partial^2 T}{\partial y^2} + \frac{\partial^2 T}{\partial z^2} = \frac{1}{\kappa} \frac{\partial T}{\partial t}$$

in the rectangular coorinate system.

The solution is given as

$$(28)\qquad T_{\text{inst. point source}}(x,y,z,t) = \frac{Q}{8\rho c\left[\pi\kappa t\right]^{\frac{3}{2}}} * \exp\left[- \left[\frac{(x-x')^2 + (y-y')^2 + (z-z')^2}{4\kappa t} \right] \right]$$

where $T(x,y,z,t)$ = the temperature (in K) at a point (x,y,z) at the time t
Q = the quantity of energy liberated at $t=0$ at a point (x',y',z') (in J)
c = the specific heat (in J/(kgmK))
κ = the thermal diffusivity (in m^2/s)
ρ = the density (in kg/m^3)
t = the time (in s)

Now,

a) expand the expression for an instantaneous point source into an expression for an instantaneous circular surface source with a Gaussian distribution
b) make the expression valid for a noninstantaneous source
c) make the expression valid for a semi-infinite solid.

But first, go over to cylindrical coordinates. The cosine theorem gives (see Fig. 23)

$$(29)\qquad (x-x')^2 + (y-y')^2 = r'^2 + r^2 - 2rr'\cos(\theta-\theta')$$

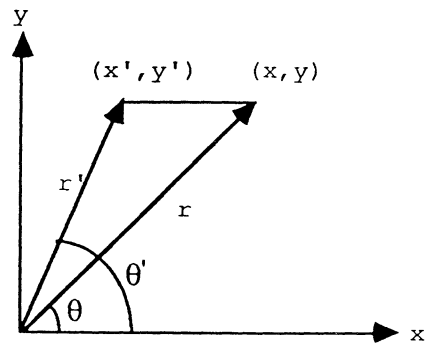

Fig. 23. Relation rectangular - cylindrical coordinate system.

(28) and (29) give (with z'=0)

$$(30)\qquad T_{\text{inst. point source}}(r,\theta,z,t) = \frac{Q}{8\rho c\left[\pi\kappa t\right]^{\frac{3}{2}}} * \exp\left[- \left[\frac{r'^{2} + r^{2} - 2rr'\cos(\theta-\theta') + z^{2}}{4\kappa t} \right] \right]$$

where r' is the location of the source in the r direction.

In order to form an instantaneous ring source at t=0 with radius r' in the plane z'=0, with totally radiated energy Q, we sum up (integrate) an infinite number of point sources in a circle, as in Fig. 24.

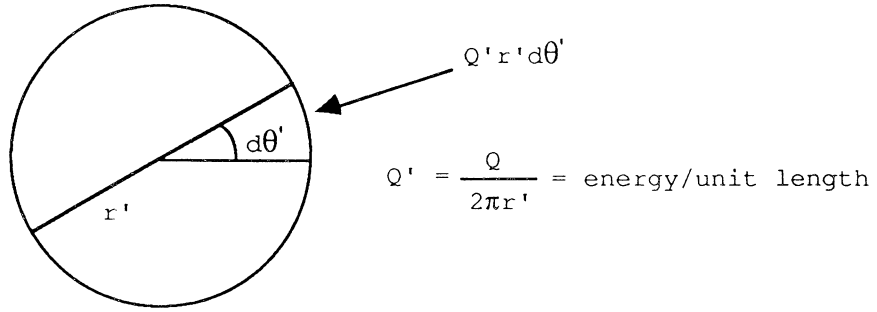

Fig. 24. A ring source and the used energy relation between the point source Q' and the ring source Q.

Integrate the expression:

$$(31)\qquad T = \int_{0}^{2\pi} \frac{Q'r'}{8\rho c\left[\pi\kappa t\right]^{\frac{3}{2}}} * \exp\left[- \left[\frac{r'^{2} + r^{2} - 2rr'\cos(\theta-\theta') + z^{2}}{4\kappa t} \right] \right] d\theta' =$$

$$= \left[\text{with } Q' = \frac{Q}{2\pi r'} \right] = \frac{Q}{16\pi\rho c\left[\pi\kappa t\right]^{\frac{3}{2}}} * \exp\left[- \left[\frac{r^{2} + r'^{2} + z^{2}}{4\kappa t} \right] \right] *$$

$$* \int_{0}^{2\pi} \exp\left[\frac{2rr'\cos(\theta-\theta')}{4\kappa t} \right] d\theta'$$

A table of integrals, series and products gives the value of the integral as [31]

$$(32) \qquad \int_0^{2\pi} \exp\left[\frac{2rr'\cos(\theta-\theta')}{4\kappa t}\right] d\theta' = 2\pi I_0\left[\frac{rr'}{2\kappa t}\right]$$

where I_0 = the modified Bessel function of order zero.

We have

$$(33) \qquad T_{\text{inst. ring source}}(r,z,t) = \frac{Q}{8\rho c[\pi\kappa t]^{\frac{3}{2}}} * \exp\left[-\left[\frac{r'^2 + r^2 + z^2}{4\kappa t}\right]\right] * I_0\left[\frac{rr'}{2\kappa t}\right]$$

Now look at a ring as in Fig. 25.

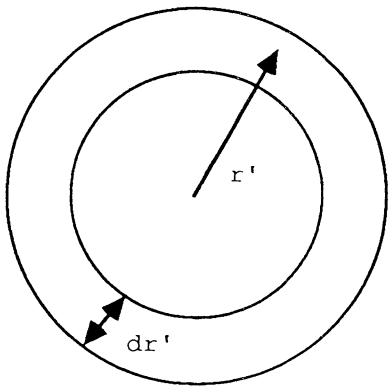

Fig. 25. A ring source.

For an instantaneous Gaussian source the energy liberated in a ring as in Fig. 25. is

$$(34) \qquad Q_{\text{Gaussian ring dr'}} = 2\pi r'Q'' * \exp\left[-\frac{r'^2}{a^2}\right] dr'$$

where r' = the radial distance from origin (in m)
d = the Gaussian beam radius (in m)
Q" = the energy liberated per unit area at the origin (in J/m^2)

To get the total energy liberated over the whole area by a Gaussian source we integrate over r', after replacing Q in (33) with (34). The result is

(35) $T_{\text{inst. Gaussian area source}}(r,z,t) =$

$$\frac{2\pi Q''}{8\rho c\left[\pi\kappa t\right]^{\frac{3}{2}}} * \exp\left[-\left[\frac{r^2 + z^2}{4\kappa t} \right] \right] * \int_0^{\infty} \left[\exp\left[-r'^2 \left[\frac{1}{4\kappa t} + \frac{1}{a^2} \right] \right] * I_0\left[\frac{rr'}{2\kappa t} \right] \right] r'dr'$$

We use the mentioned tables again. Setting

$$\beta = \frac{1}{4\kappa t} + \frac{1}{a^2}$$

and

$$\iota = \frac{r}{2\kappa t}$$

we obtain

$$\int_0^{\infty} \left[r'\exp\left[-r'^2\beta \right] * I_0(\iota r') \right] dr'$$

Setting $y = r'^2$ gives

$$\frac{1}{2} * \int_0^{\infty} \left[\exp(-\beta y) * I_0\left[\iota y^{\frac{1}{2}} \right] \right] dy$$

Using [32] gives

$$(36)\qquad \frac{1}{2} * \int_0^{\infty} \left[\exp(-\beta y) * I_0\left[\imath y^{\frac{1}{2}} \right] \right] dy =$$

$$= \frac{\exp\left[\frac{\imath^2}{8\beta} \right]}{2\left[\frac{\beta \imath^2}{4} \right]^{\frac{1}{2}}} * M_{-\frac{1}{2},\,0}\left[\frac{\imath^2}{4\beta} \right]$$

where M is a Whittaker function

[33] gives

$$(37)\qquad M_{-\frac{1}{2},\,0}\left[\frac{\imath^2}{4\beta} \right] = \left[\frac{\imath^2}{4\beta} \right]^{\frac{1}{2}} * \exp\left[\frac{-\imath^2}{8\beta} \right] * A\left[1 , 1 ; \frac{\imath^2}{4\beta} \right]$$

where A is a degenerate hypergeometric function

[34] gives

$$(38)\qquad A\left[1 , 1 ; \frac{\imath^2}{4\beta} \right] = \exp\left[\frac{\imath^2}{4\beta} \right]$$

Combining (36), (37) and (38) gives

$$(39)\qquad \frac{1}{2} * \int_0^{\infty} \left[\exp(-\beta y) * I_0\left[\imath y^{\frac{1}{2}} \right] \right] dy = \frac{1}{2\beta} \exp\left[\frac{\imath^2}{4\beta} \right]$$

Going back to the original variables and substituting into (35) gives

$$(40)\qquad T_{\text{inst. Gaussian area source}}(r,z,t) =$$

$$\frac{a^2 Q''}{2\rho c\left[\pi\kappa t\right] * \left[4\kappa t + a^2\right]^{\frac{1}{2}}} * \exp\left[- \frac{z^2}{4\kappa t} - \frac{r^2}{4\kappa t + a^2} \right]$$

For a source that has a duration in time we must integrate. Set

(41) $Q'' = \varepsilon F(0,t')dt'$

where $\varepsilon F(0,t)$ is the absorbed power per unit area at the centre of the Gaussian spot (in W/m^2)

We arrive at

(42) $T_{\text{noninst. Gauss. area source}}(r,z,t) =$

$$= \frac{a^2}{2\rho c[\pi\kappa]^{\frac{1}{2}}} * \int_0^t \left[\frac{\varepsilon F(0,t')}{(t-t')^{\frac{1}{2}} * [\,4\kappa(t-t') + a^2\,]} * \right.$$

$$\left. * \exp\left[- \frac{z^2}{4\kappa(t-t')} - \frac{r^2}{4\kappa(t-t') + a^2} \right] \right] dt'$$

(t' is the time when a source is "born" and starts to emit energy. The important time is the time between the birth of a source and its observation (at a time t). If we perform an integration where we let t' go from 0 to t, we will cover the duration of the source. (Observe that in earlier calculations we have set t'=0.))

Set

(43) $p(t) = \frac{F(0,t)}{F_{max}}$

where $F_{max} = \max (F(0,t))$

(That is, p(t) is the temporal shape of the pulse normalised to its maximum value.)

Also, we have the relation

$$\kappa = \frac{K}{\rho c}$$

where K = the thermal conductivity (in W/mK)

Using these two relations, we obtain

(44) $T_{\text{noninst. Gauss. area source}}(r,z,t) =$

$$= \frac{\varepsilon F_{max} a^2}{2K} \left[\frac{\kappa}{\pi}\right]^{\frac{1}{2}} * \int_0^t \left[\frac{p(t')}{(t-t')^{\frac{1}{2}} * \left[4\kappa(t-t') + a^2 \right]} * \right.$$

$$\left. * \exp\left[- \frac{z^2}{4\kappa(t-t')} - \frac{r^2}{4\kappa(t-t') + a^2} \right] \right] dt'$$

$$= (\text{ with } t'' = t-t') =$$

$$= \frac{\varepsilon F_{max} a^2}{2K} \left[\frac{\kappa}{\pi}\right]^{\frac{1}{2}} * \int_0^t \left[\frac{p(t-t'')}{(t'')^{\frac{1}{2}} * \left[4\kappa t'' + a^2 \right]} * \right.$$

$$\left. * \exp\left[- \frac{z^2}{4\kappa t''} - \frac{r^2}{4\kappa t'' + a^2} \right] \right] dt''$$

This expression is only valid for an infinite medium, however. To make it valid for a semi-infinite medium, we simply multiply by two.

The explanation is as follows. Assume that a surface in an infinite medium continuously produces the energy Q_0. This energy is divided into two parts, which flow in different directions, forming a symmetrical temperature distribution around the surface. (See Fig. 26a.)

If we "remove" half of the infinite medium, the energy Q_0 just has one way to flow. (We assume no loss by radiation.) This means that the temperature doubles in this direction. (See Fig. 26b.)

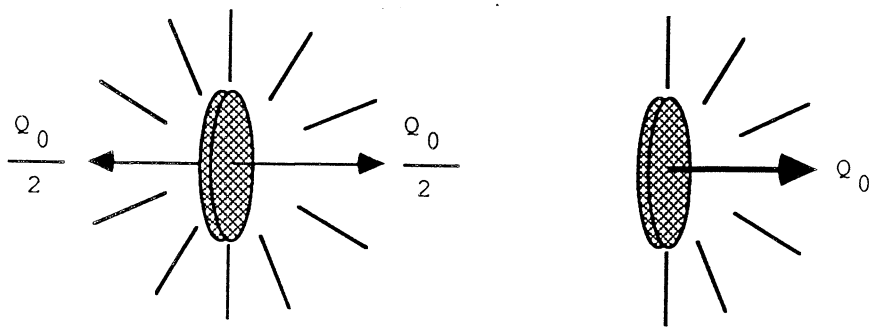

Fig. 26a. and Fig. 26b. A surface source in an infinite medium and in a finite medium, respectively.

Introducing dimensionless variables

$$\tau = \frac{4\kappa t}{a^2}$$

$$\tau'' = \frac{4\kappa t''}{a^2}$$

$$\kappa = \frac{r}{a}$$

$$\upsilon = \frac{z}{a}$$

$$\Phi = \frac{2K\pi^{\frac{1}{2}}\, T}{\varepsilon a F_{max}}$$

and multiplying by 2 (semi-infinite medium), (44) turns to

$$(45) \qquad \Phi(\kappa,\upsilon,\tau) = \int_0^{\tau} \left[\frac{p(\tau-\tau'')}{(\tau'')^{\frac{1}{2}}\,(\tau''+1)} * \exp\left[-\frac{\kappa^2}{(\tau''+1)} - \frac{\upsilon^2}{\tau''} \right] \right] d\tau''$$

For a cw (continuous-wave) laser $p(\tau-\tau'')=1$ and $F_{max} = F_0$. We get

$$(46) \qquad \Phi_{cw}(\kappa,\upsilon,\tau) = \int_0^{\tau} \frac{\exp\left[-\frac{\kappa^2}{(\tau''+1)} - \frac{\upsilon^2}{\tau''} \right]}{(\tau'')^{\frac{1}{2}}\,(\tau''+1)} * d\tau''$$

The temperature at the centre of the focal spot is:

$$(47) \qquad \Phi_{\text{cw centre}}(0,0,\tau) = \int_0^{\tau} \frac{d\tau''}{(\tau'')^{\frac{1}{2}}\,(\tau''+1)} = 2\arctan(\tau^{\frac{1}{2}})$$

That is

$$(48) \qquad T_{\text{cw centre}}(0,0,t) = \frac{\varepsilon F_0 a}{K(\pi)^{\frac{1}{2}}} \arctan\left[\frac{4\kappa t}{a^2}\right]$$

Assuming steady state ($t \to \infty$), we finally get

$$(49) \qquad T_{\text{cw centre steady state}} = \frac{\varepsilon F_0 a \pi^{\frac{1}{2}}}{2K}$$

More extensive calculations have been made by Brugger [35] and Bechtel [36]. Bechtel also compares surface generation of heat (that is, the situation when the absorption coefficient is infinite) with volume generation of heat (where the absorption coefficient is not infinite).

Note that since the depth heated by a pulse of duration t is $\approx (\kappa t)^{\frac{1}{2}}$ the results may be used for a solid of finite thickness, if the thickness is several times larger than the heated depth. Furthermore, if the Gaussian beam radius a is about as large as the depth heated, the surface of the sheet removed from the focal area will not be heated significantly during the laser pulse. The results can therefore be used to estimate the temperature rise in sheets of finite lateral extension, provided the above condition is satisfied.

2. A thin slab irradiated by a Gaussian beam

Configuration, see Fig. 27.

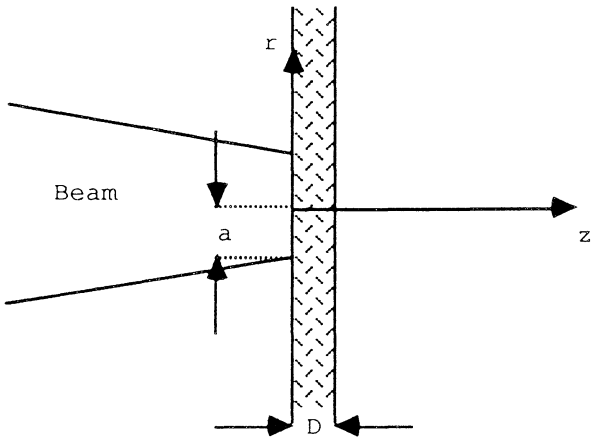

Fig. 27. A thin sheet of thickness D irradiated by a Gaussian laser beam.

We assume uniform thermal conductivity and a surface source (that is, the absorption coefficient of the material is infinite). The slab is thermally thin, that is

$$(50) \qquad \frac{D^2}{4\kappa t} << 1$$

where D = the thickness of the slab (in m)
κ = the thermal diffusivity (m^2/s)

(This implies that during the time duration of the laser pulse the back surface of the sheet reaches approximately the same temperature as the front surface (where the radiation is incident)).

We include losses by convection into a medium at zero temperature.

The beam has a Gaussian shape

$$(51) \qquad F = F_0 \exp\left[-\frac{r^2}{a^2} \right]$$

where F = the intensity at the surface (in W/m^2)
F_0 = the intensity at the centre of the irradiated spot

Ready, and Duley [37] are again used. Carslaw and Jaeger [38] give the partial differential equation of heat conduction for an instantaneous point source in a thin sheet as

(52) $$\frac{\partial^2 T}{\partial x^2} + \frac{\partial^2 T}{\partial y^2} - k^2 T = 0 \qquad \text{(in the rectangular coordinate system)}$$

where $k^2 = \frac{2H}{KD}$

where H = the surface coductance (in W/m^2K)
K = the thermal conductivity (W/mK)

The solution is given [39] as

(53) $$T_{\text{inst. point source}}(x,y,z,k^2) = \frac{Q}{4\pi KDt} *$$

$$* \exp\left[- \kappa k^2 t - \left[\frac{(x-x')^2 + (y-y')^2}{4\kappa t} \right] \right]$$

where Q = the quantity of energy liberated at t=0 at a point (x',y',0) (in J)

We use the trick mentioned before (page 32) to make the expression valid for a noninstantaneous Gaussian surface source.

Using pages 32 - 34, we find an expression for an instantaneous circular source of radius r' at z'=0

(54) $$T_{\text{inst. ring source}}(r,t,k^2) =$$

$$= \int_0^{2\pi} \left(\frac{Q'r'}{4\pi KDt} * \exp\left[-\kappa k^2 t\right] * \right.$$

$$\left. * \exp\left[- \left[\frac{r'^2 + r^2 - 2rr'\cos(\theta-\theta')}{4\kappa t} \right] \right] \right) d\theta' =$$

$$= \left[\text{with } Q' = \frac{Q}{2\pi r'} \right] = \frac{Q}{8\pi^2 KDt} * \exp\left[-\kappa k^2 t\right] *$$

$$* \exp\left[- \left[\frac{r^2 + r'^2}{4\kappa t} \right] \right] * \int_0^{2\pi} \exp\left[\frac{2rr'\cos(\theta-\theta')}{4\kappa t} \right] d\theta'$$

Further, we obtain

(55) $$T_{\text{inst. ring source}}(r,t,k^2) =$$

$$= \frac{Q}{4\pi KDt} * \exp\left[- \kappa k^2 t - \left[\frac{r^2 + r'^2}{4\kappa t} \right] \right] * I_0\left[\frac{rr'}{2\kappa t} \right]$$

where I_0 = the modified Bessel function of order zero

In order to get the total energy liberated over the whole area by a Gaussian surface source, we use the method described previously, replacing Q in (55) with (34) and then integrating r'. We get the integral as

(56) $$T_{\text{inst. Gaussian area source}}(r,t,k^2) =$$

$$= \frac{Q''}{2KDt} * \exp\left[- \kappa k^2 t - \frac{r^2}{4\kappa t} \right] *$$

$$* \int_0^{\infty} \left[\exp\left[-r'^2 \left[\frac{1}{4\kappa t} + \frac{1}{a^2} \right] \right] * I_0\left[\frac{rr'}{2\kappa t} \right] \right] r'dr'$$

The integral is now evaluated the same way as on pages 35 - 36. The result is

(57) $$T_{\text{inst. Gaussian area source}}(r,t,k^2) =$$

$$= \frac{\kappa a^2 Q''}{KD\left[4\kappa t + a^2\right]} * \exp\left[- \kappa k^2 t - \frac{r^2}{4\kappa t + a^2} \right]$$

For a source that has a duration in time we must integrate.

Set

(58) $$Q'' = \varepsilon F(0,t')dt'$$

where $\varepsilon F(0,t)$ = the absorbed power per unit area (in W/m^2)

We obtain

$$(59)\qquad T_{\text{noninst. Gauss. area source}}(r,t,k^2)=$$

$$= \int_0^t \left[\frac{\kappa a^2 \varepsilon F(0,t')}{KD\left[\, 4\kappa(t-t') + a^2 \,\right]} * \right.$$

$$\left. * \exp\left[- \kappa k^2 (t-t') - \frac{r^2}{4\kappa(t-t') + a^2} \right] \right] dt'$$

(For a discussion about the integration of t', see page 37.)

Set

$$(43)\qquad p(t)= \frac{F(0,t)}{F_{max}}$$

where $F_{max} = \max (F(0,t))$

(That is, p(t) is the temporal shape of the pulse normalised to its maximum value.) It gives

$$(60)\qquad T_{\text{noninst. Gauss. area source}}(r,t,k^2)=$$

$$= \frac{\varepsilon F_{max} \kappa a^2}{KD} * \int_0^t \left[\frac{p(0,t')}{\left[\, 4\kappa(t-t') + a^2 \,\right]} * \right.$$

$$\left. * \exp\left[- \kappa k^2 (t-t') - \frac{r^2}{4\kappa(t-t') + a^2} \right] \right] dt'$$

$$= \text{(with } t''=t-t' \text{) =}$$

$$= \frac{\varepsilon F_{max} \kappa a^2}{KD} * \int_0^t \left[\frac{p(0,t-t'')}{\left[\, 4\kappa t'' + a^2 \,\right]} * \right.$$

$$\left. * \exp\left[- \kappa k^2 t'' - \frac{r^2}{4\kappa t'' + a^2} \right] \right] dt''$$

Introduce dimensionless variables

$$\tau = \frac{4\kappa t}{a^2}$$

$$\tau'' = \frac{4\kappa t''}{a^2}$$

$$\kappa = \frac{r}{a}$$

$$\zeta = \frac{k^2 a^2}{4}$$

$$\theta(\kappa,\tau,\zeta) = \frac{4KD}{\varepsilon a^2 F_{max}} T(r,t,k^2)$$

(60) becomes

$$(61) \qquad \theta(\kappa,\tau,\zeta) = \int_0^{\tau} \frac{p(\tau-\tau'')d\tau''}{\tau'' + 1} * \exp\left[- \zeta\tau'' - \frac{\kappa^2}{(\tau'' + 1)}\right]$$

For a cw (continuous-wave) laser $p(\tau-\tau'')=1$ and $F_{max} = F_0$. (61) becomes

$$(62) \qquad \theta_{cw}(\kappa,\tau,\zeta) = \int_0^{\tau} \frac{d\tau''}{\tau'' + 1} * \exp\left[- \zeta\tau'' - \frac{\kappa^2}{(\tau'' + 1)}\right]$$

The temperature at the centre of the spot is

$$(63) \qquad \theta_{cw\ centre}(0,\tau,\zeta) = \int_0^{\tau} \frac{d\tau''}{\tau'' + 1} * \exp(-\zeta\tau'')$$

This expression has to be solved numerically, if a solution is required. If we assume the convection losses to be zero (k=0), we get

$$(64) \qquad \theta_{cw\ centre\ no\ conv.}(0,\tau,0) = \int_0^{\tau} \frac{d\tau''}{\tau'' + 1} = \ln(\tau + 1)$$

That is

$$(65) \qquad T_{cw\ centre\ no\ conv.} = \frac{\varepsilon F_0 a^2}{4KD} * \ln\left[1 + \frac{4\kappa t}{a^2}\right]$$

However, we soon realize that (65) is not suitable for a steady-state approximation, since T → infinity when t → infinity.
But we can use (63) instead. [40] gives

$$(66) \qquad \theta_{\text{cw centre}}(0,\tau,\zeta) = \int_0^{\tau} \frac{d\tau''}{\tau'' + 1} * \exp(-\zeta\tau'') = -\exp(-\zeta)*Ei(-\zeta)$$

where Ei is an exponential integral function.

Furthermore, we have [41]

$$(67) \qquad -\exp(-\zeta)*Ei(-\zeta) = -\exp(-\zeta)\left[C + \ln(\zeta) + \int_0^{\zeta} \frac{\exp(-t) - 1}{t}\, dt \right]$$

where C = 0.5772 (Euler's constant)

Now, assuming that ζ is small

$$(68) \qquad \int_0^{\zeta} \frac{\exp(-t) - 1}{t}\, dt \approx 0$$

and

$$(69) \qquad \exp(-\zeta) \approx 1$$

We get

$$(70) \qquad \theta_{\text{cw centre steady state}}(0,\tau,\zeta) \approx - C - \ln(\zeta)$$

for small ζ.

Or, in the original variables

$$(71) \qquad T_{\text{cw centre steady state}}(0,t,k^2) \approx - C - \ln\left[\frac{k^2 a^2}{4} \right]$$

where C = 0.5772 (Euler's constant)

More extensive calculations for different cases of heating of a sheet have been performed by Brugger [42].

3. A thin film on a semi-infinite substrate irradiated by a Gaussian laser beam

Configuration, see Fig. 28.

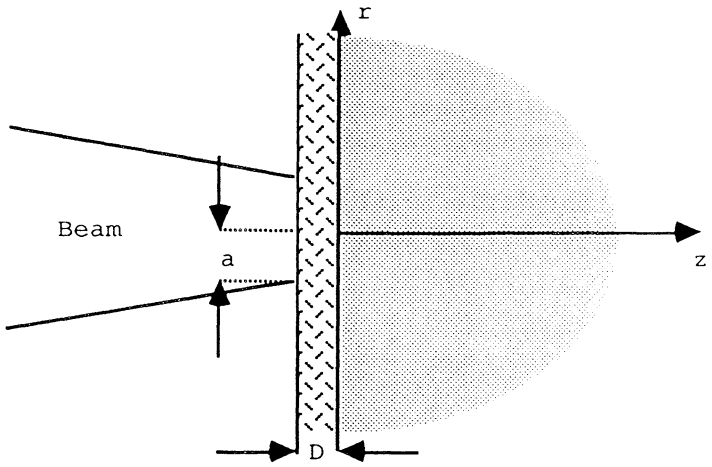

Fig. 28. Irradiated sheet on a semi-infinite substrate.

We assume uniform thermal conductivity. We also assume that the transmitted light is completely absorbed in the film (that is, all the heat is generated in the film (or, if we want to use the absorption coeffecient α, $1/\alpha < D$)).

Finally, we assume that both surfaces of the film have the same temperature. This assumption can be expressed as

$$\frac{D^2}{4\kappa t} << 1 \qquad (72)$$

where D = the thickness of the film (in m)
κ = the thermal diffusivity of the film (in m^2/s)
t = (here) the length of the laser pulse (in s)

We follow a solution obtained by Peak and Kestenbaum [43].

The beam has a Gaussian shape

$$F = F_0 \exp\left[-\frac{r^2}{a^2} \right] \qquad (73)$$

where F = the intensity at the surface (in W/m^2)
F_0 = the intensity at the centre of the irradiated spot
a = the beam radius at the surface (in m)

εF is absorbed within the film where ε is the absorbtion (in percent)

The general differential equation of heat conduction is (see page 28)

$$(74) \qquad \nabla^2 T + \frac{g}{K} = \frac{1}{\kappa} \frac{\partial T}{\partial t}$$

where T = the temperature (in K)
g = the source term (that is, the heat generated per unit time and volume) (in W/m^3)
K = the thermal conductivity (in W/mK)
κ = the thermal diffusivity (in m^2/s)

In order to get the differential equation for the film (index 1) and the substrate (index 2), we look at a small volume (see Fig. 29).

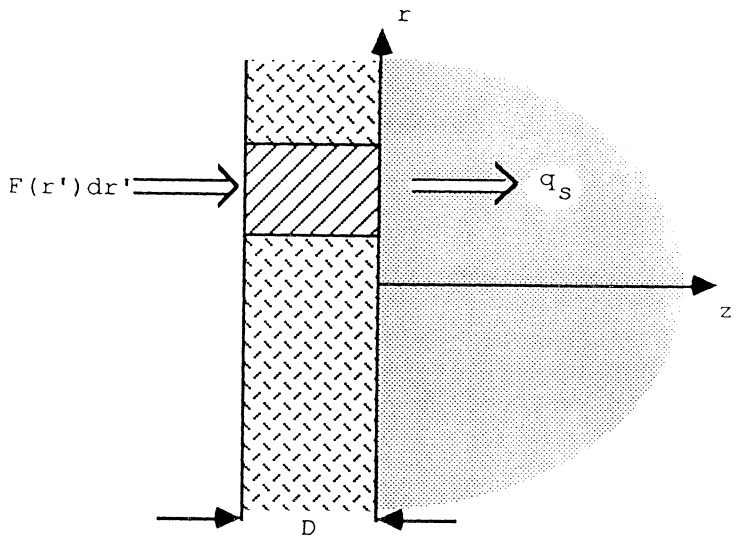

Fig. 29. A small volume.

The differential equations for the film and the substrate are

$$(75) \qquad \nabla^2 T_1 + \frac{g_1}{K_1} = \frac{1}{\kappa_1} \frac{\partial T_1}{\partial t}$$

and

$$(76) \qquad \nabla^2 T_2 + \frac{g_2}{K_2} = \frac{1}{\kappa_2} \frac{\partial T_2}{\partial t}$$

Since we use cylindrical coordinates, and z=0 for the film, we get, by definition

$$(77) \qquad \nabla^2 T_1 = \frac{\partial^2 T_1}{\partial r^2} + \frac{1}{r} \frac{\partial T_1}{\partial r}$$

and

$$(78) \qquad \nabla^2 T_2 = \frac{\partial^2 T_2}{\partial r^2} + \frac{1}{r} \frac{\partial T_2}{\partial r} + \frac{\partial^2 T_2}{\partial z^2}$$

To evaluate g_1, we look at Fig. 29. and understand that

$$(79) \qquad g_1 = \frac{\varepsilon F(r) - q_s}{D}$$

where $\varepsilon F(r)$ = the total incoming flux minus the flux reflected from the first surface of the film (in W/m^2)

q_s = the heat flux transmitted to the substrate (in W/m^2)

We have, by definition

$$(80) \qquad q_s = -K_2 * \left.\frac{\partial T_2}{\partial z}\right|_{z=0}$$

Substituting (73) and (80) into (79) gives

$$(81) \qquad g_1 = \frac{\varepsilon F_0}{D} \exp\left[-\frac{r^2}{a^2}\right] + \frac{K_2}{D} * \left.\frac{\partial T_2}{\partial z}\right|_{z=0}$$

The assumptions we made give us $g_2=0$.

Substituting the values of g_1 and g_2 into (75) and (76), and then using (77) and (78), we arrive at two differential equations for heat conduction, one for the film and one for the substrate:

$$(82) \qquad \frac{1}{\kappa_1}\frac{\partial T_1}{\partial t} = \frac{\partial^2 T_1}{\partial r^2} + \frac{1}{r}\frac{\partial T_1}{\partial r} + \frac{\varepsilon F_0}{DK_1}\exp\left[-\frac{r^2}{a^2}\right] + \frac{K_2}{DK_1} * \left.\frac{\partial T_2}{\partial z}\right|_{z=0}$$

and

$$(83) \qquad \frac{\partial T_2}{\partial t} = \kappa_2 * \left[\frac{\partial^2 T_2}{\partial r^2} + \frac{1}{r}\frac{\partial T_2}{\partial r} + \frac{\partial^2 T_2}{\partial z^2}\right]$$

The boundary conditions for the film are

$$\frac{\partial T_1}{\partial r} = 0 \qquad \text{at } r = 0$$

$$(84) \qquad T_1 = 0 \qquad \text{at } r \to \infty$$

$$T_1 = 0 \qquad \text{at } t = 0$$

and for the substrate

$$T_2 = T_1(t,r) \qquad \text{at } r = 0$$

$$T_2 = 0 \qquad \text{at } z \to \infty \tag{85}$$

$$T_2 = 0 \qquad \text{at } \tau = 0$$

Now we introduce dimensionless variables

$$\theta_1 = \frac{T_1}{T_v} \qquad \theta_2 = \frac{T_2}{T_v} \qquad \tau = \frac{K_1 t}{D^2}$$

$$\xi = \frac{r}{a} \qquad Z = \frac{z}{D} \tag{86}$$

$$\beta = \frac{K_2}{K_1} \qquad \sigma = \frac{K_2}{K_1}$$

$$\Lambda = \frac{\varepsilon F_0 D}{K_1 T_v} \qquad \Xi = \frac{D^2}{a^2}$$

where T_v is the vaporization temperature of the film (in K)

(82) and (83) become

$$\frac{\partial \theta_1}{\partial \tau} = \Xi \left[\frac{\partial^2 \theta_1}{\partial \xi^2} + \frac{1}{\xi} \frac{\partial \theta_1}{\partial \xi} \right] + \beta \left. \frac{\partial \theta_2}{\partial Z} \right|_{Z=0} + \Lambda \exp(-\xi^2) \tag{87}$$

and

$$\frac{\partial \theta_2}{\partial \tau} = \sigma \left[\Xi \left[\frac{\partial^2 \theta_2}{\partial \xi^2} + \frac{1}{\xi} \frac{\partial \theta_2}{\partial \xi} \right] + \frac{\partial^2 \theta_2}{\partial Z^2} \right] \tag{88}$$

respectively, with the boundary conditions

$$\frac{\partial \theta_1}{\partial \xi} = 0 \qquad \text{at } \xi = 0$$

$$\theta_1 = 0 \qquad \text{at } \xi \to \infty$$

$$\theta_1 = \theta_2 = 0 \qquad \text{at } \tau = 0 \tag{89}$$

$$\theta_2 = \theta_1(\tau,\xi) \qquad \text{at } Z = 0$$

$$\theta_2 = 0 \qquad \text{at } Z \to \infty$$

The solutions θ_1 and θ_2 are expanded in terms of the perturbation parameter Ξ.

$$(90) \qquad \theta_1 = \exp(-\xi^2)\mu_{11}(\tau) + \Xi\theta_{12} + \Xi^2\theta_{13} + \ldots$$

and

$$(91) \qquad \theta_2 = \exp(-\xi^2)\mu_{21}(\tau,Z) + \Xi\theta_{22} + \Xi^2\theta_{23} + \ldots$$

where θ_{1i} = the i:th-order perturbed solution of θ_1

θ_{2i} = the i:th-order perturbed solution of θ_2

μ_{ij} = the j:th order nonradial solution in the film or substrate

As can be seen in (87) and (88), the perturbation parameter multiplies the conduction terms in the radial direction, and thus the conduction effect does not contribute to the first-order solution, but to solutions of higher orders. Thus it can be concluded that the Gaussian factor will be included in the first-order solution. We get

$$(92) \qquad \theta_{11} = \exp(-\xi^2)\mu_{11}(\tau)$$

and

$$(93) \qquad \theta_{21} = \exp(-\xi^2)\mu_{21}(\tau,Z)$$

Now, if we take θ_{11} and θ_{21} and put them into (87) and (88), respectively, we will get two equations by collecting the terms of the first order. We obtain

$$(94) \qquad \frac{\partial\mu_{11}}{\partial\tau} = \beta \left.\frac{\partial\mu_{21}}{\partial Z}\right|_{Z=0} + \Lambda$$

and

$$(95) \qquad \frac{\partial\mu_{21}}{\partial\tau} = \sigma \frac{\partial^2\mu_{21}}{\partial Z^2}$$

Since μ_{11} is a function of τ only, (94) and (95) show that

$$\left.\frac{\partial\mu_{21}}{\partial Z}\right|_{Z=0}$$

is only a function of τ.

Let us define $f_1(\tau)$ as

$$(96) \qquad f_1(\tau) = \left.\frac{\partial \mu_{21}}{\partial Z}\right|_{Z=0}$$

Now, solve (94) and (95). (94) is easy. We obtain

$$(97) \qquad \mu_{11}(\tau) = \beta \int_0^\tau f_1(\tau')d\tau' + \Lambda\tau$$

(95) is more complicated. The solution can be found in appendix 1.

Summary: We get the solution of (94) as

$$(98) \qquad \mu_{11} = \beta \int_0^\tau f_1(\tau')d\tau' + \Lambda\tau$$

and the solution of (95) as

$$(99) \qquad \mu_{21}(\tau,Z) = \frac{Z}{2(\pi\sigma)^{\frac{1}{2}}} * \int_0^\tau \frac{\mu_{11}(\tau')}{(\tau-\tau')^{\frac{3}{2}}} \exp\left[- \frac{Z^2}{4\sigma(\tau-\tau')} \right] d\tau'$$

The next step in order to obtain the complete solution is to evaluate $f_1(\tau)$. We put this evaluation in appendix 2.

We get the result

$$(100) \qquad f_1(\tau) = - \frac{\Lambda}{\beta} \left[1 - \frac{1}{1 + \tau^{\frac{1}{2}} \left[\frac{2\beta}{(\sigma\pi)^{\frac{1}{2}}} \right]} \right]$$

In order to solve (98) we have to integrate (100).

Let $\Gamma = \dfrac{2\beta}{(\sigma\pi)^{\frac{1}{2}}}$ and let $\gamma = \Gamma\tau^{\frac{1}{2}}$

Then

$$(101) \qquad \int \frac{1}{1 + \Gamma\tau^{\frac{1}{2}}} d\tau = \frac{2}{\Gamma^2} \int \frac{\gamma}{1+\gamma} d\gamma = \frac{2}{\Gamma^2}\gamma - \frac{2}{\Gamma^2} \ln(1+\gamma) + G$$

$$= \frac{2}{\Gamma} \tau^{\frac{1}{2}} - \frac{2}{\Gamma^2} \ln(1 + \Gamma\tau^{\frac{1}{2}}) + G$$

where G is a constant

We get

$$(102)\quad \int_0^{\tau} f_1(\tau')d\tau' = -\frac{\Lambda}{\beta}\tau + \frac{(\sigma\pi)^{\frac{1}{2}}}{\beta^2}\Lambda\tau^{\frac{1}{2}} - \frac{\sigma\pi\Lambda}{2\beta^3}\ln\left[1 + \frac{2\beta}{(\pi\sigma)^{\frac{1}{2}}}\tau^{\frac{1}{2}}\right] + \frac{G\Lambda}{\beta}$$

This gives, according to (98)

$$(103)\quad \mu_{11}(\tau) = \beta\int_0^{\tau} f_1(\tau')d\tau' + \Lambda\tau =$$

$$= \frac{(\sigma\pi)^{\frac{1}{2}}}{\beta}\Lambda\tau^{\frac{1}{2}} - \frac{\sigma\pi\Lambda}{2\beta^2} * \ln\left[1 + \frac{2\beta}{(\pi\sigma)^{\frac{1}{2}}}\tau^{\frac{1}{2}}\right] + \Lambda G$$

Since $\mu_{11}(0) = 0$, then $G = 0$. We put this into (92) and finally obtain the first-order perturbed solution for the temperature rise in the film as

$$(104)\quad \theta_{11}(\tau,\xi) = \exp(-\xi^2)\left[\frac{(\sigma\pi)^{\frac{1}{2}}}{\beta}\Lambda\tau^{\frac{1}{2}} - \frac{\sigma\pi\Lambda}{2\beta^2} * \ln\left[1 + \frac{2\beta}{(\pi\sigma)^{\frac{1}{2}}}\tau^{\frac{1}{2}}\right]\right]$$

Going back to the original variables, we get

$$(105)\quad T_1 = \exp\left[\frac{-r^2}{a^2}\right] * \left[\frac{\varepsilon F_0 (\pi\kappa_2)^{\frac{1}{2}}}{K_2}t^{\frac{1}{2}} - \right.$$

$$\left. - \frac{\varepsilon F_0 \pi K_1 \kappa_2 D}{2K_2^2 \kappa_1} * \ln\left[1 + \frac{2K_2\kappa_1}{K_1 D(\pi\kappa_2)^{\frac{1}{2}}}t^{\frac{1}{2}}\right]\right]$$

where index 1 stands for the film
index 2 stands for the substrate
and

- r = the radial coordinate (in m)
- a = the beam radius (in m)
- εF_0 = the absorbed part of the intensity at the centre of the irradiated spot (in W/m^2)
- K = the thermal conductivity (in W/mK)
- κ = the thermal diffusivity (in m^2/s)
- t = the time (in s)
- D = the thickness of the film (in m)

As mentioned before, this solution does not take into account the radial heat conduction in the film. This conduction becomes important when we are using longer pulses (μs). Since this can be the case, we will also derive the second-order solution (which is always negative). We do this in appendix 3.

The result is

$$(106)\quad \theta_{12}(\tau,\xi) = \tfrac{1}{4}(\xi^2 - 1)\exp(-\xi^2)\left[\int_0^{\tau} \mu_{11}(\tau'')d\tau'' + \right.$$

$$+ \beta\int_0^{\tau}\left[\frac{1}{\left(1 + 2\beta\left[\frac{\tau''}{\sigma\pi}\right]^{\frac{1}{2}}\right)} *\right.$$

$$* \left[\frac{-2}{(\sigma\pi)^{\frac{1}{2}}}(\tau''^{\frac{1}{2}})\mu_{11}(\tau'') + \left[\frac{\sigma}{\pi}\right]^{\frac{1}{2}}\int_0^{\tau''}\left[\mu_{11}(\tau') *\right.\right.$$

$$\left.\left.\left.\left.* \left[\frac{1}{(\tau''-\tau')^{\frac{1}{2}}} - \frac{1}{\tau''^{\frac{1}{2}}}\right]\right]d\tau'\right]\right]d\tau''\right]$$

where, from (103)

$$(107)\quad \mu_{11} = \frac{(\sigma\tau)^{\frac{1}{2}}}{\beta}\Lambda\tau^{\frac{1}{2}} - \frac{\sigma\pi\Lambda}{2\beta^2} * \ln\left[1 + \frac{2\beta}{(\pi\sigma)^{\frac{1}{2}}}\tau^{\frac{1}{2}}\right]$$

4. A multilayer solution

Configuration, see Fig. 30.

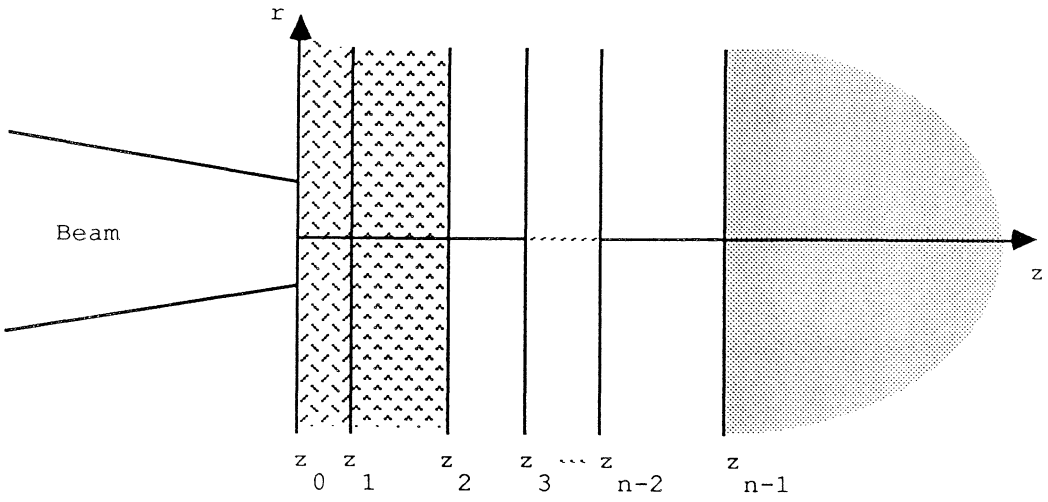

Fig. 30. Irradiated multilayer structure.

We follow the solution obtained by I. D. Calder and R. Sue [44].

We assume steady state and no heat loss at the top and bottom surfaces. The layers are homogeneous and infinite in the plane. The substrate is infinitely thick. The most correct result is obtained if all layers are assumed to have thermal conductivities of the same temperature dependence.

For each layer i we have:

$z_i - z_{i-1}$ = the thickness of layer i (in m)

K_i = the thermal conductivity of layer i (in W/mK)

$N_i = n_i(1+j^{e_i})$ = the complex index of refraction of layer i

$T_i(r,z)$ = the required temperature rise of layer i (in K)

The beam is circular, having a radial intensity distribution

$$f(r) = \frac{P(r)}{P(0)} \tag{108}$$

where P(r) = the power of the beam
P(0) = the incident power of the beam

The effective beam width can be defined by

$$(109) \quad w = \left[2 \int_0^\infty f(r) r dr \right]^{\frac{1}{2}}$$

The assumption of no heat loss at the top and bottom surfaces can be expressed as

$$(110) \quad \left. \frac{\partial T_1}{\partial z} \right|_{z=0} = \left. \frac{\partial T_n}{\partial z} \right|_{z=\infty} = 0$$

At the interfaces between layers, the temperature and the heat flow must be continuous functions of position. Therefore

$$(111) \quad T_i(z_i) = T_{i+1}(z_i)$$

and

$$(112) \quad K_i \left. \frac{\partial T_i}{\partial z} \right|_{z_i} = K_{i+1} \left. \frac{\partial T_{i+1}}{\partial z} \right|_{z_i}$$

Calder and Sue showed that the only way to allow for a temperature-dependent K and at the same time preserve the boundary condition

$$(113) \quad T_i = T_{i+1}$$

was to assume that all thermal conductivities have the same temperature dependence, that is

$$(114) \quad K_i(T) = c_i K_i(T)$$

where c_i is a constant

With the help of Born and Wolf [45] the normalised power transmitted at any depth z in layer i can be expressed as

$$(115) \quad P_i = n_i \frac{\mu_0}{\mu_i} * \frac{\left|E_i(z)\right|^2}{E_0^2}$$

where n_i = the index of refraction of layer i

$\frac{\mu_0}{\mu_i}$ = the relative magnetic permeabiltiy of layer i

$E_i(z)$ = the electric field in layer i

E_0 = the incident electric field

Making the approximation that $\frac{\partial P_i(z)}{\partial z}$ decreases exponentially with depth in an absorbing film, we define an effective intensity attenuation coeffecient of layer i as

$$(116) \quad \alpha_i = \frac{\ln\left[\frac{P_i(z_{i-1})}{P_i(z_i)}\right]}{z_i - z_{i-1}}$$

The heat generation function can now be written as (with $P_i(z_{i-1}) = P_i$)

$$(117) \quad g_i(r,z) = \frac{\partial P_i(z)}{\partial z} * \frac{f(r)}{\pi w^2} = \frac{P_i \alpha_i \exp(-\alpha_i(z_i - z_{i-1}))\, f(r)}{\pi w^2}$$

In order to find the solution, we define a set of dimensionless variables

$$W_i = \alpha_i w$$

$$R = \frac{r}{w}$$

$$Z = \frac{z}{w}$$

$$Z_i = \frac{z_i}{w}$$

Following the procedure outlined by Lax [46]

$$(118)\quad T_i(r,z) = \int_0^\infty \left[G_i(\lambda)\exp(-\lambda Z) + H_i(\lambda)\exp(\lambda Z) - B_i W_i F(\lambda)\exp(-W_i Z)\right] * \frac{J_0(\lambda R)\lambda d\lambda}{W_i^2 - \lambda^2}$$

where J_0 = the Bessel function of order 0

$F(\lambda)$ = the Bessel transform of $f(R)$,

$$F(\lambda) = \int_0^\infty f(R)J_0(\lambda R)RdR$$

B_i = a temperature coeffecient defined by

$$B_i = \frac{P_i K_1 \exp(W_i Z_{i-1})}{2\pi K_i^2 F(0) w}$$

G_i = a function determinated by the boundary condition

H_i = " -

Let us define new parameters

$$k_i = \frac{K_i \lambda}{W_i^2 - \lambda^2}$$

$$r_i = \exp(\lambda Z_i)$$

and

$$b_i = \begin{cases} \left[k_{i-1}B_{i-1} * W_{i-1}^2 \exp(-W_{i-1}Z_{i-1}) - k_i B_i * W_i^2 \exp(-W_i Z_{i-1})\right] * \frac{F(\lambda)}{\lambda} & 1 \le i \le n \\ \left[k_{i-n}B_{i-n}W_{i-n}\exp(-W_{i-n}Z_{i-n}) - k_{i-n+1}B_{i-n+1}W_{i-n+1} * \exp(-W_{i-n+1}Z_{i-n}) * \frac{K_{i-n}}{K_{i-n+1}}\right] & n+1 \le i \le 2n \end{cases}$$

with $W_0 = W_{n+1} = 0$

The boundary conditions (110) - (112) applied to these formulas will result in 2n linear equations in the 2n variables G_i (i=1...n) and H_i (i=1...n) [47].

These equations will, together with equation (118), give the solution. Calder and Sue have partially solved the equations and have obtained a reduction to n-1 linear equations in $H_1 \ldots H_{n-1}$ (H_n=0), giving

$$(119) \qquad \sum_{j=1}^{n-1} a_{ij} H_j = b_i^*$$

where

$$a_{ii} = k_i \left[\left(1 + \frac{K_i}{K_{i+1}}\right) * r_i^2 + \left(1 - \frac{K_i}{K_{i+1}}\right) * r_{i-1}^2 \right]$$

$$a_{i,i+1} = -2k_{i+1} r_i^2 \frac{K_i}{K_{i+1}}$$

$$a_{ij} = 0 \qquad j>i+1$$

$$a_{ij} = k_j (r_{j-1}^2 - r_j^2)\left(1 - \frac{K_i}{K_{i+1}}\right) \qquad j<i$$

and

$$b_i^* = \left(b_{n+i} - b_{i+1} \frac{K_i}{K_{i+1}}\right) r_i + \left(1 - \frac{K_i}{k_{i+1}}\right) * \sum_{k=1}^{i} b_k r_{k-1}$$

Then

$$(120) \qquad G_i = k_i^{-1} * \sum_{j=1}^{i} \left[k_j H_j (r_j^2 - r_j^2) - b_j r_{j-1} \right] + H_i r_i^2$$

once the H_i are known.

This solution is amenable to numerical computation. Suggestions for flow charts for a computer program based on the presented equations are given on the following pages.

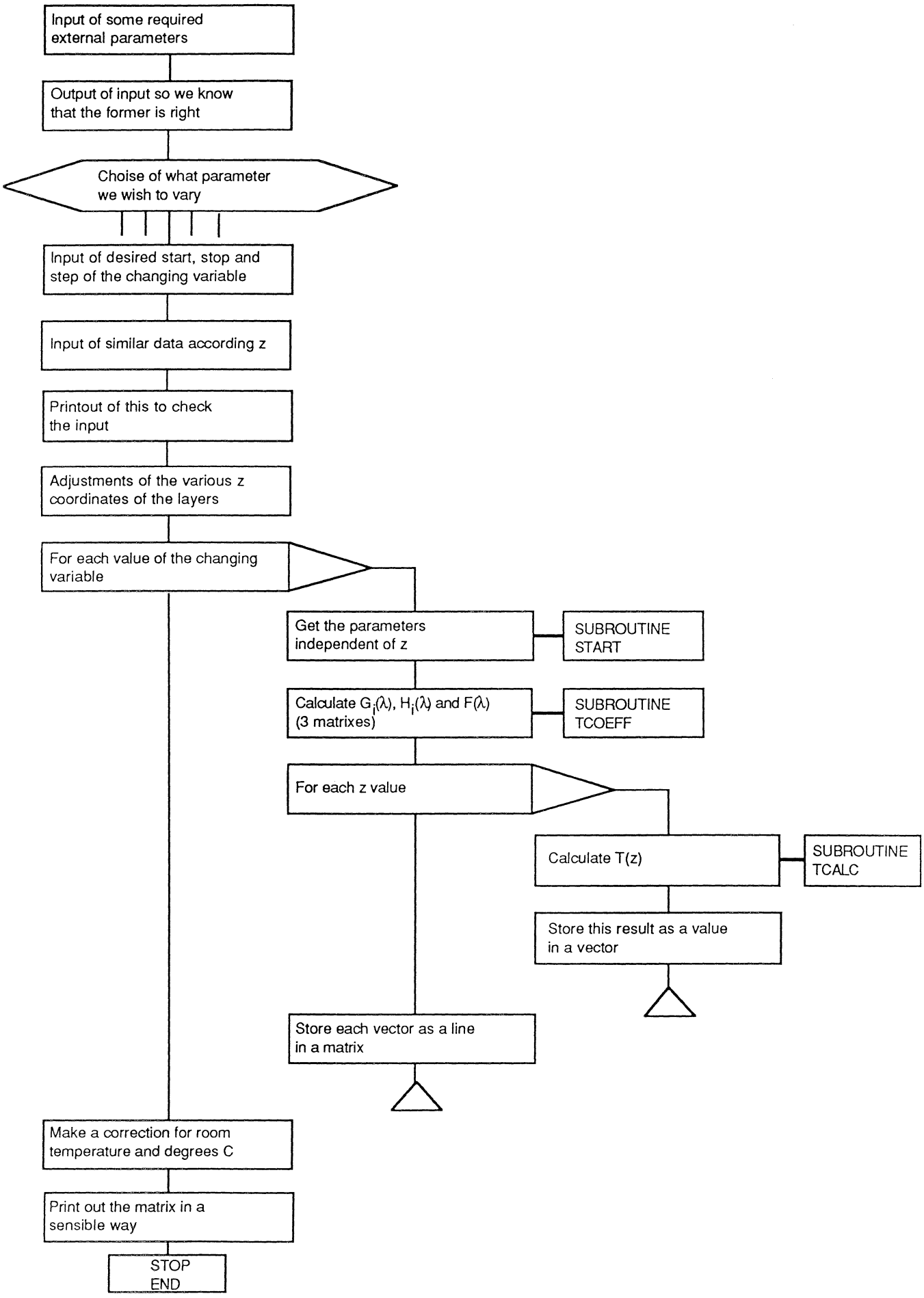

Fig. 31. Main program.

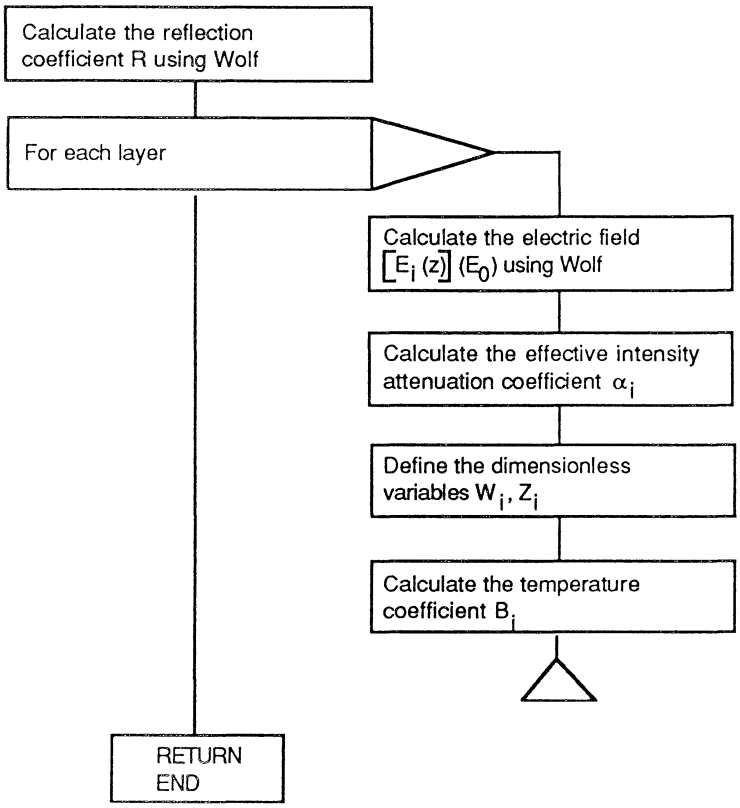

Fig. 32. Subroutine START. Calculation of parameters independent of lambda.

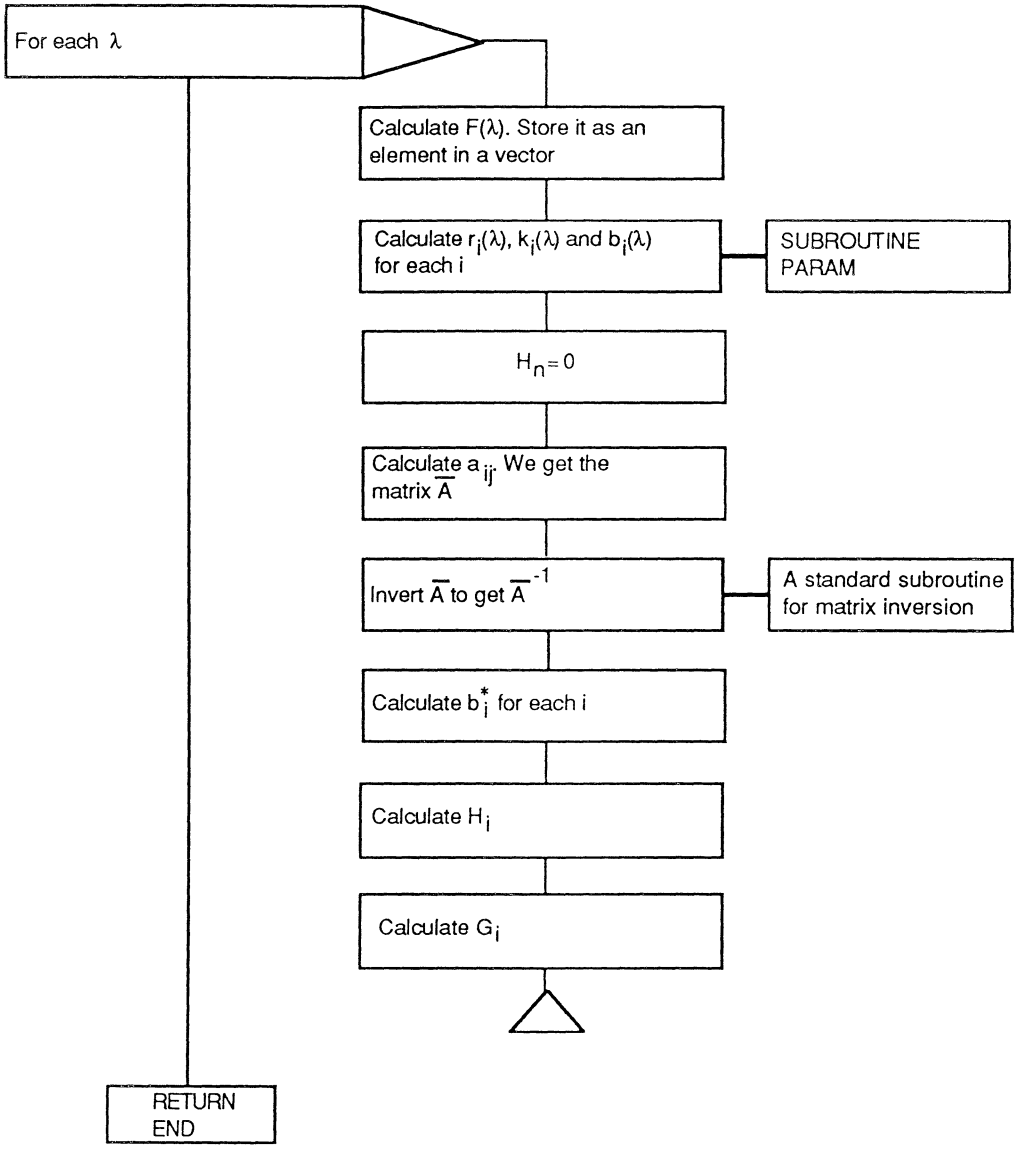

Fig. 33. Subroutine TCOEFF. Calculation of $G_i(\lambda)$, $H_i(\lambda)$ and $F(\lambda)$ for (i,λ).

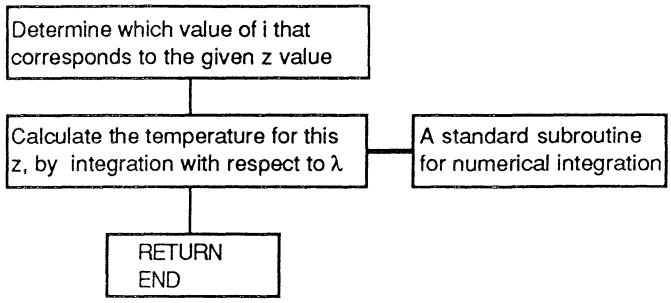

Fig. 34. Subroutine TCALC. Calculation of the temperature (z) as a vector.

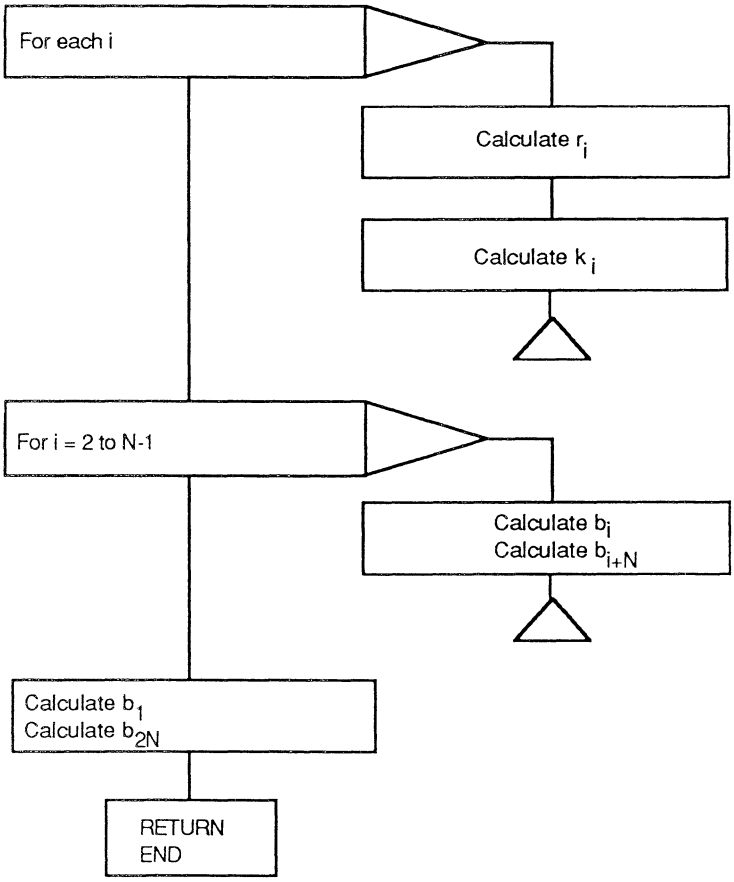

Fig. 35. Subroutine PARAM. Calculation of $r_i(\lambda)$, $k_i(\lambda)$ and $b_i(\lambda)$.

Chapter 4. Experiments

General

In order to experimentally investigate and compare the different proposals for reducing the heat in semiconductor lasers, a series of experiments were planned.

Our intention was to look at the temperature of the semiconductor in a semiconductor laser at various pump powers, obtaining a curve of the temperature versus the pump power. By doing this for each proposal, they can be compared.

The input power was measured directly with a power meter. The problem was how to measure the temperature of the semiconductor. Two ways were discussed. One was to use a sensor, developed by M. Kull [48] to measure the temperature. The other was to calculate the temperature from the expected wavelength shift of the radiation from the semiconductor when exposed to different values of pump power [49].

The first approach seemed to be the easiest. The second required a model for the temperature dependence of the wavelength shift.

But to be able to do any measurements at all in an optically pumped semiconductor laser, such a laser first had to be built. This soon became a goal itself. When doing this, the method of Roxlo et al. was used [50].

The choice and mounting of a semiconductor

The first thing to do was to choose a semiconductor. CdSe was instantly available. It was also expected to lase at 700 nm [51], which meant that the lasing output would be visible, which ought to simplify the alignment of the laser. Finally, not many lasing experiments had been done with CdSe.

CdSe can not be made to lase at room temperature, due to a decrease in the radiative efficiency [52]. It had to be cooled. To achieve this, tiny samples were mounted with oil on a sapphire window. See Fig. 36.

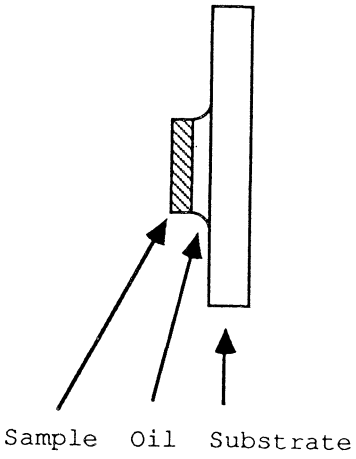

Fig. 36. The mounting of a sample.

The window was then mounted in a Dewar, which was originally constructed by Fuchs and Salour [53]. See Fig. 37.

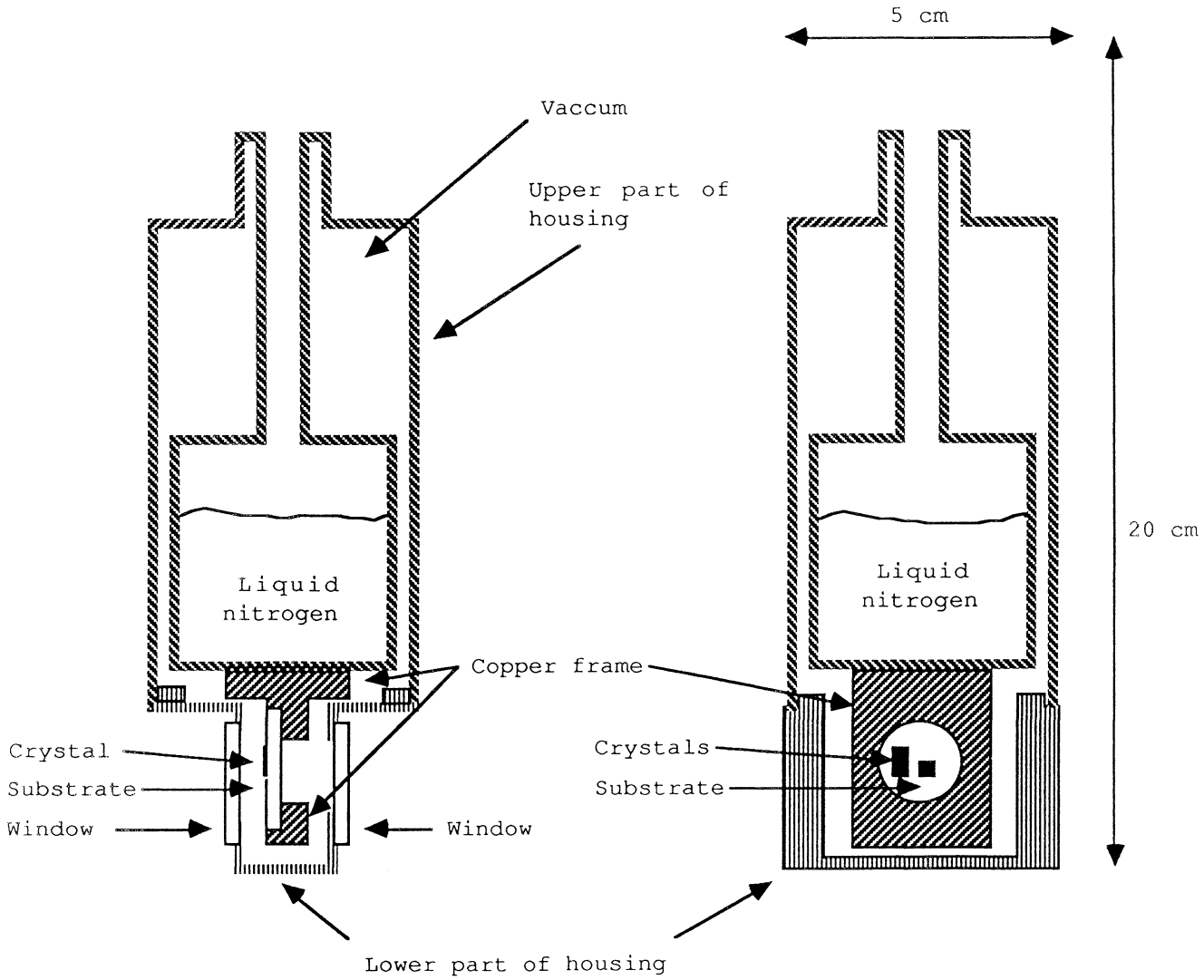

Fig. 37. Dewar construction. (a) Cutaway side view. (b) Cutaway front view.

This enabled the crystals to be cooled (by liquid nitrogen) in a vacuum, down to 77 K.

Study of the fluorescence

Now it was possible to look at the fluorescence at room temperature and at 77 K. The following set-up was constructed.

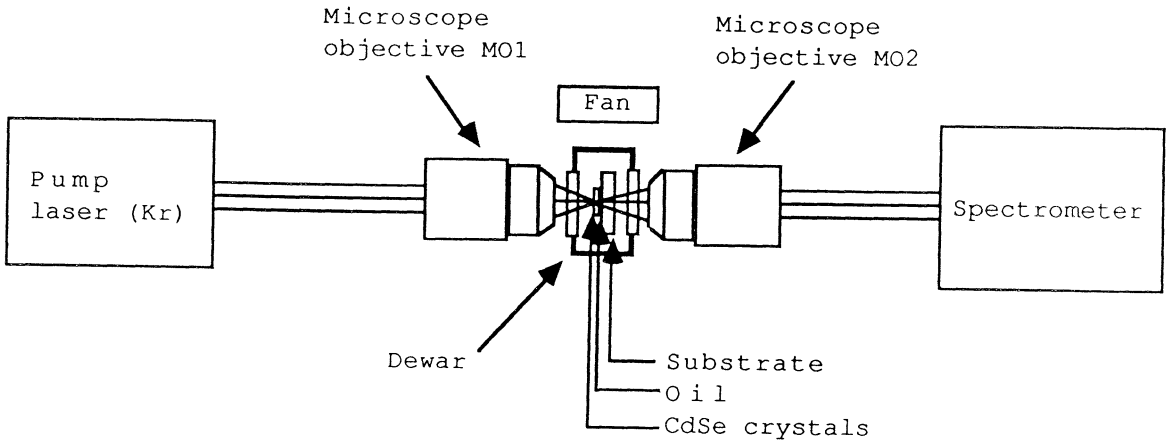

Fig. 38. Setup for studying of the flourescence from the crystals.

The set-up was constructed in such a way that it would be easy to change it into a set-up for lasing experiments at a later time.

The construction of the Dewar enabled only longitudinal pumping, but this was sufficient, since there are significant problems in obtaining lasing with transversel pumping, due to amplified spontaneous emission [54].

The pump laser used here was a Kr^+ laser, continuously radiating at 647 nm.

The microscope objective MO1 was used to focus the pump beam into a spot size of ≈ 5 μm on a CdSe sample. This focusing was necessary in order to avoid amplified spontaneous emission perpendicular to the beam in lasing experiments. Also, a larger spot size would probably have destroyed the crystal in later lasing experiments, due to the high (≈ 100 kW/cm^2 [55]) pump threshold for lasing.

The microscope objective MO2 collected the fluorescence light emitted from the semiconductor sample and collimated it.

Both microscope objectives were Leitz EF 10x 0.25 NA objectives.

The fan prevented condensation on the Dewar windows when the sample was cooled.

Two scans were taken, one at room temperature (Fig. 39) and one at 77 K (Fig. 40).

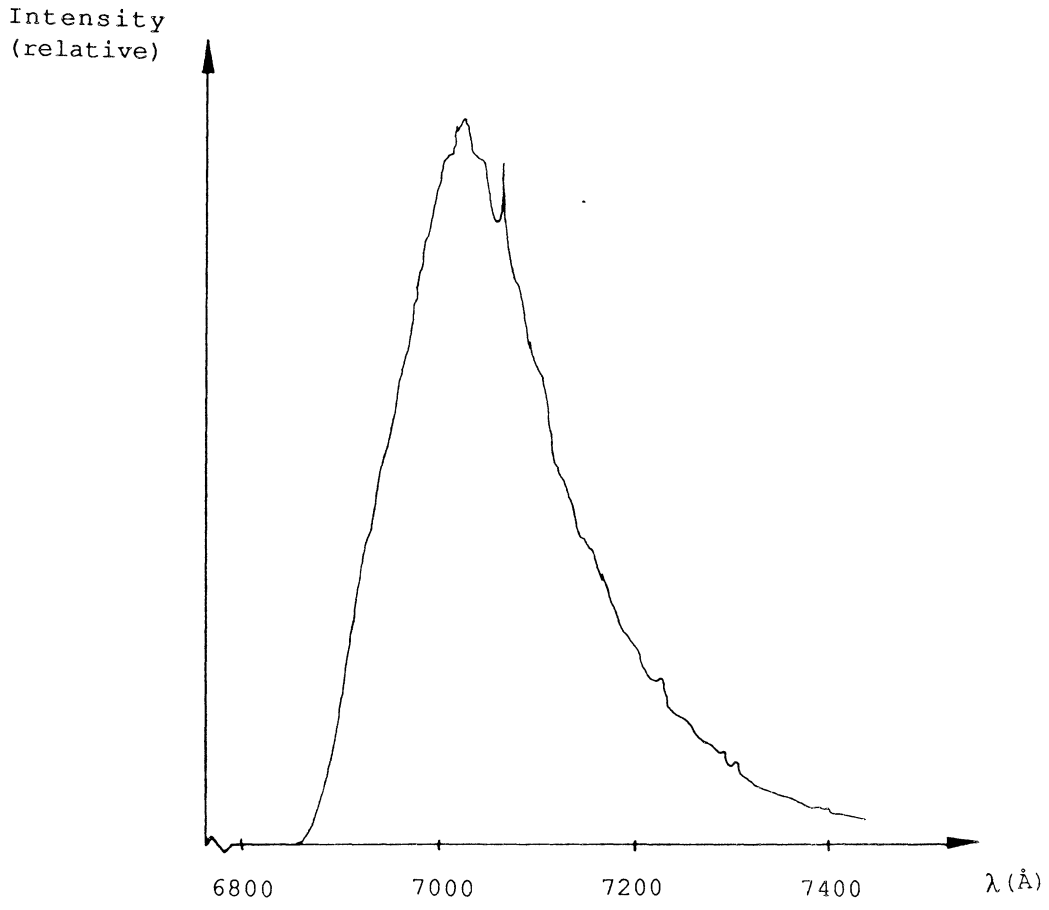

Fig. 39. Fluorescence from CdSe at room temperature (excitation wavelenght 647 nm).

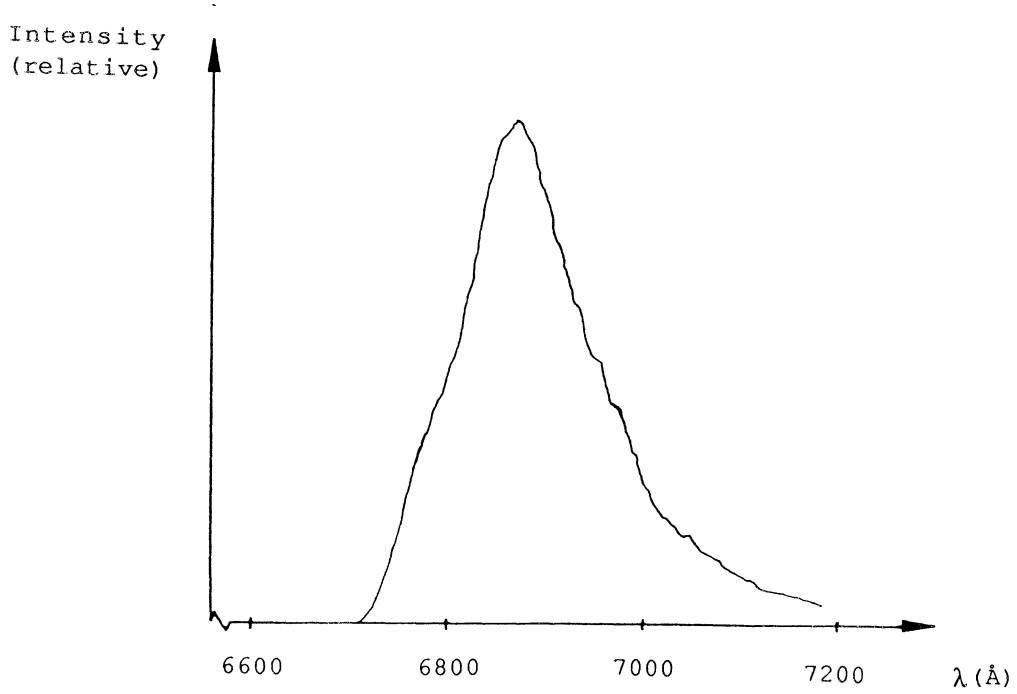

Fig. 40. Fluorescence from CdSe at 77 K (excitation wavelenght 647 nm).

A wavelength shift can immediately be seen. The main peaks are at 7020 Å (Fig. 39.) and 6870 Å (Fig. 40).

Test of the heat sensor

Now it was time to test whether the mentioned infrared heat sensor could be used to measure the temperature of the irradiated spot of the semiconductor crystal directly. The following set-up was used.

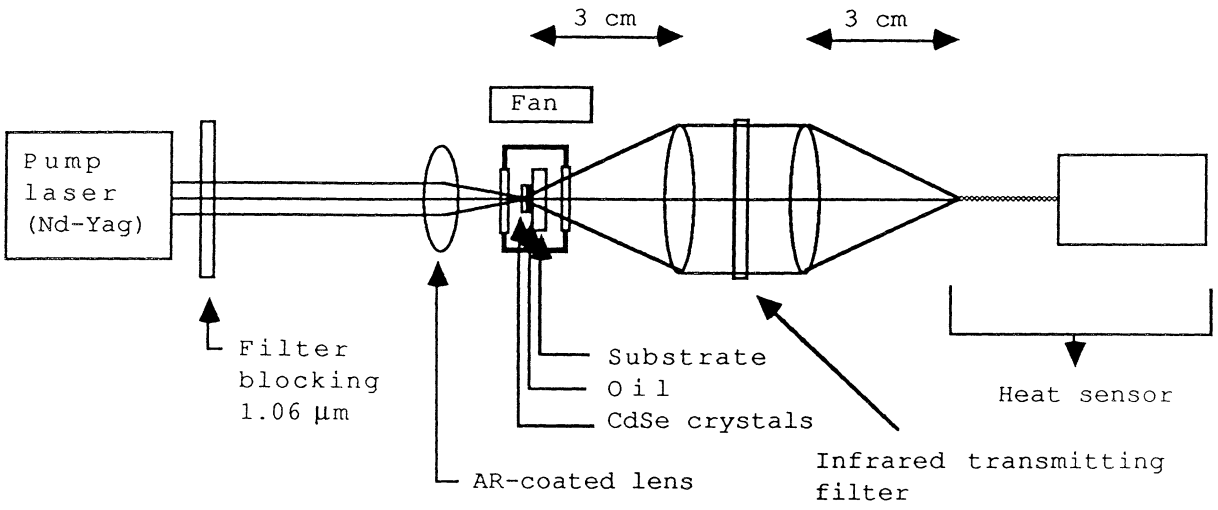

Fig. 41. Configuration used for test of the sensor.

Since the Kr^+ laser was starting to fade, a Q-switched Nd-YAG laser (Quantronics 416) was used instead as a pump source, radiating at 532 nm. The 1.06 µm radiation from the laser was blocked out by filters.

The MO1 from the former set-up was replaced by a single AR-coated lens, in order to get lower losses.

MO2 was replaced by a system of two lenses of focal length 3 cm and an infrared transmitting filter (in order to block out the pump radiation and the fluorescence, leaving the infrared heat radiation from the heated sample uneffected).

At first an ordinary optical fibre connected to a spectrometer was used instead of the heat sensor. The reason for this was to be able to find the focus of the lens system and then to optimize the total output radiation from the irradiated crystal at that point. (The infrared transmitting filter was of course not used then, it was replaced by a filter that only blocked out the pump beam.)

Some scans were taken, with the crystals initially cooled to 77 K in vacuum. When inspecting the crystals afterwards, burn marks were visible. Also, a layer of CdSe had been deposited on one of the sapphire windows!

The windows were then removed (which meant that the crystals could no longer be cooled) and the pump beam was focused less well on the crystals by moving the focusing AR-coated lens slightly. (If this was not done, we could hear the sample burning and could see the smoke.)

The next step was to remove the optical fibre and to insert the infrared heat sensor (and the infrared transmitting filter). This was done, but no signal was detectable. Since M. Kull was working on the sensor at TACAN Corporation at that time, we tried to solve the problem together, but did not succeed.

It was later shown [56] that the sensor was too insensitive, requiring a heated spot of 200 µm in diameter for a minimum detectable temperature of 800 K. Other detectors had to be used, e. g. a combination of InAs and PbS detectors. Unfortunately, such detectors were quite expensive.

In that situation a decision was made to investigate whether the expected wavelength shift would suffice.

A decision was also made to focus more on the construction of the optically pumped semiconductor laser, since time in the USA was getting short.

Building an optically pumped semiconductor laser

The ultimate goal was initially to construct a CdSe ring laser. One reason for this is that a ring cavity results in higher output powers than linear cavities [57]. Also, a semiconductor ring laser with CdSe had not been reported.

However, since it was important to quickly get a semiconductor laser going (in order to investigate the red shift) we decided to first construct a linear cavity CdSe laser, using the technique of Roxlo et al. [58], and than, if time allowed, construct a CdSe ring laser.

A new set-up was constructed (see Fig. 42). First we wanted to look at the fluorescence, in order to find a good spot for lasing experiments.

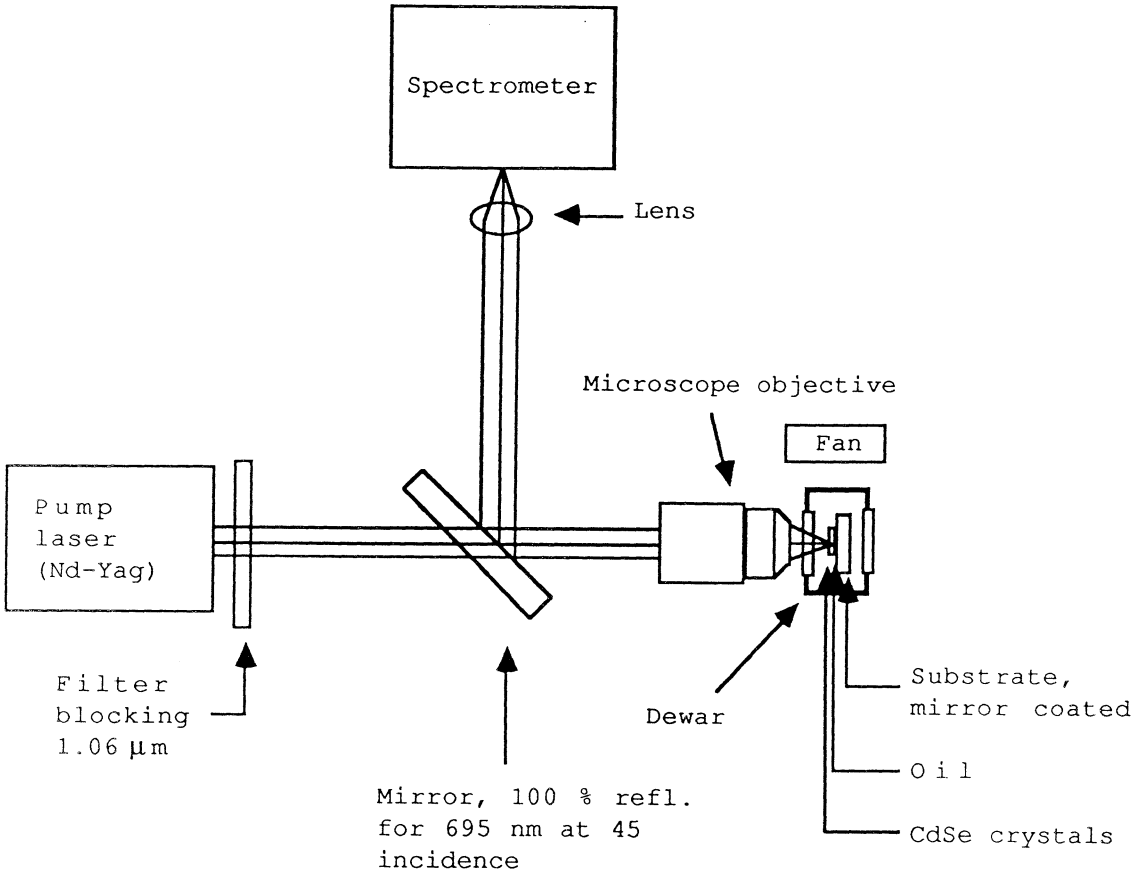

Fig. 42. Setup for studying of the flourescence.

The glass substrate in the Dewar was replaced by a mirror substrate, of 100 % reflectivity at 695 nm at an angle of incidence of 0 degrees. In other words, the semiconductor crystals now became attached with oil directly to a mirror inside the Dewar.

New sapphire windows were glued onto the Dewar, and it was again cooled to 77 K in vacuum.

The microscope objective was a Leitz EF 10x 0.25 NA objective. (The reason why the AR-coated lens was not used was that Roxlo had found [59] that the quality of the focused image was more important than low losses).

The pump laser was a Q-switched Nd-YAG laser radiating at 532 nm. Filters were used to block out the 1.06 µm radiation.

The mirror at an angle of 45 degrees was of 100 % reflectivity at 695 nm, which meant that most of the pump light went through, but the fluorescence was reflected into the spectrometer.

Some scans of the fluorescence were taken. One example is given in Fig. 43.

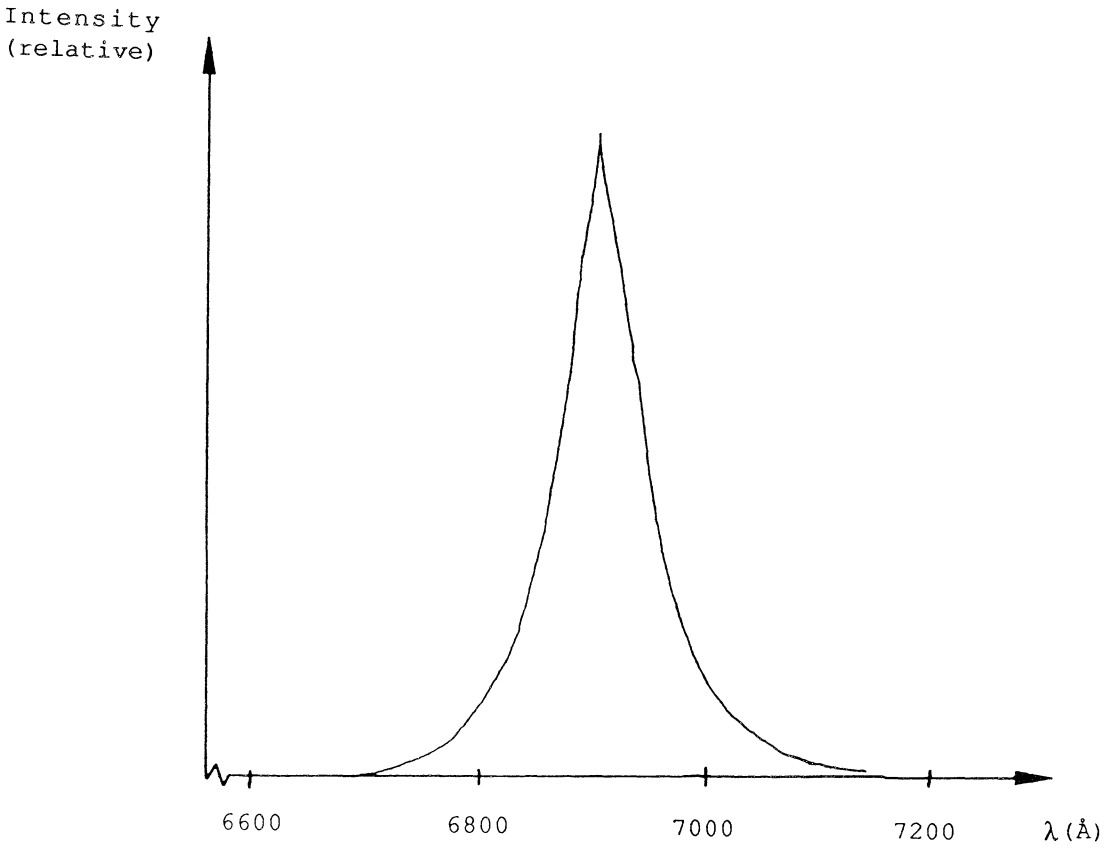

Fig. 43. Fluorescence scan.

Finally, the time had come to look for some laser action.

An output mirror of 98 % reflectivity at 695 nm at an angle of incidence of 15 degrees was inserted between the mirror and the microscope objective in Fig. 42. Its second surface was AR-coated.

This was not sufficient, however. The mirrors weakened the pump beam too much. The set-up had to be modified. See Fig. 44.

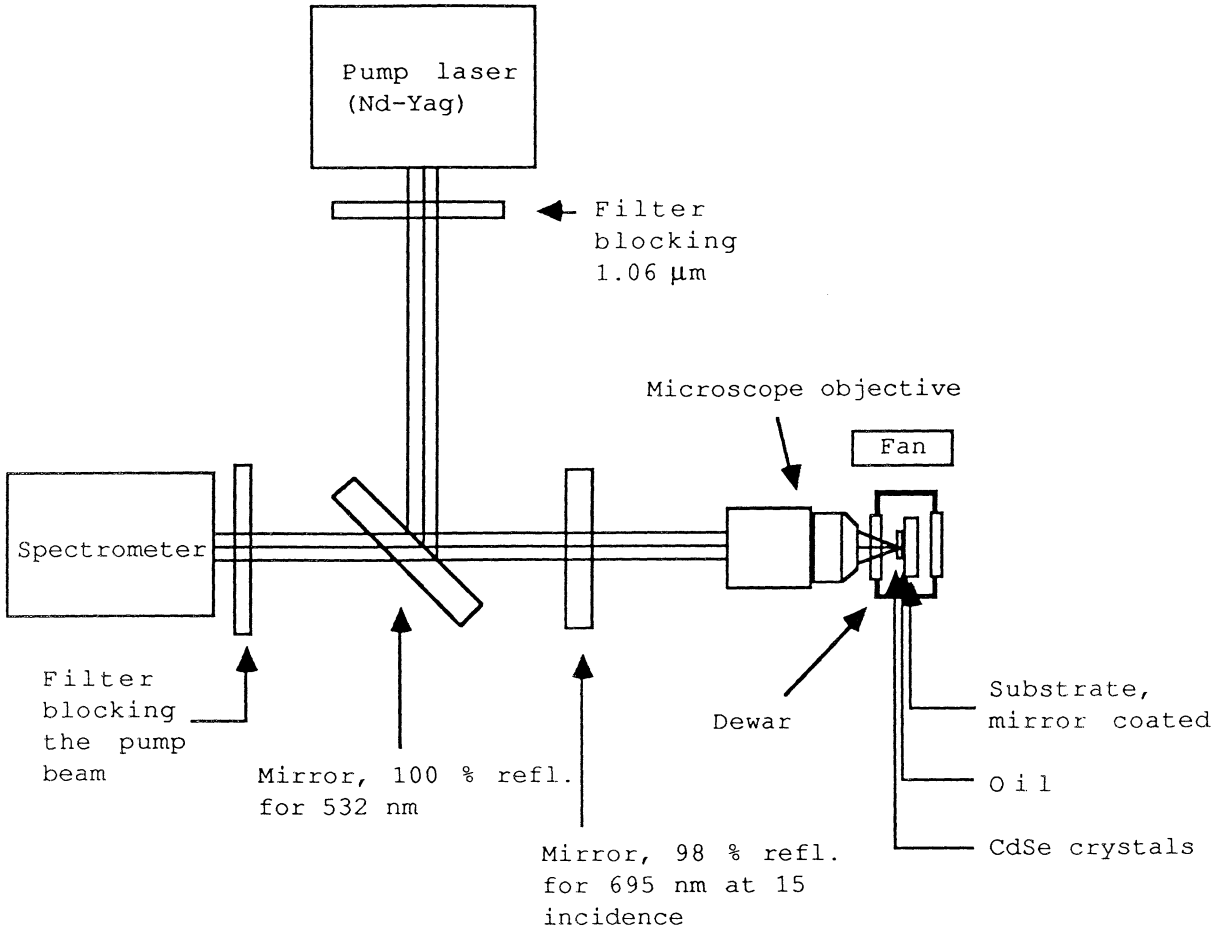

Fig. 44. A simple laser setup.

To be able to conveniently optimize the output beam, a photomultiplier was used, with a filter that blocked out the pump wavelength. The spectrometer could not be used, since it was not clear at exactly which wavelength the crystals would lase, and to optimize with repeated scannings would at this stage be a waste of time.

After some optimization, strong signals were detected. The photomultiplier and the blocking filter were removed, and were replaced by a spectrometer. The semiconductor crystal was lasing. The output could easily be seen by the naked eye.

Studying the laser radiation and the samples

Several scans were taken, in order to investigate and optimize the output.

The laser radiation usually consisted of several peaks, representing different laser modes. When optimizing, it could be seen how the modes were competing (see Fig. 45).

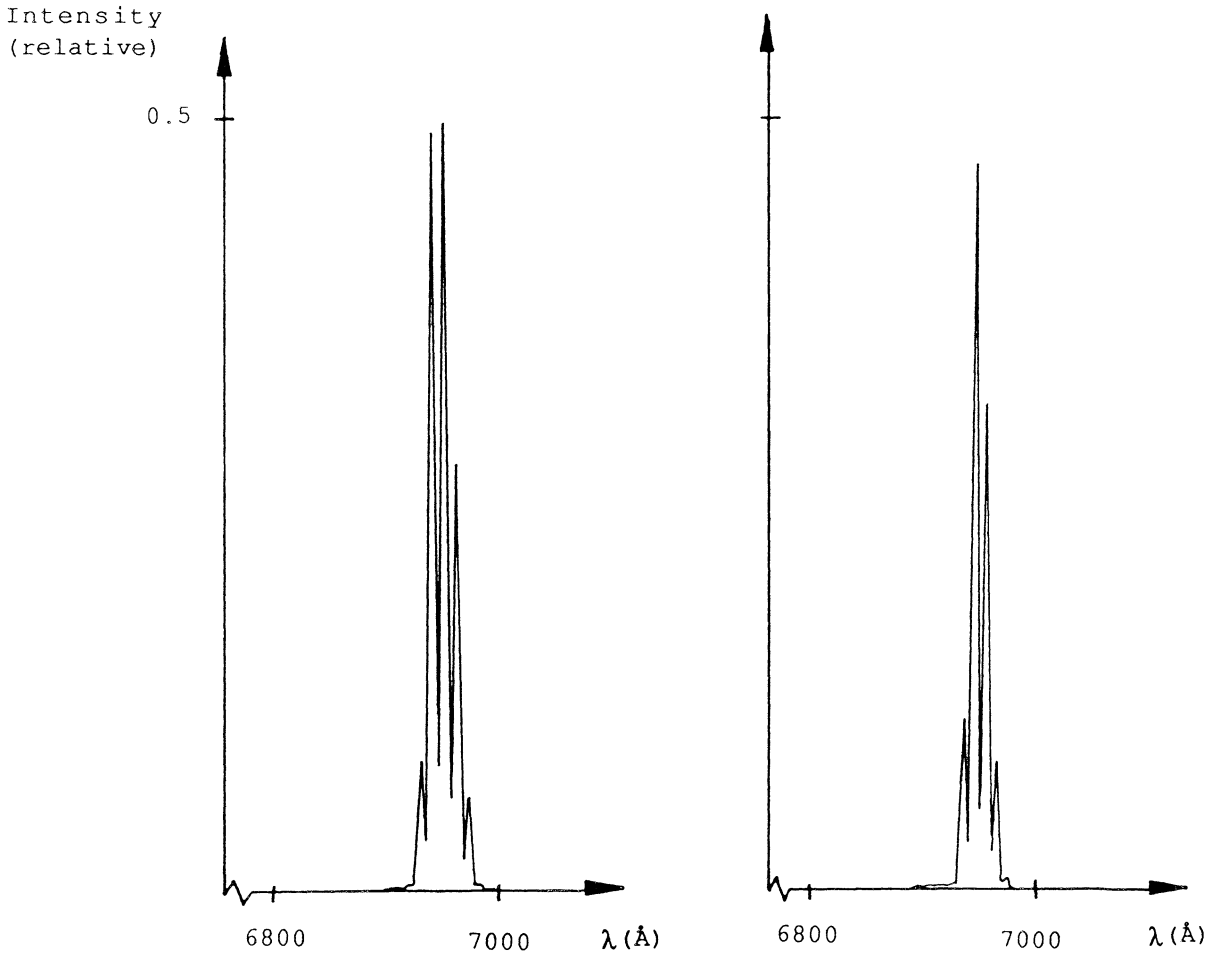

Fig. 45. Competing laser modes.

Since the modes are Fabry-Perot modes originated in the crystal, they can be used to calculate the thickness of the crystal. We have [60]

$$(121) \quad (\partial\lambda_0)_{fsr} \approx \frac{\lambda_0^2}{2n_f d}$$

where $(\Delta\lambda_0)_{fsr}$ = the free spectral range (in m)

λ_0 = the wavelength in vacuum of the beam (in m)

n_f = the refractive index of the medium in the interferometer

d = the distance between the plates in the interferometer (in m)

In our case the free spectral range is the distance between the peaks in the scans, d is the thickness of the crystal, and the refractive index is that of CdSe (2.446 [61]).

In Fig. 45 the distance between the peaks is 5 Å. The output laser radiation has a wavelength of 695 nm. Thus we can calculate the thickness of the crystal. The result is ≈ 200 µm.

This was much thicker than assumed when mounting the samples.

The output power was low, less than 1 µW average power. Assuming a pulse length of 200 ns [62], knowing the pulse repetition rate to be 5 kHz, the following rough formula can be used.

$$(122) \quad P_p \approx \frac{P_a}{L * R}$$

where P_p = the peak power (in W)

P_a = the average power (in W)

L = the pulse length (in s)

R = the repetition rate (in 1/s)

The result was that the average power of 1 µW corresponded to a peak power of 1 mW.

The energy can be calculated using the following formula:

$$(123) \quad E = P_p * L$$

where E = the energy (in J)

P_p , L , see above

The result was an energy of 0.2 nJ.

Several crystals and different spots on them were investigated. Scans showing radiation from different spots on the same sample could look quite different (different number of peaks, different distance between the peaks). The reason for this was that the samples were not uniform in thickness.

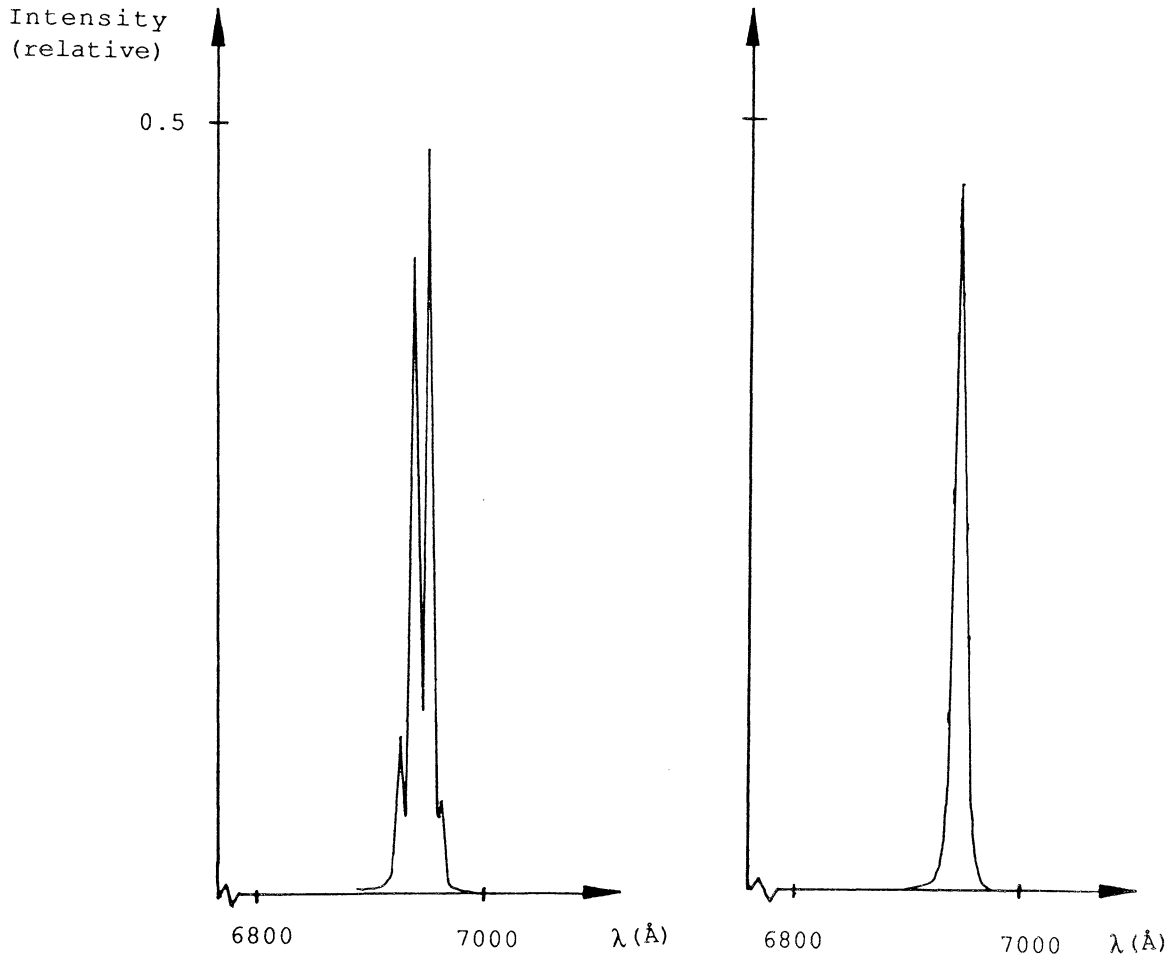

Fig. 46. Fluorescence from different spots on the same sample.

The crystals were in general much thicker than the 10 μm that we had assumed.

In search of a red shift

Now it was time to start the search for a red shift.

In order to be able to change the pump power easily, we used optical filters of different transmittance. The use of different filters enabled different values of the pump power. Also, combinations of filters could be used to get more data.

Several series of scans were taken, but no red shift was detected, except when running out of liquid nitrogen. Then a red shift of about 10 Å was seen before the sample stopped lasing. (Once a red shift of 120 Å was seen.)

An example of attenuation is shown in Fig. 47.

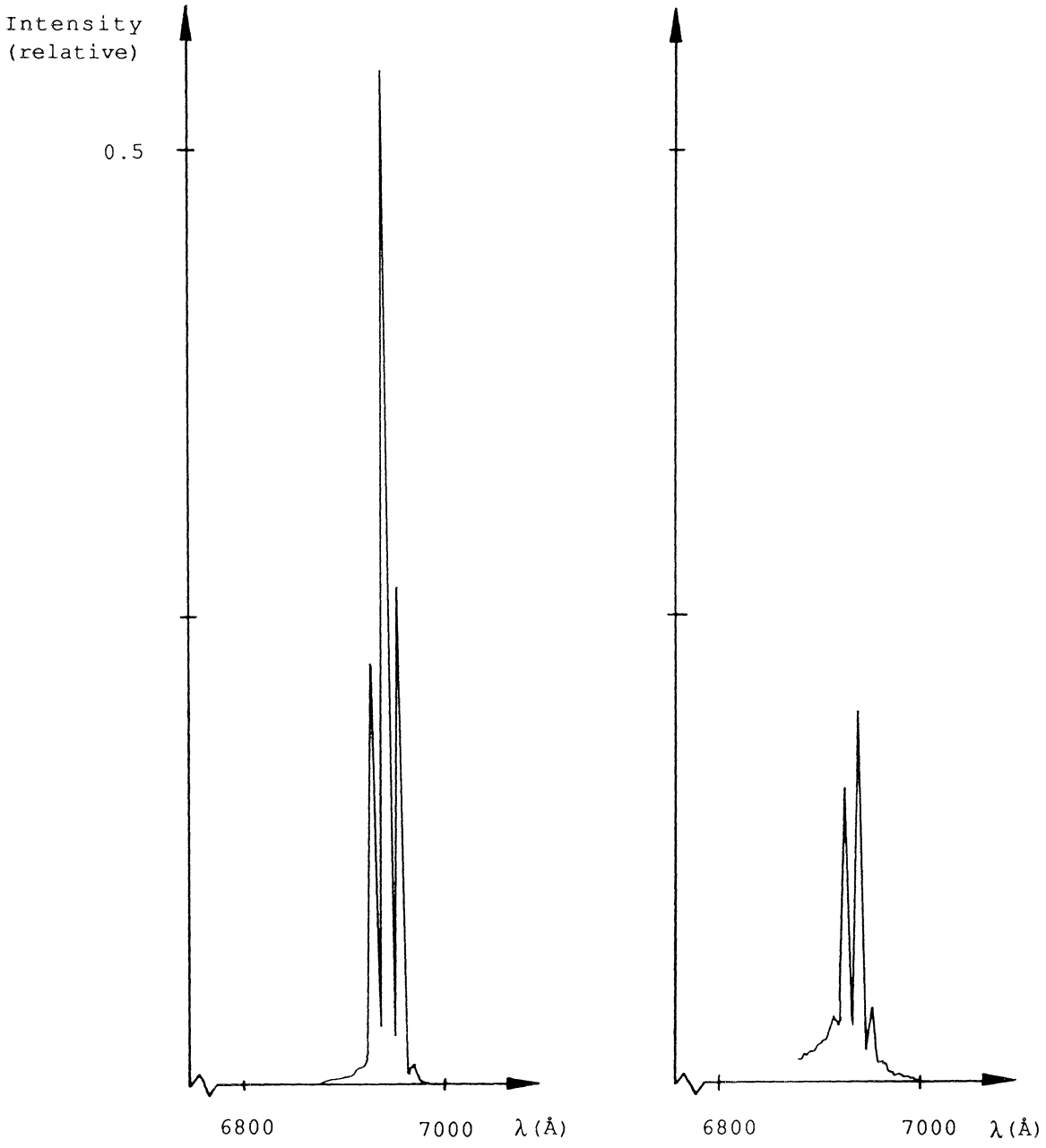

Fig. 47. Fluorescence from a certain spot. The right scan is produced after attenuation of the input laser beam with filters.

Since it could be suspected that the pulses were too short to really heat the sample at that frequency, the frequency of the Q-switched laser was increased. At about 15 kHz a red shift was suspected (see Fig. 48), but soon the sample was destroyed, probably due to overheating. This method could in other words not be used.

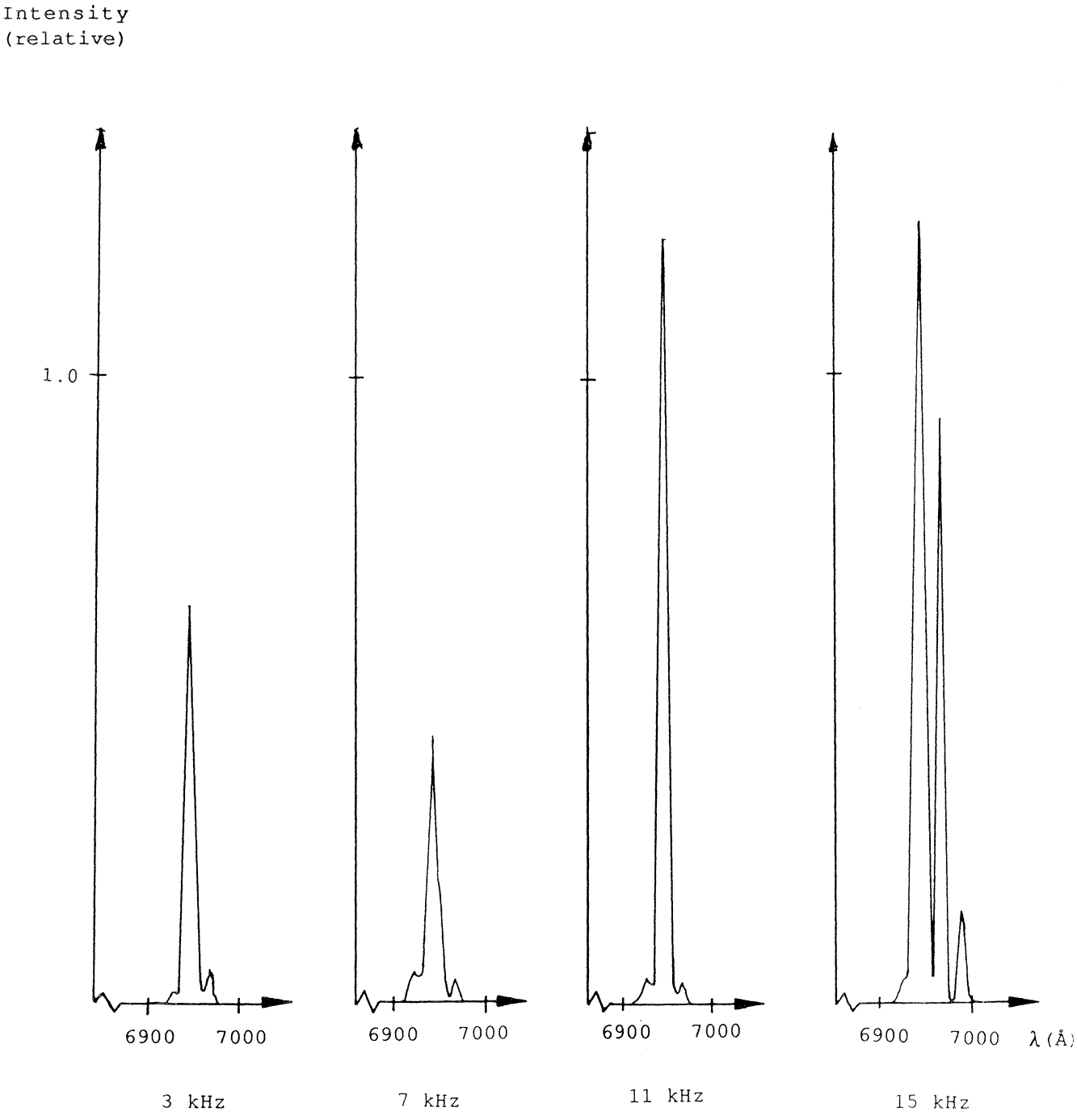

Fig. 48. Scans at various frequencies of the Q-switched pump beam.

The conclusion of these experiments was that the samples had to be continuously pumped in order to achieve a red shift.

Unfortunately, this could not be done with the Nd-YAG, since its continuous radiation at 532 nm was very weak (maximum output 10 mW [62]).

It was decided to try to use the Kr^+ laser again, in spite of the fact that it had started to fade.

Before the set-up was arranged, however, the crystals were taken out of the Dewar and were inspected with the help of a microscope.

Long burn traces could be seen in most of the samples. This showed that the samples had been burned during the experiments, probably when too much input power was used, or when running out of liquid nitrogen.

The new set-up was then constructed.

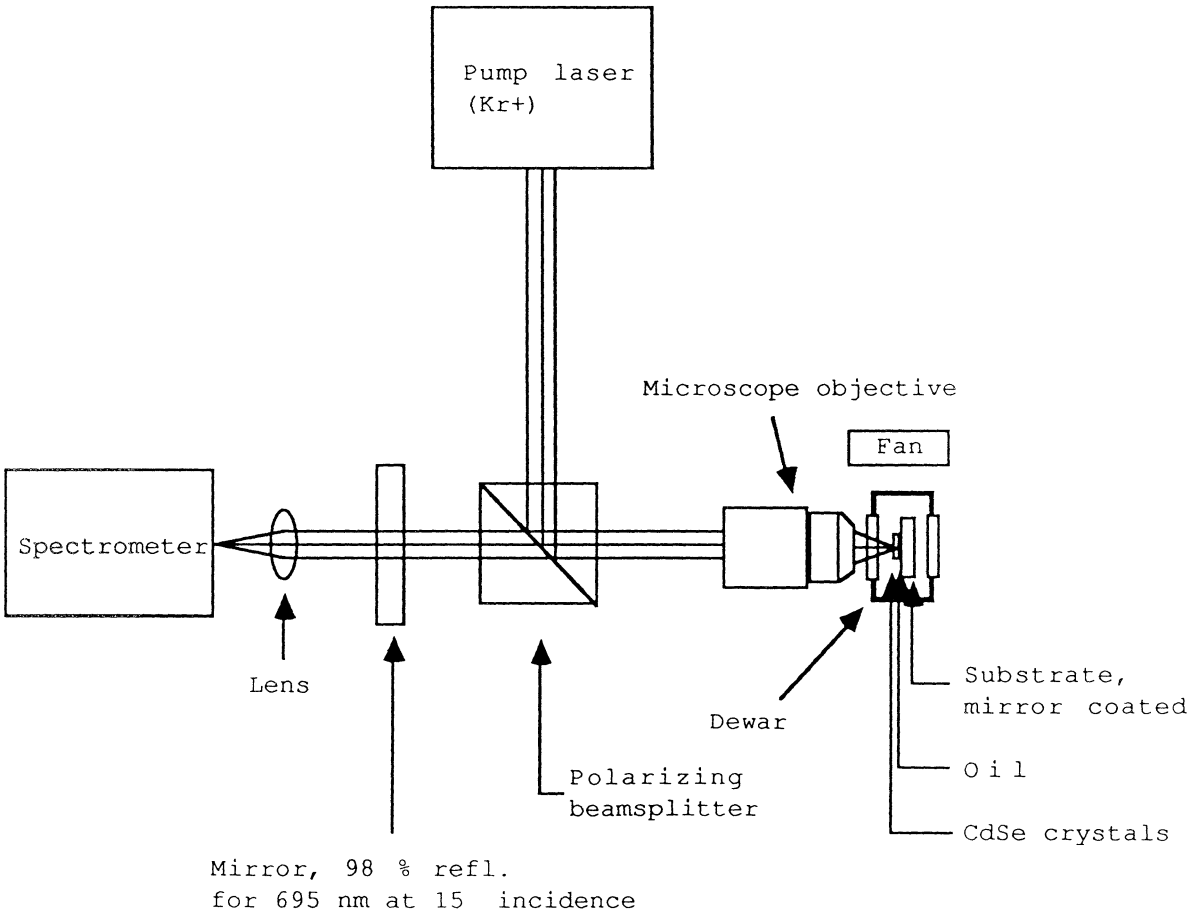

Fig. 49. Setup with Kr+ pump.

With external help the Kr^+ laser was realigned, and its output power then increased. It was radiating at 676 nm when the output power was low (up to 140 mW). At higher output powers it also radiated at 647 nm. The radiation from the laser was vertically polarized.

In order to be able to separate the pump beam from the fluorescence, a polarizing beamsplitter was used. The emission from CdSe is strongly polarized with $E \perp c$. The crystals were mounted such that their c axes were vertical, so that the emission was horizontally polarized. Since the radiation from the pump laser was vertically polarized, the polarizing beamsplitter reflected the pump beam and transmitted the emission from the crystals.

Due to lack of time, no efforts were made to obtain lasing action. The goal this time was only to obtain a red shift.

Several series of scans were taken. All of them showed a red shift when increasing the pump power. Some examples are shown in Fig. 50 (next page).

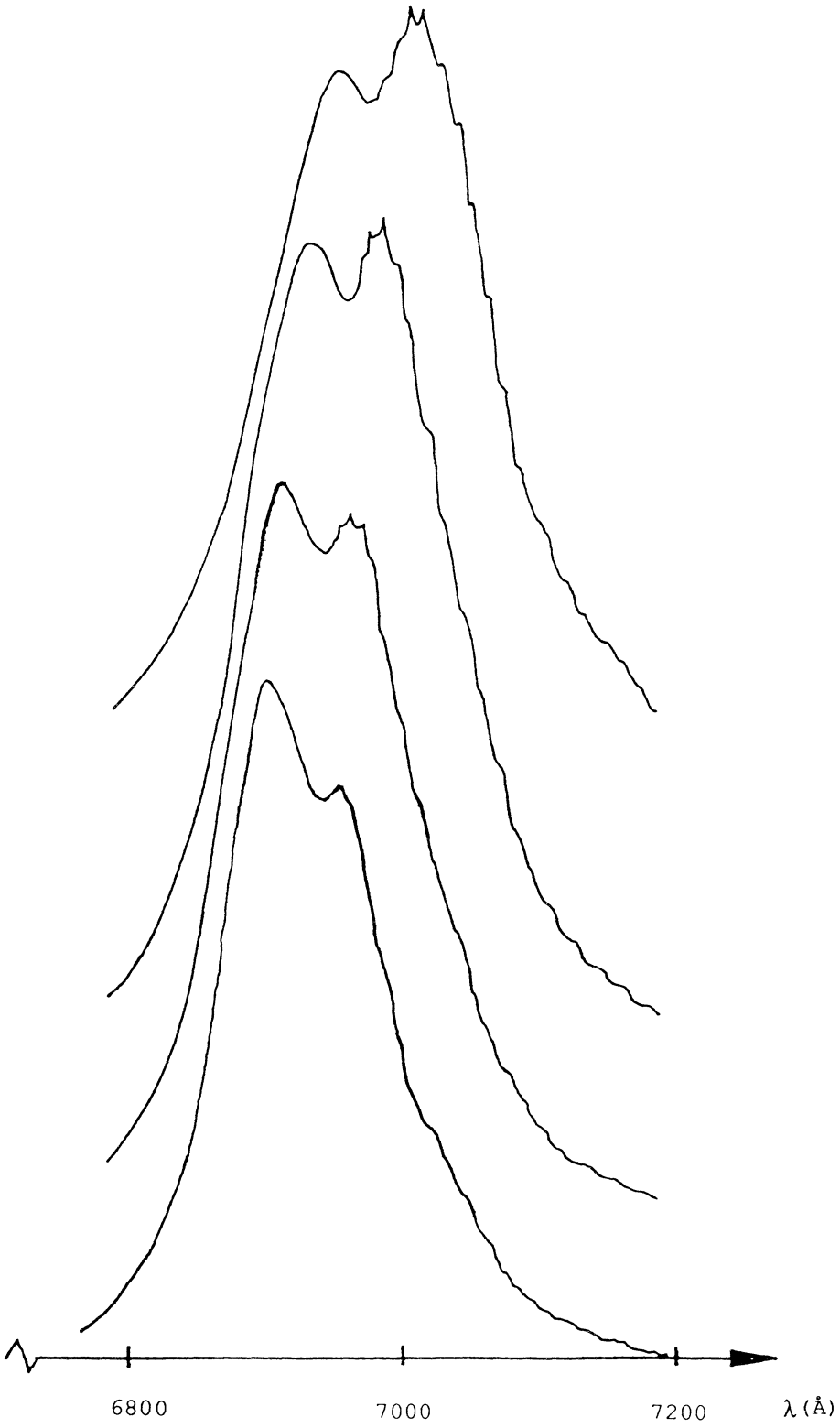

Fig. 50. Red shift in fluorescence for various pump powers.

Red shift measurements of this kind could be used to test different proposals for removing the heat in semiconductor lasers. However, there was no time to continue the experimental work. The next step would otherwise have been to experimentally test some of the proposals with this method, and also to see how they worked when the CdSe was lasing.

Chapter 5. Discussion and Conclusions

This thesis is only a first step in the development of a solution to the heat transfer problem in optically pumped semiconductor lasers. What has been given here is an investigation of some different proposals being made and some models that the proposals might be tested with.

What remains is of course to test the proposals. This will probably be costly and time-consuming work, since some of the proposals involve e. g. growing layers on semiconductor samples.

In order to be able to test the various proposals, the temperature of the semiconductor has to be measured. This can be done either directly with a sensor, or by some indirect method. In this thesis, using the red shift as such a method has been discussed, since a sufficient sensor was not available.

It remains to be seen whether the red shift will suffice to test the proposals. The best way would of course be not to use the red shift but to try to find a sensor capable of measuring the temperature.

Acknowledgements
==========

I wish to thank James H. Bechtel (TACAN) for supervision. I would also like to thank all employees at TACAN for fruitful discussions and for making my visit to the United States a very pleasant memory for me. Special thanks to Michael M. Salour (TACAN) and Sune Svanberg (LTH) for making it possible for me to do this work.

Appendices

Appendix 1

Here we will derive an expression for the solution of (95)

$$(124) \qquad \frac{\partial \mu_{21}(Z,\tau)}{\partial \tau} = \sigma \frac{\partial^2 \mu_{21}(Z,\tau)}{\partial Z^2}$$

To solve (124), we need more theory. (We have a complicating boundary condition, the surface temperature is a function of τ (equation (96)). We can use Dunhamel's theorem. Carslaw and Jaeger [63] express the theorem for this case as:

"If $T = B(x,y,z,t)$ represents the temperature at (x,y,z) at the time t in a solid in which the initial temperature is zero, while its surface is kept at temperature unity, then the solution of the problem when the surface is kept at temperature $\Phi(t)$ is given by

$$(125) \qquad T = \int_0^t \Phi(\lambda) \frac{\partial}{\partial t} B(x,y,z,t-\lambda)\, d\lambda \qquad "$$

So the first step to be taken is to find the solution for the problem with the surface temperature at unity. In order to do this, we start by saying that the temperature origin is located at $Z=z'$ and that the solid is infinite. We then have

$$(126) \qquad \frac{\partial \mu_{21}(Z,\tau)}{\partial \tau} = \sigma \frac{\partial^2 \mu_{21}(Z,\tau)}{\partial Z^2} \qquad -\infty < Z < \infty$$

and

$$(127) \qquad \mu_{21}(Z,\tau) = h(Z) \qquad \tau = 0$$

where $h(Z)$ = the initial temperature distribution

Carslaw and Jaeger [64] give one particular solution as

$$(128) \qquad \mu_{21}(Z,\tau) = \frac{1}{\tau^{\frac{1}{2}}} \exp\left[\frac{-Z^2}{4\sigma\tau}\right]$$

Also

$$(129) \qquad \mu_{21}(Z,\tau) = \frac{1}{2(\pi\sigma\tau)^{\frac{1}{2}}} \exp\left[\frac{-(Z-z')^2}{4\sigma\tau}\right]$$

where z' = the location of the source in the z-direction

is a solution.

The equations (126) - (127) being linear, the sum of any particular solution is also a particular solution. This gives

$$(130)\quad \mu_{21}(Z,\tau) = \frac{1}{2(\pi\sigma\tau)^{\frac{1}{2}}} * \int_{-\infty}^{\infty} c(z') \exp\left[\frac{-(Z - z')^2}{4\sigma\tau} \right] dz'$$

where c(z') has to be calculated. We follow Özisik [65] and set

$$(131)\quad \eta = \frac{z' - Z}{[4\sigma\tau]^{\frac{1}{2}}}$$

(130) thus becomes

$$(132)\quad \mu_{21}(Z,\tau) = \frac{1}{\pi^{\frac{1}{2}}} * \int_{-\infty}^{\infty} c(Z + [4\sigma\tau]^{\frac{1}{2}} \eta) \exp(-\eta^2)\, d\eta$$

According to (127) $\mu_{21} = h(Z)$ when $\tau = 0$. This gives us

$$(133)\quad \mu_{21}(Z,0) = h(Z) = \frac{1}{\pi^{\frac{1}{2}}} * \int_{-\infty}^{\infty} c(Z) \exp(-\eta^2)\, d\eta$$

Since

$$(134)\quad \frac{1}{\pi^{\frac{1}{2}}} * \int_{-\infty}^{\infty} \exp(-\eta^2)\, d\eta = 1$$

we arrive at

$$(135)\quad c(Z) = h(Z)$$

Putting this into (130), we obtain

$$(136)\quad \mu_{21}(Z,\tau) = \frac{1}{2(\pi\sigma\tau)^{\frac{1}{2}}} * \int_{-\infty}^{\infty} h(z') \exp\left[\frac{-(Z - z')^2}{4\sigma\tau} \right] dz'$$

In order to make the expression valid for a semi-infinite solid, we use the method of images, presented by Carslaw and Jaeger [66]. We imagine a semi-infinite solid extended into all directions. Then we put a negative image of the temperature distribution on "the other side" of the boundary plane. We then obtain zero temperature at the boundary surface.

Applying this method to (136), we get

$$(137)\quad \mu_{21}(Z,\tau) = \frac{1}{2(\pi\sigma\tau)^{\frac{1}{2}}} * \int_0^{\infty} h(z') \exp\left[\frac{-(Z - z')^2}{4\sigma\tau} \right] dz' +$$

$$+ \frac{-1}{2(\pi\sigma\tau)^{\frac{1}{2}}} * \int_{-\infty}^{0} h(-z') \exp\left[\frac{-(Z - (-z'))^2}{4\sigma\tau} \right] dz' =$$

$$= \frac{1}{2(\pi\sigma\tau)^{\frac{1}{2}}} * \int_0^{\infty} h(z') \left[\exp\left[\frac{-(Z - z')^2}{4\sigma\tau} \right] - \right.$$

$$\left. - \exp\left[\frac{-(Z + z')^2}{4\sigma\tau} \right] \right] dz'$$

Now, say that the initial temperature distribution is a constant, V, that is

$$(138)\quad h(z') = V \quad \text{at } \tau=0$$

Substitute

$$(139)\quad z' = Z + 2\eta(\sigma\tau)^{\frac{1}{2}} \quad \text{in the first part and}$$

$$(140)\quad z' = -Z + 2\eta(\sigma\tau)^{\frac{1}{2}} \quad \text{in the second part}$$

We obtain

$$(141)\quad \mu_{21}(Z,\tau) = \frac{V}{\pi^{\frac{1}{2}}} \left[\int_{\frac{-Z}{2(\sigma\tau)^{\frac{1}{2}}}}^{\infty} \exp(-\eta^2)\, d\eta - \int_{\frac{Z}{2(\sigma\tau)^{\frac{1}{2}}}}^{\infty} \exp(-\eta^2)\, d\eta \right] =$$

$$= \frac{2V}{\pi^{\frac{1}{2}}} \left[\int_0^{\frac{Z}{2(\sigma\tau)^{\frac{1}{2}}}} \exp(-\eta^2)\, d\eta \right]$$

This is the solution for a semi-infinite solid whose surface is kept at zero temperature, the initial temperature distribution being V. However, we want the surface to be kept at temperature unity, the initial temperature distribution being zero.

If we change the boundary condition from

(142) $\mu_{21}(Z,t) = 0$ at $Z=0$

to

(143) $\mu_{21}(Z,t) = V = \text{constant}$ at $Z=0$,

we can add V to the solution (141) for an initial temperature -V, thus obtaining the solution for a semi-infinite solid whose surface temperature is kept at V, and whose initial temperature distribution is zero.

$$(144) \quad \mu_{21}(Z,\tau) = V\left[1 - \frac{2}{\pi^{\frac{1}{2}}}\left[\int_0^{\frac{Z}{2(\sigma\tau)^{\frac{1}{2}}}} \exp(-\eta^2)\, d\eta\right]\right]$$

The solution for an initial temperature of zero and unity surface temperature is thus

$$(145) \quad \mu_{21}(Z,\tau) = 1 - \frac{2}{\pi^{\frac{1}{2}}}\left[\int_0^{\frac{Z}{2(\sigma\tau)^{\frac{1}{2}}}} \exp(-\eta^2)\, d\eta\right]$$

Now we can use Dunhamel's theorem, mentioned above. This gives the solution to the problem ((95), with boundary conditions from (89), (90) and (91))

$$(146) \quad \frac{\partial \mu_{21}}{\partial \tau} = \sigma \frac{\partial^2 \mu_{21}}{\partial Z^2}$$

$$\mu_{21} = 0 \quad \text{at } \tau=0$$

$$\mu_{21} = \mu_{11}(\tau) \quad \text{at } Z=0$$

as

$$(147)\qquad \mu_{21}(Z,\tau) = \int_0^{\tau} \mu_{11}(\tau') \frac{\partial}{\partial\tau} B(Z,\tau-\tau')d\tau'$$

where

$$(148)\qquad B(Z,\tau-\tau') = 1 - \frac{2}{\pi^{\frac{1}{2}}}\left[\int_0^{\frac{Z}{2[\sigma(\tau-\tau')]^{\frac{1}{2}}}} \exp(-\eta^2)\, d\eta\right]$$

Let

$$(149)\qquad X = \frac{Z}{2[\sigma(\tau-\tau')]^{\frac{1}{2}}}$$

Then

$$(150)\qquad \frac{\partial}{\partial\tau} B(Z,\tau-\tau') = \frac{\partial}{\partial X}\frac{\partial X}{\partial\tau} B(Z,\tau-\tau') = \frac{\partial}{\partial X} B(Z,\tau-\tau') * \frac{\partial X}{\partial\tau} =$$

$$= -\frac{2}{\pi^{\frac{1}{2}}} \exp\left[\frac{-Z^2}{4\sigma(\tau-\tau')}\right] * \frac{\partial}{\partial\tau}\left[\frac{Z}{2[\sigma(\tau-\tau')]^{\frac{1}{2}}}\right] =$$

$$= \frac{Z}{2(\pi\sigma)^{\frac{1}{2}}(\tau-\tau')^{\frac{3}{2}}} \exp\left[\frac{-Z^2}{4\sigma(\tau-\tau')}\right]$$

We get the solution of (95) as

$$(151)\qquad \mu_{21}(Z,\tau) = \frac{Z}{2(\pi\sigma)^{\frac{1}{2}}} * \int_0^{\tau} \frac{\mu_{11}(\tau')}{(\tau-\tau')^{\frac{3}{2}}} \exp\left[-\frac{Z^2}{4\sigma(\tau-\tau')}\right] d\tau'$$

==========

Appendix 2 ==========

Here we evaluate $f_1(\tau) = \left.\frac{\partial \mu_{21}}{\partial Z}\right|_{Z=0}$

We use

$$(149) \quad X = \frac{Z}{2\left[\sigma(\tau-\tau')\right]^{\frac{1}{2}}}$$

to remove τ' in (99). We obtain (99) as

$$(152) \quad \mu_{21}(\tau,Z) = \frac{2}{\pi^{\frac{1}{2}}} * \int_{\frac{Z}{2(\sigma\tau)^{\frac{1}{2}}}}^{\infty} \mu_{11}\left(\tau - \frac{Z^2}{4\sigma X^2}\right) \exp(-X^2)\, dX$$

We must be careful when differentiating, since Z is included in one integration limit.

We use Leibniz's formula. It can be expressed as

$$(153) \quad \frac{d}{d\S} \int_{u_0(\S)}^{u_1(\S)} P(x,\S)dx = P(u_1,\S)\frac{du_1}{d\S} - P(u_0,\S)\frac{du_0}{d\S} + \int_{u_0(\S)}^{u_1(\S)} \frac{\partial P(x,\S)}{\partial \S}\, dx$$

We have

$$\S = Z$$

$$u_1(\S) = \infty$$

$$(154)$$

$$u_0(\S) = \frac{Z}{2(\sigma\tau)^{\frac{1}{2}}}$$

$$P(x,\S) = \frac{2}{\pi^{\frac{1}{2}}} * \mu_{11}\left(\tau - \frac{Z^2}{4\sigma X^2}\right) \exp(-X^2)$$

We obtain

$$(155)\quad \frac{\partial \mu_{21}(\tau,Z)}{\partial Z} = \frac{2}{\pi^{\frac{1}{2}}} * \mu_{11}\left(\tau - \frac{Z^2}{4\sigma X^2}\right) \exp(-X^2)\Big|_{X=\infty} * 0 -$$

$$- \frac{2}{\pi^{\frac{1}{2}}} * \mu_{11}\left(\tau - \frac{Z^2}{4\sigma\left[\frac{Z}{2(\sigma\tau)^{\frac{1}{2}}}\right]^2}\right) \exp\left[-4\sigma\left[\frac{Z}{2(\sigma\tau)^{\frac{1}{2}}}\right]^2\right] *$$

$$* \frac{1}{2(\sigma\tau)^{\frac{1}{2}}} + \frac{2}{\pi^{\frac{1}{2}}} * \int_{\frac{Z}{2(\sigma\tau)^{\frac{1}{2}}}}^{\infty} \frac{\partial \mu_{11}\left(\tau - \frac{Z^2}{4\sigma X^2}\right)}{\partial Z} * \exp(-X^2)\, dX$$

$\mu_{11}(0) = 0$, by definition (see the initial conditions). Thus

$$(156)\quad \frac{\partial \mu_{21}(\tau,Z)}{\partial Z} = \frac{2}{\pi^{\frac{1}{2}}} * \int_{\frac{Z}{2(\sigma\tau)^{\frac{1}{2}}}}^{\infty} \frac{\partial \mu_{11}\left(\tau - \frac{Z^2}{4\sigma X^2}\right)}{\partial Z} * \exp(-X^2)\, dX$$

In order to evaluate this integral we expand

$$\mu_{11}\left(\tau - \frac{Z^2}{4\sigma X^2}\right)$$

in a Maclaurin series for small Z.

The formula is

$$(157)\quad \mu_{11}(\tau - \frac{z^2}{4\sigma X^2}) = \mu_1(\tau - \frac{z^2}{4\sigma X^2})\Big|_{Z=0} +$$

$$+ \frac{\partial \mu_{11}(\tau - \frac{z^2}{4\sigma X^2})}{\partial z}\Big|_{Z=0} * z + \frac{\partial^2 \mu_{11}(\tau - \frac{z^2}{4\sigma X^2})}{\partial z^2}\Big|_{Z=0} * \frac{z^2}{2} +$$

$$+ \text{terms of order} > z^2$$

Thus, substituting μ_{11} from equation (97) into (157), we obtain

$$(158)\quad \mu_{11} = \beta * \int_0^{\tau - \frac{z^2}{4\sigma X^2}} f_1(\tau')d\tau'\Big|_{Z=0} + \Lambda * \left[\tau - \frac{z^2}{4\sigma X^2}\right]\Big|_{Z=0} +$$

$$+ \left[\beta \frac{\partial}{\partial z}\int_0^{\tau - \frac{z^2}{4\sigma X^2}} f_1(\tau')d\tau' + \Lambda \frac{\partial}{\partial z}\left[\tau - \frac{z^2}{4\sigma X^2}\right]\right]\Big|_{Z=0} * z +$$

$$+ \left[\beta \frac{\partial^2}{\partial z^2}\int_0^{\tau - \frac{z^2}{4\sigma X^2}} f_1(\tau')d\tau' + \Lambda \frac{\partial^2}{\partial z^2}\left[\tau - \frac{z^2}{4\sigma X^2}\right]\right]\Big|_{Z=0} * \frac{z^2}{2} +$$

$$+ \text{terms of order} > z^2$$

Having

$$(159)\quad \frac{\partial}{\partial z}\int_0^{\tau - \frac{z^2}{4\sigma X^2}} f_1(\tau')d\tau' = \frac{\partial}{\partial(\tau - \frac{z^2}{4\sigma X^2})} * \frac{\partial(\tau - \frac{z^2}{4\sigma X^2})}{\partial z} * \int_0^{\tau - \frac{z^2}{4\sigma X^2}} f_1(\tau')d\tau' =$$

$$= -\frac{z}{2\sigma X^2} * f_1(\tau - \frac{z^2}{4\sigma X^2})$$

then

$$(160)\quad \frac{\partial^2}{\partial z^2}\int_0^{\tau-\frac{z^2}{4\sigma X^2}} f_1(\tau')d\tau' = \frac{\partial}{\partial z}\left[-\frac{z}{2\sigma X^2} * f_1\left(\tau - \frac{z^2}{4\sigma X^2}\right)\right] =$$

$$= -\frac{z}{2\sigma X^2} * \frac{\partial f_1\left(\tau - \frac{z^2}{4\sigma X^2}\right)}{\partial z} - \frac{1}{2\sigma X^2} * f_1\left(\tau - \frac{z^2}{4\sigma X^2}\right)$$

Putting (159) and (160) into (158), we obtain

$$(161)\quad \mu_{11}\left(\tau - \frac{z^2}{4\sigma X^2}\right) = \left[\beta * \int_0^{\tau-\frac{z^2}{4\sigma X^2}} f_1(\tau')d\tau' + \Lambda * \left[\tau - \frac{z^2}{4\sigma X^2}\right]\right]\Bigg|_{z=0} +$$

$$+ \left[\frac{-z\beta}{2\sigma X^2} * f_1\left(\tau - \frac{z^2}{4\sigma X^2}\right) + \frac{-z\Lambda}{2\sigma X^2}\right]\Bigg|_{z=0} * z +$$

$$+ \left[\frac{-z\beta}{2\sigma X^2} * \frac{\partial f_1\left(\tau - \frac{z^2}{4\sigma X^2}\right)}{\partial z}\right]\Bigg|_{z=0} * \frac{z^2}{2} +$$

$$+ \left[\frac{-\beta}{2\sigma X^2} * f_1\left(\tau - \frac{z^2}{4\sigma X^2}\right) + \frac{-\Lambda}{2\sigma X^2}\right]\Bigg|_{z=0} * \frac{z^2}{2} +$$

$$+ \text{terms of order} > z^2$$

Put Z=0 in appropriate places. We get

$$(162)\quad \mu_{11}\left(\tau - \frac{Z^2}{4\sigma X^2}\right) = \left[\beta * \int_0^{\tau - \frac{Z^2}{4\sigma X^2}} f_1(\tau')d\tau'\right]\Bigg|_{Z=0} + \Lambda\tau -$$

$$- \left[\frac{\beta}{2\sigma X^2} * f_1(\tau) + \frac{\Lambda}{2\sigma X^2}\right] * \frac{Z^2}{2} +$$

$$+ \text{terms of order} > Z^2$$

Differentiate with respect to Z. We get

$$(163)\quad \frac{\partial \mu_{11}\left(\tau - \frac{Z^2}{4\sigma X^2}\right)}{\partial Z} = -\left[\frac{\beta}{2\sigma X^2} * \frac{\partial f_1(\tau)}{\partial Z}\right] * \frac{Z^2}{2} - \left[\frac{\beta}{2\sigma X^2} * f_1(\tau) +\right.$$

$$\left. + \frac{\Lambda}{2\sigma X^2}\right] * Z + \text{terms of order} > Z$$

Since f_1 in (163) is only a function of τ, we can immediately see that

$$(164)\quad \frac{\beta}{2\sigma X^2} * \frac{\partial f_1(\tau)}{\partial Z} = 0$$

Put (163) into (156). It gives

$$(165)\quad \frac{\partial \mu_{21}(\tau, Z)}{\partial Z} = -\frac{2}{\pi^{\frac{1}{2}}} * \frac{\int_Z^\infty \left[\left[\frac{\beta Z}{2\sigma} f_1(\tau) + \frac{\Lambda Z}{2\sigma} + \text{terms of}\right.\right.}{2(\sigma\tau)^{\frac{1}{2}}}$$

$$\left.\left. \text{order} > Z\right] * \frac{\exp(-X^2)}{X^2}\right] dX$$

Looking at (162), (163) and (164), we see that no more X will come out from the higher-order terms.

[67] gives

$$(166)\qquad \int_{\frac{Z}{2(\sigma\tau)^{\frac{1}{2}}}}^{\infty} \left[\frac{\exp(-X^2)}{X^2} \right] dX = \frac{2(\sigma\tau)^{\frac{1}{2}}}{Z} \exp\left[\frac{-Z^2}{4\sigma\tau} \right] -$$

$$- \pi^{\frac{1}{2}} \left[1 - \frac{2}{\pi^{\frac{1}{2}}} \left[\int_{0}^{\frac{Z}{2(\sigma\tau)^{\frac{1}{2}}}} \exp(-\xi^2)\, d\xi \right] \right]$$

Putting (166) into (165) gives

$$(167)\qquad \frac{\partial u_{21}(\tau,Z)}{\partial Z} = -\frac{2}{\pi^{\frac{1}{2}}} * \left[\frac{\beta Z}{2\sigma} f_1(\tau) + \frac{\Lambda Z}{2\sigma} + \text{terms of order} > Z \right] *$$

$$* \left[\frac{2(\sigma\tau)^{\frac{1}{2}}}{Z} \exp\left[\frac{-Z^2}{4\sigma\tau} \right] - \right.$$

$$\left. - \pi^{\frac{1}{2}} \left[1 - \frac{2}{\pi^{\frac{1}{2}}} \left[\int_{0}^{\frac{Z}{2(\sigma\tau)^{\frac{1}{2}}}} \exp(-\xi^2)\, d\xi \right] \right] \right]$$

$$= \text{(if we collect terms of different orders of Z)}$$

$$= -\frac{2}{\pi^{\frac{1}{2}}} * \left[\frac{\beta}{\sigma} f_1(\tau) + \frac{\Lambda}{\sigma} \right] * (\sigma\tau)^{\frac{1}{2}} * \exp\left[\frac{-Z^2}{4\sigma\tau} \right] +$$

$$+ \text{terms of order} > Z$$

If we set Z=0, we get

$$(168)\qquad \left.\frac{\partial \mu_{21}(\tau,Z)}{\partial Z}\right|_{Z=0} = -\frac{2\tau^{\frac{1}{2}}}{(\sigma\pi)^{\frac{1}{2}}} * \left[\beta f_1(\tau) + \Lambda\right]$$

(96) gives

$$(169)\qquad f_1(\tau) = \left.\frac{\partial \mu_{21}}{\partial Z}\right|_{Z=0}$$

Equating (96) and (168) gives

$$(100)\qquad f_1(\tau) = -\frac{\Lambda}{\beta}\left[1 - \frac{1}{1 + \tau^{\frac{1}{2}}\left[\frac{2\beta}{(\sigma\pi)^{\frac{1}{2}}}\right]}\right]$$

==========

Appendix 3

Here we evaluate the second-order perturbed solution. We use approximately the same method as when we derived the first-order perturbed solution. We use the "new" variables introduced in (86).

Put

$$\theta_1 = \theta_{11} + \Xi\theta_{12} + \Xi^2\theta_{13} + \dots$$
$$\theta_2 = \theta_{21} + \Xi\theta_{22} + \Xi^2\theta_{23} + \dots \tag{170}$$

(obtained from (90) - (93)) into (87) and (88). Select the terms with Ξ of power 1. They form

$$\frac{\partial\theta_{12}}{\partial\tau} = \frac{\partial^2\theta_{11}}{\partial\xi^2} + \frac{1}{\xi}\frac{\partial\theta_{11}}{\partial\xi} + \beta\left.\frac{\partial\theta_{22}}{\partial Z}\right|_{Z=0} \tag{171}$$

and

$$\frac{\partial\theta_{22}}{\partial\tau} = \sigma * \left[\frac{\partial^2\theta_{21}}{\partial\xi^2} + \frac{1}{\xi}\frac{\partial\theta_{21}}{\partial\xi} + \frac{\partial^2\theta_{22}}{\partial Z^2}\right] \tag{172}$$

The boundary conditions are the same as in (89), except that

$$\theta_{22} = \theta_{12}(\tau,\xi) \qquad \text{at } Z=0 \tag{173}$$

We have the first-order perturbed solutions from (92) and (93):

$$\theta_{11} = \exp(-\xi^2)\mu_{11}(\tau) \tag{174}$$

and

$$\theta_{21} = \exp(-\xi^2)\mu_{21}(\tau,Z) \tag{175}$$

Putting these into (171) and (172), gives us

$$\frac{\partial\theta_{12}}{\partial\tau} = 4(\xi^2 - 1)\exp(-\xi^2)\mu_{11}(\tau) + \beta f_2(\tau,\xi) \tag{176}$$

and

$$\frac{\partial\theta_{22}}{\partial\tau} = \sigma * \left[4(\xi^2 - 1)\exp(-\xi^2)\mu_{21}(\tau,Z) + \frac{\partial^2\theta_{22}}{\partial Z^2}\right] \tag{177}$$

where $f_2(\tau,\xi)$ is defined as

$$f_2(\tau,\xi) = \left.\frac{\partial\theta_{22}}{\partial Z}\right|_{Z=0} \tag{178}$$

(177) can be solved with the help of the Green function Ψ. The Green function is the homogeneous version of the inhomogeneous problem. In this case, the homogeneous version is

$$(179) \qquad \frac{\partial \Psi}{\partial \tau} = \sigma \frac{\partial \Psi^2}{\partial Z^2}$$

$$\text{with } \Psi = 0 \quad \text{at } Z=\infty$$
$$\Psi = 0 \quad \text{at } Z=0$$

The Green function in this case can also be defined as (according to Carslaw and Jaeger [68]) the temperature at Z at the time τ due to a unit instantaneous plane source at z' at the time τ'.

The solution is given as [68]

$$(180) \qquad \Psi(\tau,Z;\tau',z') = \frac{1}{2(\pi\sigma)^{\frac{1}{2}}(\tau-\tau')^{\frac{1}{2}}} \left[\exp\left[\frac{-(Z-z')^2}{4\sigma(\tau-\tau')} \right] - \exp\left[\frac{-(Z+z')^2}{4\sigma(\tau-\tau')} \right] \right]$$

(This solution is easily obtained from (129), using the method of images [66].)

Now, having the Green function, we are able to directly obtain the solution to (177) with the help of Özisik [69] as

$$(181) \qquad \theta_{22}(\tau,\xi,Z) = \sigma \int_{\tau'=0}^{\tau} d\tau' \left[\int_0^{\infty} \left[\Psi(\tau,Z;\tau',z') * 4(\xi^2 - 1)\exp(-\xi^2) * \mu_{12}(\tau',z') \right] dz' \right] d\tau' +$$
$$+ \sigma \int_{\tau'=0}^{\tau} \left[\theta_{12}(\tau',\xi) \frac{\partial \Psi(\tau,Z;\tau',z')}{\partial z'} \Big|_{Z=0} \right] d\tau'$$

Equation (176) can be integrated directly. We get

$$(182) \qquad \theta_{12}(\tau,\xi) = 4(\xi^2 - 1)\exp(-\xi^2) * \int_0^{\tau} \mu_{11}(\tau')d\tau' + \beta \int_0^{\tau} f_2(\tau',\xi)d\tau'$$

We can get μ_{11} and μ_{12} from the first-order solution. This means that we "only" have to find $f_2(\tau,\xi)$. As can be seen, the strategy is, and will be, the same as for the first-order solution.

We use solution (181). For convenience it is divided into two parts, s_1 and s_2, where

$$(183) \qquad s_1 = \sigma \int_0^{\tau} \theta_{12}(\tau',\xi) \left.\frac{\partial \Psi}{\partial z'}\right|_{z'=0} d\tau'$$

and

$$(184) \qquad s_2 = 4\sigma(\xi^2 - 1)\exp(-\xi^2) \int_0^{\tau}\int_0^{\infty} \Psi u_{21}(\tau',z')dz'd\tau'$$

We know that $\theta_{22} = s_1 + s_2$. This means that if we want to evaluate

$f_2(\tau,\xi) = \left.\frac{\partial \theta_{22}}{\partial Z}\right|_{Z=0}$, we have to evaluate

$\left.\frac{\partial s_1}{\partial Z}\right|_{Z=0}$ and $\left.\frac{\partial s_2}{\partial Z}\right|_{Z=0}$

Let us do that.

First, evaluate $\left.\frac{\partial \Psi}{\partial z'}\right|_{z'=0}$

The result is obtained from differentiating (180). The result is

$$(185) \qquad \left.\frac{\partial \Psi}{\partial z'}\right|_{z'=0} = \frac{Z}{2(\pi\sigma)^{\frac{1}{2}}(\tau-\tau')^{\frac{1}{2}}} * \frac{1}{\sigma(\tau-\tau')} * \exp\left[\frac{-Z^2}{4\sigma(\tau-\tau')}\right]$$

Use, in order to get rid of τ',

$$(186) \qquad X = \frac{Z}{2\left[\sigma(\tau-\tau')\right]^{\frac{1}{2}}}$$

We obtain

$$(187) \qquad \left.\frac{\partial \Psi}{\partial z'}\right|_{z'=0} = \frac{4X^3}{Z^2\,\pi^{\frac{1}{2}}} \exp(-X^2)$$

and (183) will become

$$(188) \qquad s_1\left(\tau - \frac{Z^2}{4\sigma X^2}, \xi\right) = \int_{\frac{Z}{2(\sigma\tau)^{\frac{1}{2}}}}^{\infty} \left[\theta_{12}\left(\tau - \frac{Z^2}{4\sigma X^2}, \xi\right) \frac{2}{\pi^{\frac{1}{2}}} \exp(-X^2)\right] dX$$

To obtain $\frac{\partial s_1}{\partial Z}$ we must use Leibniz' formula (153). Using this and the fact that $\theta_{12}(\xi,0)=0$, we get

$$(189)\qquad \frac{\partial s_1}{\partial Z} = \int_{\frac{Z}{2(\sigma\tau)^{\frac{1}{2}}}}^{\infty} \left[\frac{\partial \theta_{12}(\tau - \frac{Z^2}{4\sigma X^2}, \xi)}{\partial Z} * \frac{2}{\pi^{\frac{1}{2}}} \exp(-X^2) \right] dX$$

How do we evaluate this?

As in the first-order solution, we expand θ_{12} in a Maclaurin series for small Z.

The Maclaurin formula is, in this case

$$(190)\qquad \theta_{12} = \theta_{12} + \left.\frac{\partial \theta_{12}}{\partial Z}\right|_{Z=0} * Z + \left.\frac{\partial^2 \theta_{12}}{\partial Z^2}\right|_{Z=0} * \frac{Z^2}{2} +$$

$$+ \text{terms of order } Z^3 \text{ and higher}$$

We have, according to (182)

$$(191)\qquad \theta_{12}(\tau - \frac{Z^2}{4\sigma X^2}, \xi) = \int_0^{\tau - \frac{Z^2}{4\sigma X^2}} \left[4(\xi^2 - 1)\exp(-\xi^2)\mu_{11}(\tau') + \right.$$

$$\left. + \beta f_2(\tau', \xi) \right] d\tau'$$

This will give

$$(192)\qquad \frac{\partial \theta_{12}}{\partial Z} = \frac{\partial}{\partial(\tau - \frac{Z^2}{4\sigma X^2})} * \frac{\partial(\tau - \frac{Z^2}{4\sigma X^2})}{\partial Z} \theta_{12} =$$

$$= \frac{-Z}{2\sigma X^2} * \left[4(\xi^2 - 1)\exp(-\xi^2) * \mu_{11}(\tau - \frac{Z^2}{4\sigma X^2}) + \right.$$

$$\left. + \beta f_2(\tau - \frac{Z^2}{4\sigma X^2}, \xi) \right] = \frac{-Z}{2\sigma X^2} * \Omega(Z)$$

(We define Ω this way).

We get

$$(193) \qquad \frac{\partial^2 \theta_{12}}{\partial z^2} = - \frac{\Omega(z)}{2\sigma X^2} - \frac{\partial \Omega(z)}{\partial z} * \frac{z}{2\sigma X^2}$$

We get (190) as

$$(194) \qquad \theta_{12}(\tau - \frac{z^2}{4\sigma X^2}, \xi) = \theta_{12}(\tau, \xi) - \frac{\Omega(0)}{2\sigma X^2} * \frac{z^2}{2} +$$

$$+ \text{ terms of order } z^3 \text{ and higher}$$

Differentiating (194) with respect to Z gives

$$(195) \qquad \frac{\partial \theta_{12}(\tau - \frac{z^2}{4\sigma X^2}, \xi)}{\partial z} - \frac{z}{2\sigma X^2} * \Omega(0) + \text{terms of order } z^2 \text{ and higher}$$

Now we can put this into (189), obtaining

$$(196) \qquad \frac{\partial s_1}{\partial z} = \frac{\int_z^\infty}{2(\sigma\tau)^{\frac{1}{2}}} \left[\frac{-z}{2\sigma X^2} \left[4(\xi^2 - 1)\exp(-\xi^2) * \mu_{11}(\tau) + \beta f_2(\tau, \xi) \right] * \right.$$

$$\left. * \frac{2}{\pi^{\frac{1}{2}}} \exp(-X^2) \right] dX = \left[\begin{array}{l} \text{since (192) and (193) show} \\ \text{that no further X appears} \end{array} \right] =$$

$$= \frac{-z}{\pi^{\frac{1}{2}}\sigma} * \left[4(\xi^2 - 1)\exp(-\xi^2) * \mu_{11}(\tau) + \beta f_2(\tau, \xi) \right] *$$

$$* \frac{\int_z^\infty}{2(\sigma\tau)^{\frac{1}{2}}} \left[\frac{\exp(-X^2)}{X^2} \right] dX$$

[70] gives

$$(197)\quad \int_{\frac{Z}{2(\sigma\tau)^{\frac{1}{2}}}}^{\infty} \left[\frac{\exp(-X^2)}{X^2} \right] dX = \frac{2(\sigma\tau)^{\frac{1}{2}}}{Z} * \exp\left[\frac{-Z^2}{4\sigma\tau} \right] -$$

$$- \pi^{\frac{1}{2}} \left[1 - \frac{2}{\pi^{\frac{1}{2}}} \int_0^{\frac{Z}{2(\sigma\tau)^{\frac{1}{2}}}} \exp(-\xi^2) d\xi \right]$$

Putting (197) into (196) and then setting Z=0 yields

$$(198)\quad \left.\frac{\partial s_1}{\partial Z}\right|_{Z=0} = \frac{-2}{(\sigma\pi)^{\frac{1}{2}}} \left[4(\xi^2 - 1)\exp(-\xi^2) * (\tau^{\frac{1}{2}})\mu_{11}(\tau) + (\tau^{\frac{1}{2}})\beta f_2(\tau,\xi) \right]$$

Now, calculate $\left.\frac{\partial s_2}{\partial Z}\right|_{Z=0}$

From (184) we have

$$(199)\quad s_2 = 4\sigma(\xi^2 - 1)\exp(-\xi^2) \int_0^{\tau}\int_0^{\infty} \Psi\mu_{21}(\tau',z')dz'd\tau'$$

and from (152) we have

$$(200)\quad \mu_{21}(\tau,Z) = \frac{2}{\pi^{\frac{1}{2}}} * \int_{\frac{Z}{2(\sigma\tau)^{\frac{1}{2}}}}^{\infty} \mu_{11}\left(\tau - \frac{Z^2}{4\sigma X^2} \right) \exp(-X^2)\, dX$$

The last equation can be approximated for small Z by expanding

$$(201)\quad \mu_{11}\left(\tau - \frac{Z^2}{4\sigma X^2} \right) = k(Z)$$

in a Maclaurin series. We get

$$(202)\quad k(Z) = k(0) + Zk'(Z) + \ldots$$

This implies that

(203) $k(Z) \approx k(0)$ for small Z

which means that

$$(204) \quad \mu_{11}\left(\tau - \frac{Z^2}{4\sigma X^2}\right) \approx \mu_{11}(\tau) \quad \text{for small } Z$$

This gives

$$(205) \quad \mu_{21} \approx \mu_{11}(\tau) * \frac{2}{\pi^{\frac{1}{2}}} * \int_{\frac{Z}{2(\sigma\tau)^{\frac{1}{2}}}}^{\infty} \exp(-X^2)\, dX$$

The integral equals $\operatorname{erfc}\left(\frac{Z}{2(\sigma\tau)^{\frac{1}{2}}}\right)$ [71]

Substitution of (205) into (199) gives

$$(206) \quad s_2 = 4\sigma(\xi^2 - 1)\exp(-\xi^2) \int_0^{\tau}\int_0^{\infty} \left[\Psi(\tau,Z;\tau',z')\mu_{11}(\tau') * \right.$$

$$\left. * \operatorname{erfc}\left(\frac{z'}{2(\sigma\tau')^{\frac{1}{2}}}\right) \right] dz'd\tau'$$

Now

$$(207) \quad \left.\frac{\partial s_2}{\partial Z}\right|_{Z=0} = 4\sigma(\xi^2 - 1)\exp(-\xi^2) \int_0^{\tau}\int_0^{\infty} \left[\left.\frac{\partial \Psi(\tau,Z;\tau',z')}{\partial Z}\right|_{Z=0} * \right.$$

$$\left. * \mu_{11}(\tau') * \operatorname{erfc}\left(\frac{z'}{2(\sigma\tau')^{\frac{1}{2}}}\right) \right] dz'd\tau'$$

From (180) and (185) we obtain

$$(208) \quad \left.\frac{\partial \Psi}{\partial Z}\right|_{Z=0} = \frac{z'}{2\sigma(\tau-\tau')*(\pi\sigma(\tau-\tau'))^{\frac{1}{2}}} \exp\left[\frac{-z'^2}{4\sigma(\tau-\tau')}\right]$$

We obtain

$$(209)\qquad \left.\frac{\partial s_2}{\partial Z}\right|_{Z=0} = 4\sigma(\xi^2 - 1)\exp(-\xi^2)\left[\int_0^{\tau} \frac{\mu_{11}(\tau')}{2(\pi\sigma(\tau-\tau'))^{\frac{1}{2}}} * \left[\int_0^{\infty} \frac{z'}{\sigma(\tau-\tau')} * \right.\right.$$

$$\left.\left. * \exp\left[\frac{-z'^2}{4\sigma(\tau-\tau')}\right] * \frac{2}{\pi^{\frac{1}{2}}} * \int_{\frac{z'}{2(\sigma\tau')^{\frac{1}{2}}}}^{\infty} \exp(-X^2)\,dX \right] dz' \right] d\tau'$$

Let

$$(210)\qquad p(z') = \int \frac{z'}{\sigma(\tau-\tau')} \exp\left[\frac{-z'^2}{4\sigma(\tau-\tau')}\right] dz' = -2\exp\left[\frac{-z'^2}{4\sigma(\tau-\tau')}\right]$$

and

$$(211)\qquad o(z') = \frac{2}{\pi^{\frac{1}{2}}} * \int_{\frac{z'}{2(\sigma\tau')^{\frac{1}{2}}}}^{\infty} \exp(-X^2)\,dX$$

Integration by parts, with respect to z', gives

$$(212)\qquad \int_0^{\infty} o(z')\frac{\partial p(z')}{\partial z'}\,dz' = \left[o(z')p(z')\right]_0^{\infty} - \int_0^{\infty} \frac{\partial o(z')}{\partial z'}\,p(z')\,dz'$$

We have

$$(213)\qquad \frac{\partial o(z')}{\partial z'} = \frac{\partial}{\partial\left[\frac{z'}{2(\sigma\tau')^{\frac{1}{2}}}\right]} * \frac{\partial\left[\frac{z'}{2(\sigma\tau')^{\frac{1}{2}}}\right]}{\partial z'} *$$

$$* \left[1 - \frac{2}{\pi^{\frac{1}{2}}} \int_0^{\frac{z'}{2(\sigma\tau')^{\frac{1}{2}}}} \exp(-X^2)dX\right] = \frac{-1}{(\sigma\tau'\pi)^{\frac{1}{2}}} \exp\left[\frac{-z'^2}{4\sigma\tau'}\right]$$

and

$$(214) \qquad \frac{\partial p(z')}{\partial z'} = \frac{z'}{\sigma(\tau-\tau')} \exp\left[\frac{-z'^2}{4\sigma(\tau-\tau')}\right]$$

Furthermore,

$$(215) \qquad \int_0^\infty \frac{\partial o(z')}{\partial z'} p(z')\,dz' = \int_0^\infty \frac{2}{(\sigma\tau'\pi)^{\frac{1}{2}}} \exp\left[\frac{-z'^2}{4\sigma} * \left[\frac{1}{\tau-\tau'} + \frac{1}{\tau'}\right]\right] dz'$$

[72] gives

$$(216) \qquad \int_0^\infty \frac{\partial o(z')}{\partial z'} p(z')\,dz' = 2 * \left[\frac{\tau-\tau'}{\tau}\right]^{\frac{1}{2}}$$

Finally

$$(217) \qquad \left[o(z')p(z') \right]_0^\infty = \left[\left[\frac{2}{\pi^{\frac{1}{2}}} * \int_{\frac{z'}{2(\sigma\tau')^{\frac{1}{2}}}}^\infty \exp(-X^2)\,dX \right] * \left[-2 \exp\left[\frac{-z'^2}{4\sigma(\tau-\tau')}\right] \right] \right]_0^\infty =$$

$$= \frac{4}{\pi^{\frac{1}{2}}} * \int_0^\infty \exp(-X^2)\,dX = \text{(according to [73])} = 2$$

(212), (216) and (217) gives

$$(218)\qquad \int_0^{\infty} o(z')\,\frac{\partial p(z')}{\partial z'}\,dz' = 2 - 2 * \left[\frac{\tau-\tau'}{\tau}\right]^{\frac{1}{2}}$$

Putting this into (209), we get

$$(219)\qquad \left.\frac{\partial s_2}{\partial Z}\right|_{Z=0} = 4\sigma(\xi^2-1)\exp(-\xi^2)\int_0^{\tau}\frac{\mu_{11}(\tau')}{(\pi\sigma)^{\frac{1}{2}}} * \left[\frac{1}{(\tau-\tau')^{\frac{1}{2}}} - \frac{1}{\tau^{\frac{1}{2}}}\right] d\tau'$$

Comparing pages 76 - 77, (198) and (219) yields

$$(220)\qquad \left.\frac{\partial \theta_{22}}{\partial Z}\right|_{Z=0} = \left.\frac{\partial s_1}{\partial Z}\right|_{Z=0} + \left.\frac{\partial s_2}{\partial Z}\right|_{Z=0} =$$

$$= \frac{-2}{(\sigma\pi)^{\frac{1}{2}}}\left[4(\xi^2-1)\exp(-\xi^2)*(\tau^{\frac{1}{2}})\mu_{11}(\tau) + (\tau^{\frac{1}{2}})\beta f_2(\tau,\xi)\right] +$$

$$+ 4\sigma(\xi^2-1)\exp(-\xi^2)\int_0^{\tau}\frac{\mu_{11}(\tau')}{(\pi\sigma)^{\frac{1}{2}}} * \left[\frac{1}{(\tau-\tau')^{\frac{1}{2}}} - \frac{1}{\tau^{\frac{1}{2}}}\right] d\tau'$$

Now we can go all the way back to (178). We can use this equation and (220) to evolve $f_2(\tau,\xi)$ as

$$(221)\qquad f_2(\tau,\xi) = \frac{1}{1 + 2\beta\left[\frac{\tau}{\sigma\pi}\right]^{\frac{1}{2}}}\left[\frac{-8}{(\sigma\pi)^{\frac{1}{2}}}(\xi^2-1)\exp(-\xi^2)*(\tau^{\frac{1}{2}})\mu_{11}(\tau) +\right.$$

$$\left. + 4\left[\frac{\sigma}{\pi}\right]^{\frac{1}{2}}(\xi^2-1)\exp(-\xi^2)\int_0^{\tau}\mu_{11}(\tau')*\left[\frac{1}{(\tau-\tau')^{\frac{1}{2}}} - \frac{1}{\tau^{\frac{1}{2}}}\right]d\tau'\right.$$

Putting this into equation (182), we finally get the second-order perturbed solution for the temperature rise in the film as

$$(222)\quad \theta_{12}(\tau,\xi) = 4(\xi^2 - 1)\exp(-\xi^2) * \int_0^{\tau} \mu_{11}(\tau^*)d\tau^* +$$

$$+ \beta \int_0^{\tau} \left[\frac{1}{\left[1 + 2\beta \left[\frac{\tau^*}{\sigma\pi} \right]^{\frac{1}{2}}\right]} * \right.$$

$$* \left[\frac{-8}{(\sigma\pi)^{\frac{1}{2}}} (\xi^2 - 1)\exp(-\xi^2) * (\tau^{*\frac{1}{2}})\mu_{11}(\tau^*) + \right.$$

$$+ 4\left[\frac{\sigma}{\pi} \right]^{\frac{1}{2}} (\xi^2 - 1)\exp(-\xi^2) \int_0^{\tau^*} \left[\mu_{11}(\tau') * \right.$$

$$\left. \left. \left. * \left[\frac{1}{(\tau^* - \tau')^{\frac{1}{2}}} - \frac{1}{\tau^{*\frac{1}{2}}} \right] \right] d\tau' \right] \right] d\tau^* = \text{(see next page)}$$

$$= 4(\xi^2 - 1)\exp(-\xi^2) \left[\int_0^{\tau} \mu_{11}(\tau^*)d\tau^* + \right.$$

$$+ \beta \int_0^{\tau} \left[\frac{1}{1 + 2\beta \left[\frac{\tau^*}{\sigma\pi} \right]^{\frac{1}{2}}} * \right.$$

$$* \left[\frac{-2}{(\sigma\pi)^{\frac{1}{2}}} (\tau^{*\frac{1}{2}})\mu_{11}(\tau^*) + \left[\frac{J}{\pi} \right]^{\frac{1}{2}} \int_0^{\tau^*} \left[\mu_{11}(\tau') * \right. \right.$$

$$\left. \left. \left. * \left[\frac{1}{(\tau^* - \tau')^{\frac{1}{2}}} - \frac{1}{\tau^{*\frac{1}{2}}} \right] \right] d\tau' \right] \left. \right] d\tau^* \left. \right]$$

where, from (103)

$$\mu_{11} = \frac{(\sigma\tau)^{\frac{1}{2}}}{\beta} \Lambda\tau^{\frac{1}{2}} - \frac{\sigma\pi\Lambda}{2\beta^2} * \ln \left[1 + \frac{2\beta}{(\pi\sigma)^{\frac{1}{2}}} \tau^{\frac{1}{2}} \right]$$

==========

References
==========

[1] E. Hecht and A Zajac; Optics (Addison-Wesley Publishing Company. Inc, 1979 (fourth printing), page 487)

[2] P. P. Sorokin and J. R. Lankard; IBM J. Res. Dev. 10, 162 (1966)

[3] F. P. Schäfer, W. Schmidt and J Volozo; Appl. Phys. Lett. 9, 506 (1966)

[4] A. M. Weiner and E. P. Ippen; Optics Lett. 9, 53 (1984)

[5] A. Corney, J. Manners and C. E. Webb; Pot. Comm. 31, 354 (1979)

W. Huffer, R. Schieder, H. Telle, R. Raue and W Brinkwerth; Opt. Comm. 33, 85 (1980)

J. N. Eckstein, A. I. Ferguson, T. W. Hansch, C. A. Minard, and C. K. Chan; Opt. Comm. 27, 466 (1978)

[6] A. Ferrario; Opt. Comm. 30, 85 (1979)

M. Leduc; Opt. Comm. 31, 66 (1979)

[7] G. White and J. G. Pruett, Opt. Lett. 6, 473 (1981)

[8] L. F. Mollenauer and D. H. Olson; J. Appl. Phys. 46, 3109 (1975)

L. F. Mollenauer and D. M. Bloom; Pot. Lett. 4, 247 (1979)

I. Schneider and M. J. Marrone; Opt. Lett. 4, 390 (1979)

[9] J. C. Walling and O. G. Peterson; IEEE J. Quan. Elec. QE-16, 119 (1980)

J. C. Walling, O. G. Peterson and R. C. Morris; IEEE J. Quan. Elec. QE-16, 120 (1980)

[10] P. F. Moulton and A. Mooradian; Appl. Phys. Lett. 35, 838 (1979)

[11] M. I. Nathan, W. P. Dumke, G. Burns, F. H. Dill, and G. Lasher; Appl. Phys. Lett. 1, 62 (1962)

T. M. Quist, R. H. Rediker, R. J. Keyes, W. E. Kras, B. Lax, A. L. McWhorter, H. J. Zeigler; Appl. Phys. Lett. 1, 91 (1962)

R. N. Hall, G. E. Fenner, J. D. Kingsley, T. J. Soltys, and R. O. Carlson; Phys. Rev. Lett. 9, 366 (1962)

[12] C. B. Roxlo, Optically pumped semiconductor lasers (Ph. D. thesis), Massachusetts Institute of Technology (1981), page 27

[13] C. B. Roxlo, Optically pumped semiconductor lasers (Ph. D. thesis), Massachusetts Institute of Technology (1981), page 17

[14] D. G. Thomas and J. J. Hopfield; J. Appl. Phys. 33, 3243 (1962)

[15] R. J. Phelan and R. H. Rediker; Appl. Phys. Lett. 6, 70 (1965)

[16] C. B. Roxlo, D. Bebelaar and M. M. Salour; Appl. Phys. Lett. 38, 7 (1981)

[17] C. B. Roxlo, Optically pumped semiconductor lasers (Ph. D. thesis), Massachusetts Institute of Technology (1981), page 108

[18] C. B. Roxlo, Optically pumped semiconductor lasers (Ph. D. thesis), Massachusetts Institute of Technology (1981), page 23 and 108

[19] C. B. Roxlo, Optically pumped semiconductor lasers (Ph. D. thesis), Massachusetts Institute of Technology (1981), page 128

[20] V. N. Martynov, S. A. Medvedev, L. L. Adsenova, and Yu. D. Avchukhov; Sov. Phys. Crystallogr. 24, 743 (1979)

[21] C. B. Roxlo, Optically pumped semiconductor lasers (Ph. D. Thesis), Massachusetts Institute of Technology (1981), page 104

[22] N. Holonyak, Jr. and D. R. Scifres; The Review of Scientific Instruments, Vol 42, number 12 (1971)

[23] D. B. Tuckerman, Heat-Transfer Microstructures for Integrated Circuits (Ph.D Thesis), Lawrence Livermore National Laboratory, (February 1984), chapter 4-5

[24] D. B. Tuckerman, Heat-Transfer Microstructures for Integrated Circuits (Ph.D Thesis), Lawrence Livermore National Laboratory, (February 1984), chapter 2-3

[25] Private communication

[26] M. N. Özisik, Basic heat transfer, McGraw-Hill Kogakusha Ltd (1977), page 20-23

[27] C. B. Roxlo, Optically pumped semiconductor lasers (Ph. D. thesis), Massachusetts Institute of Technology (1981), page 107

[28] N. N. Rykalin, A. A. Uglov, and N. I. Makarov, DAN, 174, 4, 824, (1967) (Soviet Physics - Doklady, Vol. 12, No. 6, Dec 1967, page 636)

[29] J. F. Ready, Effects of High-Power Laser Radiation, Academic Press (1971), page 75 - 83

W. W. Duley, CO_2 Lasers, Effects and Applications, Academic Press (1976), page 149 - 152

[30] H. S. Carslaw and J. C. Jaeger, Conduction of Heat in Solids, Oxford University Press (1959), second edition, page 256

[31] I. S. Gradshteyn and I. M. Ryzhik, Table of Integrals, Series and Products, Academic Press (1965), fourth edition, page 310

[32] - " -, page 709

[33] - " -, page 1059

[34] - " -, page 22 and 1058

[35] K. Brugger; J. Appl. Phys., Vol. 43, No. 2, (1972)

[36] J. H. Bechtel; J. Appl. Phys., Vol. 46, No. 4, (1975)

[37] J. F. Ready, Effects of High-Power Laser Radiation, Academic Press (1971), page 83 - 87

W. W. Duley, CO_2 Lasers, Effects and Applications, Academic Press (1976), page 161 - 166

[38] H. S. Carslaw and J. C. Jaeger, Conduction of Heat in Solids, Oxford University Press (1959), second edition, page 169

[39] - " -, page 258

[40] I. S. Gradshteyn and I. M. Ryzhik, Table of Integrals, Series and Products, Academic Press (1965), fourth edition, page 311

[41] - " -, page 925

[42] K. Brugger; J. Appl. Phys., Vol. 43, No. 2, (1972)

[43] U.C. Peak and A. Kestenbaum; J. Appl. Phys., Vol 44, No. 5, (May 1973)

[44] I. D. Calder and R. Sue: Modeling of cw laser annealing of multilayer structures, J. Appl. Phys. 53(11), November 1982

[45] M. Born and E. Wolf, Principles of optics (Pergamon, New York, 1959)

[46] J. Y. Chen, G. Eckhardt, and L. D. Hess, Semiconductor Silicon 1981 (Electrochem. Society, New Jersey (1981), page 694

[47] I. D. Calder and R. Sue: Modeling of cw laser annealing of multilayer structures, J. Appl. Phys. 53(11), November 1982 equation (17)

[48] M. Kull, Methods of optical temperature measurements (Diploma Thesis); The Royal Institute of Technology, Departement of physics II, S-100 44 Stockholm, Sweden (Nov 1984)

[49] H. Friedrich; Phys. Stat. Sol. 5, K27 (1964)

[50] C. B. Roxlo, R. S. Putnam, and M. M. Salour; IEEE J. of Quantum Electronics, Vol. QE-18, No. 3, (March 1982)

A. Fuchs, D. Bebelaar, and M. M. Salour; Appl. Phys. Lett. 43(1), 1 July 1983

[51] C. B. Roxlo, R. S. Putnam, and M. M. Salour; IEEE J. of Quantum Electronics, Vol. QE-18, No. 3, (March 1982)

[52] C. B. Roxlo, Optically pumped semiconductor lasers (Ph. D. Thesis), Massachusetts Institute of Technology (1981), page 43

[53] A. Fuchs and M. M. Salour; Rev. Sci. Instrum. 54(9), (Sept. 1983)

[54] C. B. Roxlo, Optically pumped semiconductor lasers (Ph. D. Thesis), Massachusetts Institute of Technology (1981), page 67

[55] C. B. Roxlo and M. M. Salour; Rev. Sci. Instrum. 53(4), Apr. (1982)

[56] M. Kull, Methods of optical temperature measurements (Diploma Thesis); The Royal Institute of Technology, Departement of physics II, S-100 44 Stockholm, Sweden (Nov 1984), page 39

[57] A. Fuchs, D. Bebelaar, and M. M. Salour; Appl. Phys. Lett. 43(1), 1 July 1983

[58] C. B. Roxlo, R. S. Putnam, and M. M. Salour; IEEE J. of Quantum Electronics, Vol. QE-18, No. 3, (March 1982)

[59] C. B. Roxlo, Optically pumped semiconductor lasers (Ph. D. Thesis), Massachusetts Institute of Technology (1981), page 83

[60] E. Hecht and A Zajac; Optics (Addison-Wesley Publishing Company. Inc, 1979 (fourth printing), page 311

[61] N. I. Vitrikhovskii, L. F. Gudymenko, A. F. Maznichenko, V. N. Malinko, E. V. Pidlisnyi, and S. F. Tereknova, Uk. Fiz. Zh. 12 (1967), page 796

[62] Information from S. Thornegård, Quantronics Corp.

[63] H. S. Carslaw and J. C. Jaeger, Conduction of Heat in Solids, Oxford University Press (1959), second edition, page 31

[64] - " -, page 50, 53

[65] M. N. Özisik, Heat conduction, Wiley-Interscience publication (1980), page 45

[66] H. S. Carslaw and J. C. Jaeger, Conduction of Heat in Solids, Oxford University Press (1959), second edition, page 58

[67] I. S. Gradshteyn and I. M. Ryzhik, Table of Integrals, Series and Products, Academic Press (1965), fourth edition, page 337 and 930

[68] H. S. Carslaw and J. C. Jaeger, Conduction of Heat in Solids, Oxford University Press (1959), second edition, page 357

[69] M. N. Özisik, Heat conduction, Wiley-Interscience publication (1980), chapter 6

[70] I. S. Gradshteyn and I. M. Ryzhik, Table of Integrals, Series and Products, Academic Press (1965), fourth edition, page 337 and 930

[71] H. S. Carslaw and J. C. Jaeger, Conduction of Heat in Solids, Oxford University Press (1959), second edition, page 51

[72] I. S. Gradshteyn and I. M. Ryzhik, Table of Integrals, Series and Products, Academic Press (1965), fourth edition, page 307

[73] - " -